Determining the Requirement for Wnt Signaling in HAM-1 Regulated Asymmetric Cell Divisions

by

Diana Mohan

B.Sc. (Genetics), University of Manitoba, 2020

Thesis Submitted in Partial Fulfillment of the
Requirements for the Degree of
Master of Science

in the
Department of Molecular Biology and Biochemistry
Faculty of Science

SIMON FRASER UNIVERSITY
Summer 2024

Declaration of Committee

Name:	**Diana Mohan**
Degree:	**Master of Science (Molecular Biology and Biochemistry)**
Title:	**Determining the Requirement for Wnt Signaling in HAM-1 Regulated Asymmetric Cell Divisions**
Committee:	**Chair:** **Dustin King** Assistant Professor, Molecular Biology and Biochemistry
	Nancy Hawkins Supervisor Associate Professor, Molecular Biology and Biochemistry
	Harald Hutter Committee Member Professor, Biological Sciences
	Esther Verheyen Committee Member Professor, Molecular Biology and Biochemistry
	Michel Leroux Examiner Professor, Molecular Biology and Biochemistry Simon Fraser University

Abstract

Asymmetric cell division is the process wherein a mother cell divides to generate daughter cells with distinct fates, and dysregulation is linked to cancer. *C. elegans* is an excellent model for studying asymmetric cell division due to its well-mapped cell lineage. In *C. elegans*, *ham-1* functions to regulate asymmetric neuroblast division. HAM-1 is a putative transcription factor that localizes to both the nucleus and the cell cortex during embryogenesis. Using 4D microscopy, we characterized GFP::HAM-1 polarization during cell division and its asymmetric distribution in daughter cells. In *C. elegans,* Wnt signaling polarizes asymmetrically dividing cells along the anterior-posterior axis. Therefore, we hypothesize that Wnts may function to regulate asymmetric division in *ham-1* dependent lineages. We found several of the Wnts functioned redundantly to control asymmetric divisions in the lineages that generated the PLM and PHB neurons. This suggests that Wnt signalling may function with HAM-1 to regulate asymmetric cell division.

Keywords: *C. elegans*; Asymmetric Cell Division; HAM-1; Wnt Signalling

Dedication

For my mother Diana, my brothers Daniel, Devin and Dempsey, my sister Emma, and my loving aunt and uncle Linda and Mohsen, who have given me support, love, and encouragement throughout this adventure.

Acknowledgements

A huge thank you to my supervisor Nancy Hawkins who has guided me through every success and supported me after every failure. I am grateful for her patience, wisdom, and the time she has dedicated to my development as a scientist.

Thank you to my committee members, Harald Hutter and Esther Verheyen for their astute guidance in committee meetings and their kindness offered as I learn.

Thank you to my friends Hamida, Lili, Trang, Rachel, Yuuka, Aleksa, Teodora, Matt, and J-Dog who have buffered every bad day in the lab and made every good day even better. You have all made this journey a fun and special ride!

Finally, I would like to thank my boyfriend Jackson, for your unyielding love and support.

Table of Contents

List of Tables

List of Figures

Chapter 1. Introduction

1.1. Asymmetric Cell Division

Asymmetric cell division (ACD) is an evolutionarily conserved mechanism present in eukaryotes and is the process by which a mother cell divides to produce daughter cells of distinct identities or fates (Horvitz & Herskowitz, 1992). This is separate from symmetric cell division, which produces daughter cells of the same fate. In many tissues dysregulated ACD is associated with loss of homeostasis, defective tissue repair, and cancer (Chao et al., 2024). A thorough mechanistic understanding of ACD is consequently essential to understand cell fate decisions for both health and disease.

Several steps are essential to ensure proper asymmetric division: first, a polarity axis must be established; this is followed by the alignment of the mitotic spindle and the asymmetric distribution of cell fate determinants along this polarity axis. These steps are controlled by both cell intrinsic mechanisms and cell extrinsic mechanisms (Fig. 1-1) (Hawkins & Garriga, 1996). An essential feature of an intrinsic ACD mechanism is the asymmetric localization of cell fate determinants and cell structures during mitosis using an inherent axis of polarity. This axis of polarity is also used to orient the mitotic spindle and ultimately ensures that there is a bias during inheritance of cell fate determinants between the daughter cells. Cell fate decisions can be induced through either asymmetric RNA and/or protein distribution. The polarized distribution of molecules often precedes division such that biased segregation of mRNAs into one sibling cell can affect gene expression, protein localization and function (Sunchu & Cabernard, 2020). Conversely, extrinsic mechanisms of ACD rely on extracellular signals to orient the mitotic spindle during mitosis (Sunchu & Cabernard, 2020). These signals include direct cell to cell contact and chemical cues. For example, the stem cell niche is a known environment that provides both physical and chemical cues to regulate stem cell development (Chao et al., 2024). Cell to cell contact is known to denote apical domains, and provide mechanical forces that can direct myosin flow, directing ACD. In the *C. elegans* zygote, the sperm centrosome acts as a polarizing cue that initiates an actomyosin cortical flow at one end of the cell (Pacquelet, 2017). Chemical cues include signalling molecules that provide an extrinsic cue for ACD, where after cleavage of the mother cell the relative positioning of each daughter cell to the signal continues to affect

cell fate decisions. Both mechanisms of ACD ensure the generation of daughter cells of different fate. Additionally, ACD can generate two daughter cells that are not only different in fate but also in size (Pacquelet, 2017). This occurs when the mitotic spindle is displaced favorably toward one pole of the mother cell, thereby leading to daughter cell size asymmetry. These ACD events are often preceded by cell polarity formation and symmetry breaking events. Polarity formation in ACD has been broadly explored using *Drosophila* and *C. elegans* as model systems (Hawkins & Garriga, 1996).

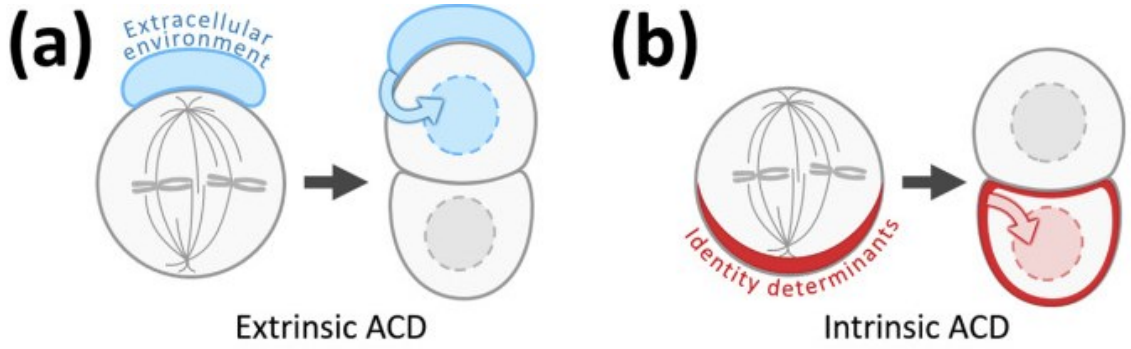

Figure 1-1 Models of ACD.
(a) In extrinsic ACD, the orientation of the division is regulated according to the cellular environment so that the two daughter cells are exposed to different extrinsic factors determining their fates. (b) In intrinsic ACD, alignment of the spindle with asymmetrically segregated intracellular determinants results in the daughter cells inheriting different determinants, conferring them different identities (Loyer & Januschke, 2020).

1.1.1. Asymmetric Cell Divisions in *Drosophila*

In *Drosophila,* mechanisms of asymmetric cell divisions are most studied in neuroblasts, the precursors of the central nervous system, and in sensory organ precursor (SOP) cells, the found cells of external sensory organs of the peripheral nervous system (Hawkins & Garriga, 1996). These asymmetric cell divisions share the use of *Drosophila* orthologs of PAR-3, PAR-6, and atypical protein kinase C (aPKC) to establish polarity (Fig. 1-2).

After three rounds of asymmetric cell division in the *Drosophila* peripheral nervous system the SOP precursor gives rise to four cells of an external sense organ. These are the two “inner support cells” the neuron and its sheath cell, and two “outer

support cells" that form the hair and socket (Rhyu et al., 1994). The first division generates the anterior pIIa and posterior pIIb cells. In the second, the pIIb cell divides, giving rise to an apical pIIIb cell and an apoptotic basal glia cell. In the third, pIIa and pIIIb divide to form the two outer support and the two inner support cells of the organ. In loss of function mutants for the membrane associated Notch inhibiting protein Numb, the SOP divides symmetrically, generating two pIIa cells and therefore four outer support neurons (Rhyu et al., 1994). When Numb is overexpressed in the SOP and its daughter cells the opposite phenotype is observed, instead generating four inner support cells. Numb is therefore required as a cell fate determinant in all three asymmetric cell divisions of the SOP lineage (Rhyu et al., 1994) During asymmetric cell division in SOP cells, the Par-3/6/aPKC complex localizes to the posterior cell cortex, and Pins and Gαi are on the opposite anterior side, establishing an axis of polarity (Neumüller & Knoblich, 2009). aPKC regulates the phosphorylation of Numb. In all divisions of pI phosphorylated Numb is polarized to an anterior crescent and segregates to the anterior daughter cell where it can specify the cell fate through inhibition of the Notch/Delta pathway (Gho & Schweisguth, 1998)(Neumüller & Knoblich, 2009). This highlights both the use of intrinsic and extrinsic mechanisms to establish polarity and regulate asymmetric cell division.

In neuroblast divisions of the CNS, asymmetric cell division is controlled by apical and basal determinants. The apical determinants are PAR-3 PAR-6, aPKC. The basal determinants are Miranda, Brat and Prospero (Loyer & Januschke, 2020). Prior to division the PAR proteins are dispersed uniformly at the cortex. During division aPKC forms a complex with PAR-3 and PAR-6 at the apical side, leading to both phosphorylation of PAR-6 and activation of aPKC. aPKC then leaves this complex to phosphorylate Numb causing the activation of Notch signalling and inducing stemness of the apical daughter. PAR-3 also localizes the cytoskeletal adaptor protein Inscuetable to the apical cortex where it forms a complex with Pins/Gαi/Mud and microtubule proteins, establishing the mitotic spindle on the apical basal axis (Loyer & Januschke, 2020) (Chao et al., 2024). On the basal cortex, degradation of the adapter protein Miranda releases the transcription factor Prospero and the translational repressor of proliferation Brat (Gallaud et al., 2017). This promotes cellular differentiation in the basal daughter (Chao et al., 2024).

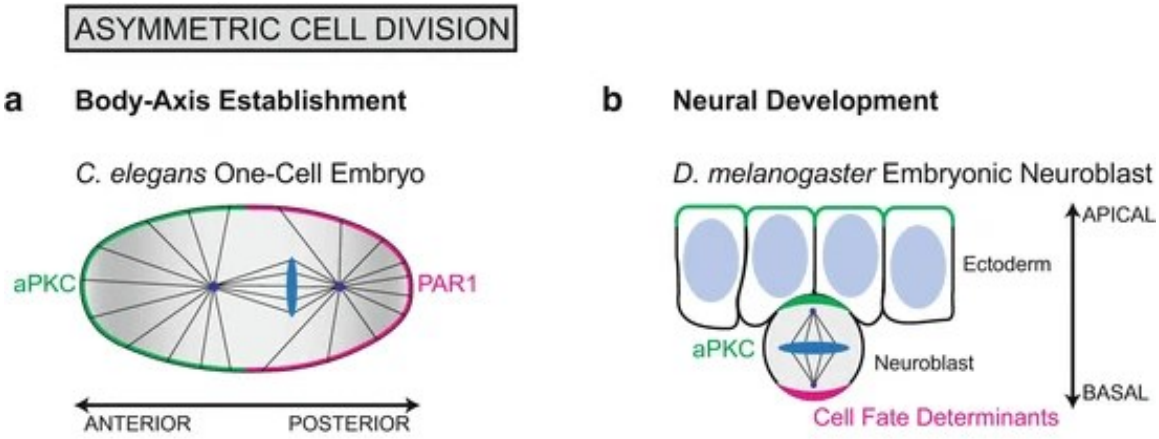

Figure 1-2 Function of the aPKC-PAR complex in various cellular contexts. Localization of the aPKC-PAR complex during asymmetric cell division in the *C. elegans* one-cell embryo (**a**) and *D. melanogaster* embryonic neuroblast (**b**) (Ohno et al., 2015)

1.1.2. Asymmetric Cell Divisions in *Caenorhabditis elegans*

C. elegans is a great model system to study asymmetric cell division as the entire cell lineage of the organism is known (Sulston & Horvitz, 1977) (Sulston et al., 1983).. There are 949 nongonadal cell divisions of which 807 are asymmetric. Furthermore, all 302 neurons arise from asymmetric divisions. In *C. elegans* the most studied ACD is the first cleavage of the single cell zygote (Horvitz & Herskowitz, 1992). The egg first divides asymmetrically to form two differently sized daughters with distinct fates that undergo different patterns of cell divisions, AB and P1. The AB cell divides symmetrically to produce daughter cells of equal size, Aba and ABp, the descendants of which contribute to the ectoderm. P1 is a stem cell that undergoes asymmetric cell divisions that produces daughter cells, EMS and P2, unequal in size and fate. EMS divides to produce a posterior daughter E, which gives rise to the intestine, and an anterior daughter MS, which primarily produces pharyngeal and body wall muscle (Horvitz & Herskowitz, 1992). In the single cell zygote ACD is not a single event but more accurately a series of consecutive events dependent on the distribution of PAR proteins to establish cell polarity. Symmetry is first disrupted at the pole after sperm entry and centrosome donation, denoting it the posterior pole. At this time the anterior PAR proteins, PAR-3, PAR-6, PKC-3, and CDC-42 and enriched at uniformly around the cortex (Pacquelet, 2017). Concurrently, the actin-myosin network in the cell cortex contracts from the site of

posterior end and stops around the center of the cell, initiating diffusive currents within the cell. These currents establish an asymmetric distribution of PAR proteins in the membrane. The anterior PAR proteins PAR-3, PAR-6, PKC-3, and CDC-42 localize to the anterior cell pole while the posterior PAR proteins PAR-1, PAR-2, LGL-1, and CHIN-1 localize to the posterior pole, with their polarization maintained through mutual antagonism (Reich et al., 2019). The PAR proteins then control other essential mechanisms of ACD including similar polarity events for cytoplasmic proteins and positioning of the mitotic spindle along the axis of polarity (Guo & Kemphues, 1996). This results in ACD around a cleavage plane producing two daughter cells AB and P1 which exhibit differences in gene expression, function, and size (Hawkins & Garriga, 1996). In *C. elegans* both Numb and the PAR complex are not known to be involved in asymmetric neuroblast division, therefore it is pertinent to investigate other proteins that may have a role in asymmetric cell division.

1.2. HAM-1

1.2.1. HAM-1 Regulates Asymmetric Neuroblast Division in the HSN/PHB Lineage

My overarching goal is to understand the mechanism by which the *C. elegans* gene *ham-1* (HSN abnormal migration) regulates asymmetric neuroblast division. *ham-1* was discovered in a screen for mutants with HSN migration defects (Desai et al., 1988), but the primary defect in *ham-1* mutants was a disruption of asymmetric division in the lineage that generates the hermaphrodite specific neuron (HSN). In wildtype animals, an HSN/PHB neuroblast divides asymmetrically to generate a smaller anterior daughter that undergoes cell death and a large posterior cell that divides to generate the HSN and PHB neurons (Fig. 1-3). In a *ham-1* mutant the asymmetric division is disrupted often resulting in a symmetric division and the transformation of the anterior daughter into a second posterior-like daughter thus leading to neuronal duplications (Guenther & Garriga, 1996). The daughter cell size asymmetry in these mutant divisions is also disrupted, leading to a larger anterior daughter cell and a smaller posterior daughter cell. A plausible interpretation of this phenotype is that the asymmetric division of the HSN/PHB neuroblast is intrinsically determined and that the distribution of developmental determinants to daughter cells is disturbed in *ham-1* animals. In this case HAM-1 may work to identify or restrict developmental determinants. Alternatively, if the

HSN/PHB division is extrinsically influenced by cell interactions, HAM-1 may be functioning in a cell signaling process that eventually determines sister cell fate. In a *ham-1 (gm279)* null background the duplication phenotype of the HSN and PHB is 24% and 33% respectively. This HSN duplication phenotype is incompletely penetrant but is over 95% in a *ced-3* mutant background. As *ced-3* is required for programmed cell death in the worm, this result means cell fate transformations in *ham-1* mutants are masked by apoptosis.

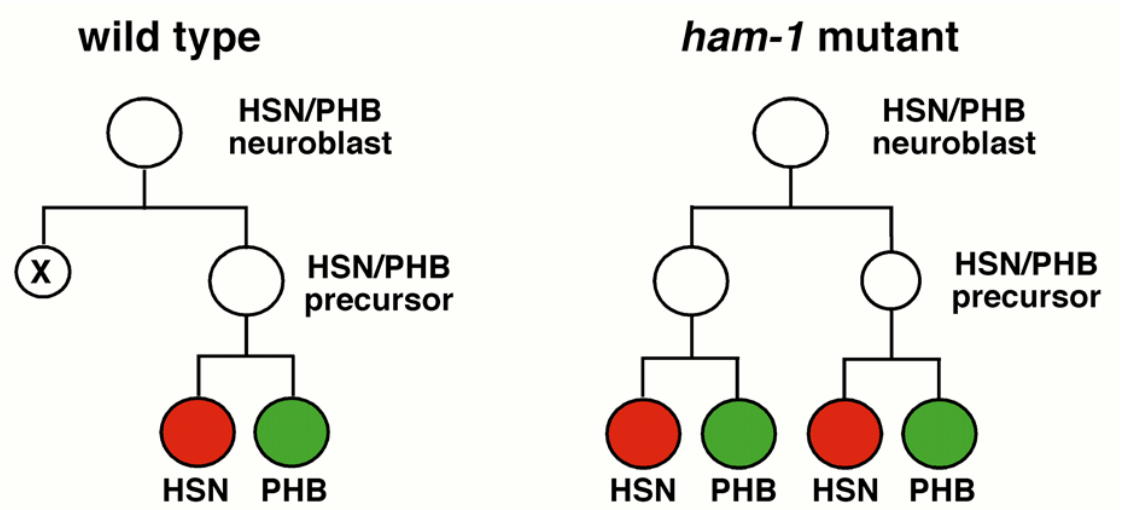

Figure 1-3. Divisions of the HSN/PHB Lineage

The HSN/PHB neuroblast undergoes asymmetric division to give rise to a smaller apoptotic anterior daughter and a larger posterior daughter, the HSN/PHB precursor. The HSN/PHB precursor then gives rise to two types of neurons, the HSN and the PHB.

1.2.2. HAM-1 is Required for Many Embryonic Asymmetric Cell Divisions

The HSN/PHB lineage is not the only asymmetrically dividing lineage affected by *ham-1* (Guenther & Garriga, 1996). HAM-1 is involved in a subset of asymmetric cell divisions during embryogenesis (Fig. 1-4) (Frank et al., 2005). Using GFP reporter constructs and antibodies, Frank et al., 2005 examined additional neuronal lineages that generate apoptotic daughters. Most of the lineages are bilaterally symmetric and are found to be affected by *ham-1* mutations by scoring the presence of extra neurons. All

eleven *ham-1* affected lineages were found produce at least one neuron and one apoptotic daughter and occur around the same time during embryogenesis, except for one lineage. The lineage that produces the dying aunt of the CEPso socket cell, was identified by an abnormally large cell death corpse. There were additional lineages examined but these were found to be unaffected by a *ham-1* mutation.

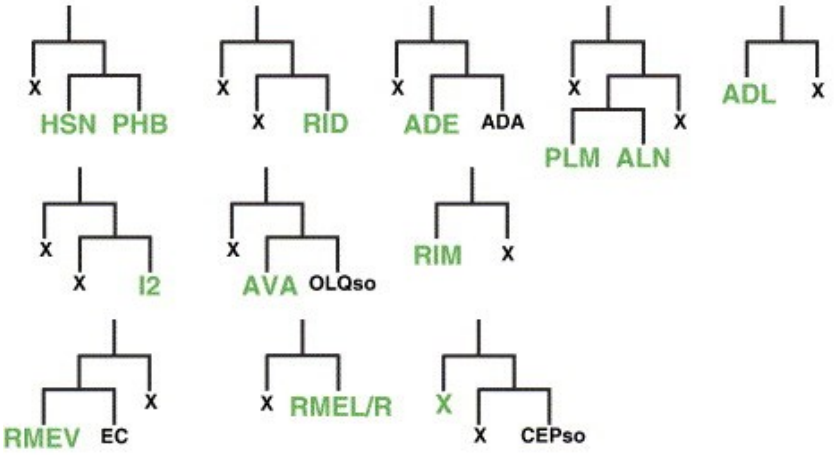

Figure 1-4. Lineages that require HAM-1 Function.
Lineages examined using GFP reporter constructs and antibodies found to be affected by a *ham-1* mutation. Adapted from (Frank et al., 2005).

ham-1 causes neuronal losses in the embryonic ALN/PLM Lineage

A more in-depth phenotypic analysis has been undertaken for the lineage that generates the ALN sensory neuron and the PLM mechanosensory neuron. In the wildtype division there are three asymmetric divisions (Sulston et al., 1983). The first division occurs at 295 minutes of embryogenesis where the neuroblast divides to produce an apoptotic anterior daughter and a posterior neuroblast. Next at 395 minutes the posterior neuroblast then divides asymmetrically producing the anterior PLM/ALN precursor and a posterior apoptotic cell. The PLM/ALN precursor then divides to generate the PLM and ALN neurons (Fig. 1-5). In a *ham-1* null mutant there is an 81% penetrant loss of the PLM neurons. The ALN neuron is also lost at a comparable frequency. By lineage analysis the asymmetric division defect is hypothesized to occur at 395 during the second division, as the first division is unaffected in *ham-1* null mutants (Leung et al., 2016). The defect may be transforming the anterior daughter into an

apoptotic posterior daughter, leading to the loss of the PLM and ALN neurons. It was found that this neuronal loss is suppressed by a mutation in *ced-4*, a homolog of the cell death gene APF-1 required for all 131 programmed cell deaths in the worm. This indicates that HAM-1 is not required for PLM cell fate and instead it is more likely an asymmetric cell division defect in the lineage (Leung et al., 2016).

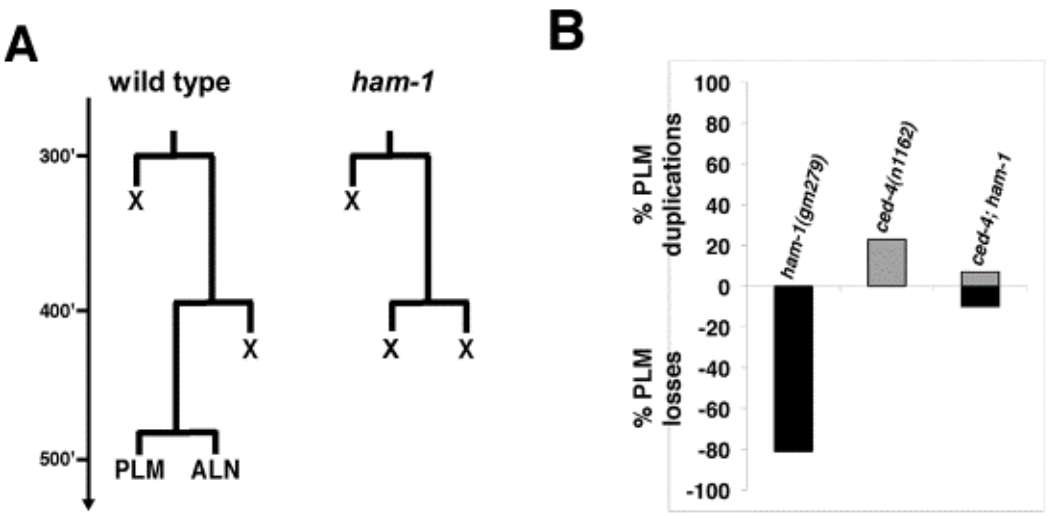

Figure 1-5. HAM-1 is a negative regulator of cell death in the PLM/ALN Lineage
(A) Wildtype division of the cell lineage generating the PLM and ALN neurons is possibly affected around the 400 min mark in a *ham-1* mutant causing a defect in the second asymmetric division causing loss of the PLM and ALN neurons. (B) A *ham-1(gm279)* mutant has an 81% penetrant PLM loss defect that is rescued by a mutation in the cell death gene *ced-4(n1162).* Adapted from (Leung et al., 2016).

ham-1 causes neuronal duplications and loss of size asymmetry in the larval Q Neuroblast Lineage

Loss of *ham*-1 function has also been shown to affect asymmetric division post-embryonically in the division of the Q neuroblasts. In wildtype worms, the pair of bilateral Q neuroblasts on the left side (QL) and right side (QR) undergoes three rounds of asymmetrical cell divisions during L1 larva development. This generates two apoptotic daughters, the A/PQR oxygen sensory neurons, A/PVM mechanosensory neurons, and SDQL/R interneurons (Sulston & Horvitz, 1977). The first division generates two cells,

Q.a.and Q.p. Q.a divides once producing a small anterior apoptotic daughter and a large posterior daughter, the A/PQR neuron. Q.p divides twice to generate a large anterior daughter, the A/PVM and SDQL/R precursor, and a small posterior apoptotic daughter (Fig 1-6). In *ham-1* mutants there is a duplication of the A/PQR neurons, the daughters of the Q.a division. No defects are observed for the A/PVM or SDQL/R neurons, indicating the specificity of HAM-1 for the anterior Q division. During Q.a cell division the mitotic spindle is positioned in the center of the cell while myosin II (NMY-2) is asymmetrically polarized to the anterior cortex making it tense and stiffer. This asymmetric tension at the anterior cortex and along with other cortical proteins is thought to generate a stiff and inward-contracting anterior pole, capable of pushing cytoplasm toward the relaxed posterior pole leading to its expansion. This would generate a smaller anterior daughter and a large posterior daughter after division. During Q.p cell division, the spindle is displaced posteriorly, and myosin II is depleted at both poles during telophase, leading to a larger anterior daughter and a smaller posterior daughter (Ou et al., 2010). It appears that HAM-1 is responsible for the regulation of spindle positioning and myosin polarization in the Q.a neuroblast, causing the duplication of the A/PQR neurons (Feng et al., 2013a). In *ham-1* mutants the Q.a division phenotype is slightly varied. In some Q.a cells the mitotic spindle is positioned normally in the center and myosin II is not asymmetrically distributed. Other Q.a cells had the mitotic spindle posteriorly displaced and symmetrically localized myosin II. This would cause the development of equal sized daughter cells that have the same fate. This phenotype parallels that of the *ham-1* mutant HSN/PHB division where instead of generating a small anterior apoptotic daughter and a large posterior HSN/PHB precursor, we see the division appear more symmetric. The anterior daughter survives and is equal to or slightly larger than the posterior daughter and assumes the same fate of the posterior HSN/PHB precursor. This also leads to a duplication of the terminal HSN and PHB neurons (Frank et al., 2005).

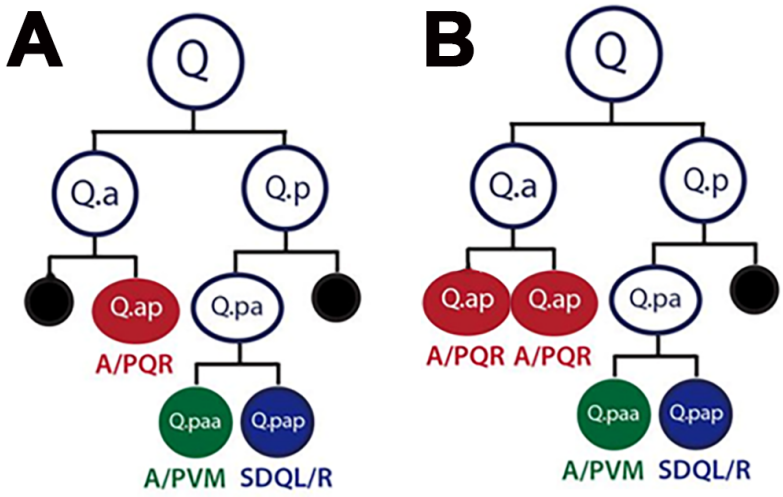

Figure 1-6. Divisions of the Q Neuroblast

(A) Both Q neuroblasts undergo an identical pattern of symmetric and asymmetric cell divisions generating two cells that undergo apoptosis (Q.aa and Q.pp) and three cells that after completing their migration differentiate into specific sensory neurons and interneurons (B) In *ham-1* mutants there is a duplication of the A/PQR neurons, the daughters of the Q.a division. No defects are observed for the A/PVM or SDQL/R neurons. Adapted from (Feng et al. 2013).

1.2.3. HAM-1 Encodes a Putative Transcription Factor

HAM-1 is a small 414 amino acid protein. The N-terminus of the protein contains a winged helix DNA binding domain, and the C-terminus two nuclear localization sequences (NLS) that function redundantly (Leung et al., 2016). HAM-1 shows 33% sequence similarity to Storkhead box 1 (STOX1), a human transcription factor, and 31% to Knockout in *Drosophila* (Fig 1-7). Knockout is a target gene of the transcription factor Kruppel. Kruppel is a zinc finger-type transcription factor known to act as both a concentration dependent repressor and activator of transcription (Hartmann et al., 1997). Knockout is first expressed during gastrulation in various tissues. In muscle precursor cells maintenance of Knockout expression requires the expression of Kruppel. Knockout's activity was determined to be required for motor innervation patterning in a subset of muscle cells (Hartmann et al., 1997). STOX1 is a transcription factor and has been implicated in early onset pre-eclampsia, a complication with pregnancy causing high blood pressure (van Dijk et al., 2010). STOX1 has also been implicated in late

onset Alzheimer's, where its expression correlates with the severity of the disease (Van Dijk et al., 2010). STOX1 encodes a winged helix DNA binding protein and is related to the Forkhead (FOX) family. The FOX gene family contains nuclear localization and nuclear export signals that permit nuclear-cytoplasmic shutting of FOX proteins. Accordingly, an isoform of STOX1 has been seen in both the cytoplasm and the nucleus of brain and placenta cells (van Dijk et al., 2010). The only known human paralogue of STOX1 is Storkhead box 2 (STOX2) (van Dijk et al., 2005). Like STOX1, STOX2 has been found to be associated with pre-eclampsia (Fenstad et al., 2010). It also has a role in oral squamous cell carcinoma progression (Sasahira et al., 2016). The structure and sequence similarities of HAM-1 allude to its putative function in asymmetric division as a transcription factor in the nucleus (Leung et al., 2016).

Figure 1-7. Alignment of the N-terminus of HAM-1 with *Drosophila* Knockout and human STOX-1.
The winged helix domain is indicated with a black line above the corresponding sequence (Leung et al., 2016).

1.2.4. HAM-1 Localizes to the Cell Cortex and the Nucleus

To further elucidate the mechanism of *ham-1* function both HAM-1 specific antibodies and expression of a GFP::HAM-1 transgene were used to determine subcellular localization. Immunofluorescence using anti-HAM-1 antibodies in wild type embryos revealed HAM-1 to be localized specifically to the cell cortex (Fig. 1-8). HAM-1 is first detectable around the cell cortex in non-dividing cells and seen asymmetric at the posterior cell cortex in dividing cells (Frank et al., 2005). HAM-1 was not detected in the nucleus, however suspecting that this could be due to epitope masking by an inability to penetrate the nuclear envelope, further studies were performed. A subcellular nuclear-cytoplasmic fractionation experiment and western blot analysis confirmed endogenous

HAM-1 to be predominantly in the nucleus (Leung et al., 2016). Analysis of transgenic embryos expressing an N-terminus GFP::HAM-1 fusion protein driven by the UNC-119 promoter revealed a broader distribution of the protein. UNC-119 expression begins at the 60-cell stage of embryogenesis and is broadly expressed throughout the nervous system and head (Maduro, 2015). Expression of GFP::HAM-1 was observed at the cell cortex, however unlike the antibody staining of HAM-1 there was strong expression in cell nuclei (Fig. 1-9). This information suggests that endogenous HAM-1 may have a function in the nucleus during asymmetric divisions in *C. elegans* embryogenesis (Leung et al., 2016). In the Q cell lineage time-lapse imaging analysis has showed that a c-terminal GFP-tagged HAM-1 protein under the control of the *ham-1* promoter (P*ham-1::ham-1::gfp)* was restricted to interphase nuclei and was evenly distributed in the cytoplasm of dividing Q.a and Q.p cell (Feng et al., 2013).

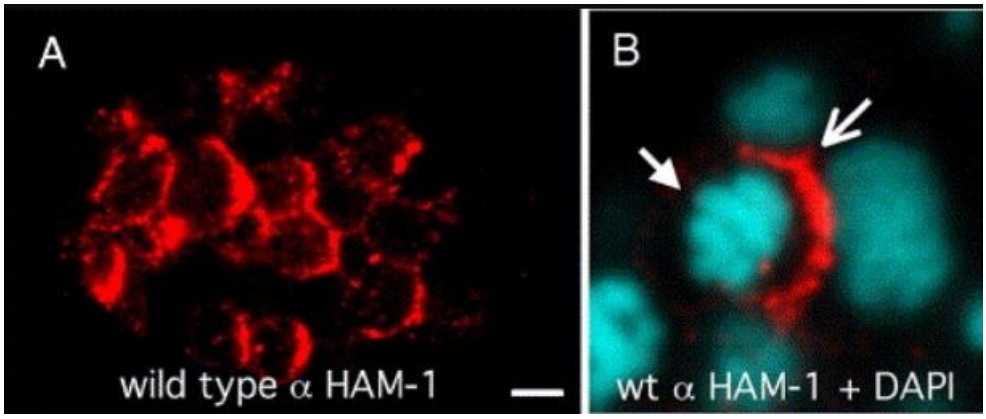

Figure 1-8. Antibody Staining reveals HAM-1 localization at cell cortex in WT embryos

(A) HAM-1 expression in a wild-type embryo. Scale bar, 5 μm. (B) When HAM-1 (open arrow) is asymmetric, chromosomes (closed arrow) appear condensed, indicating that cells are mitotic (Frank et al., 2005).

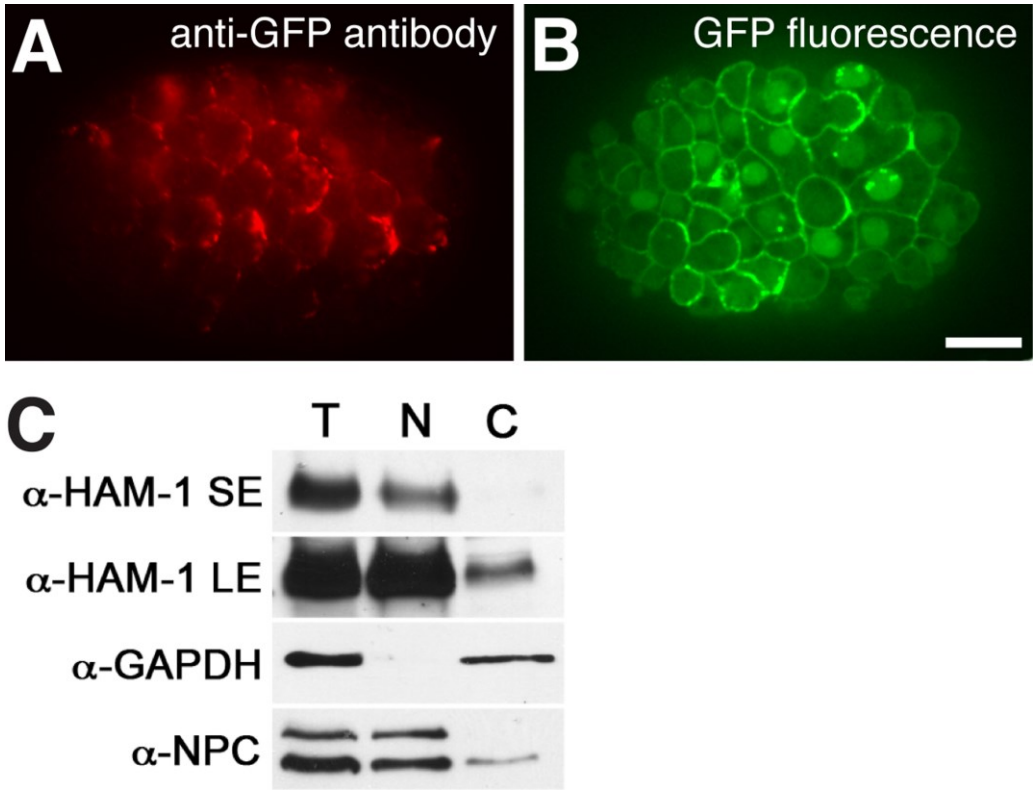

Figure 1-9. GFP::HAM-1 localizes to both the cell periphery and in the nucleus. (A) A transgenic embryo expressing GFP::HAM-1 stained with anti-GFP antibodies. (B) A transgenic embryo expressing GFP::HAM-1 examined directly for GFP fluorescence. (C) Western blot analysis of total (T), nuclear (N) and cytoplasmic fractions from embryos with antibodies against GAPDH (a cytosolic marker), a nuclear pore complex (NPC) protein (nuclear marker) or HAM-1. In a short exposure (SE) for HAM-1, HAM-1 is only seen in the nuclear fraction. Upon a longer exposure (LE), cytosolic HAM-1 is also detected. Scale bar 10 μm. (Leung et al., 2016)

1.2.5. Regions of HAM-1 required for Function and Localization

Sequences required for function and localization were identified by creating a series of N- and C- terminal deletions in the GFP::HAM-1 fusion protein (Leung et al., 2016). Function was assessed by the ability to rescue the *ham-1 (*gm279) PLM neuronal defects. Truncations of HAM-1 from either C-terminus or N-terminus abolished ability to rescue loss of PLM neurons in *ham-1*(*gm279*). Specifically, the N-terminal 31 amino acids and the C-terminal 50 amino acids were determined to be essential for function. These C-terminus or N-terminus deletions also decrease membrane localization of

GFP::HAM-1. The study revealed that the N-terminus is required for cortical membrane association and the C-terminus of the protein confer nuclear localization. Using bioinformatics two nuclear localization sequences (NLS) were found in the C-terminal region (Fig. 1-10A). Mutation of each NLS on their own had little effect on nuclear localization and function. Mutation of both eliminated nuclear localization of GFP::HAM-1 and functional rescue was determined to be unaffected due to low levels of protein still in the nucleus. Therefore, the two NLSs are functionally redundant and required for nuclear localization. This bioinformatics analysis also predicted polyproline rich SH3 binding motifs within the region required for cortical association and was found to be essential but not sufficient for cortical localization. Eight *ham-1* mutants with known phenotypes in other lineages were examined for their effects on HAM-1 localization and PLM defects (Fig. 1-10B). Every mutant that reduced membrane localization had almost no defects in the PLM lineage. Only *ham-1(gm214),* a small deletion in the C terminus, had unaffected HAM-1 localization and highly penetrant PLM loss defects. Therefore, in the PLM lineage it appears HAM-1 cortical localization is not necessary for function.

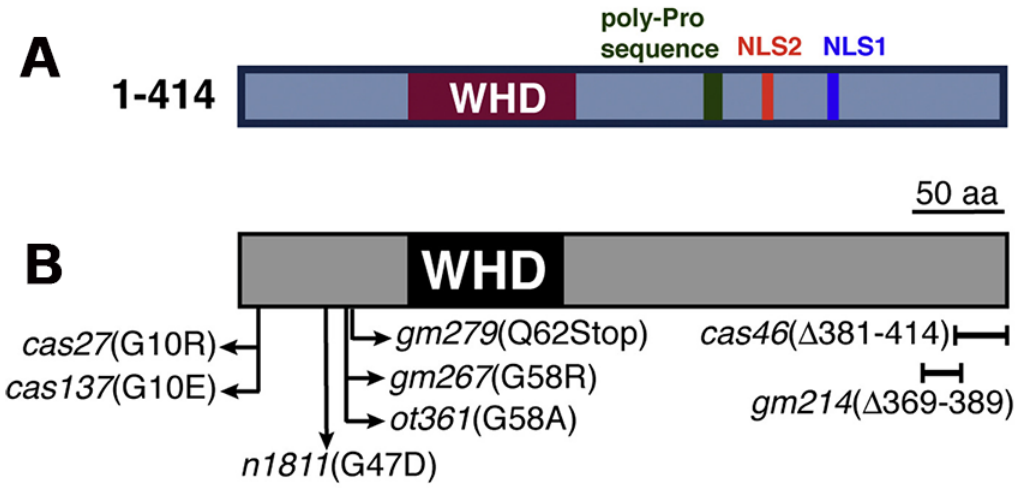

Figure 1-10. Schematic representations of the HAM-1 protein

(A) HAM-1 protein with poly-pro sequence, nuclear localization signal (NLS) 1 and 2. (B) HAM-1 protein with the position of mutant alleles and corresponding amino acid changes indicated. Only the null allele, *ham-1(gm279)* as well as *ham-1(gm214),* an in-frame 21 amino acid deletion near the C-terminus, display penetrant defects in the PLM lineage as assayed using the MEC-4::GFP reporter *zdIs5.* (Leung et al., 2016)

1.2.6. HAM-1 is a Transcriptional Regulator of PIG-1

Through a combination of live cell imaging and genetic analysis HAM-1 was found to be a transcriptional regulator of the PAR-1-like kinase PIG-1 (Cordes et al., 2006)(Feng et al., 2013). *pig-1* is the worm ortholog of MELK, a conserved member of the polarity-regulating family of AMPK-related serine/threonine kinases. PIG-1 was first identified as having asymmetric neuroblast division defects in HSN/PHB lineage. Physiologically, PIG-1 has been shown to control cell size asymmetry and neuroblast daughter cell fate in some neuroblast lineages (Fig 1-17). Notably, it was also found to be acting cell autonomously in affected lineages and is thought to regulate ACD by controlling polarity (Cordes et al., 2006). It was seen that the inhibition of *pig-1* phenocopied the *ham-1* extra neuron phenotype in the Q.a cell (Cordes et al., 2006) and that myosin polarization during Q.a cytokinesis was also disrupted in *pig-1* mutants (Ou et al., 2010). Expression using a *pig-1::gfp* translational fusion to the upstream region of *pig-1 (*Ppig-*1::pig-1::gfp)* found that *pig-1::gfp* is present throughout the cytoplasm and excluded from the nucleus in all embryonic cells. Using cell specific GFP reporters six lineages were found to produce extra neurons in *pig-1* mutants: the HSN/PHB, I2, M4 and PLM/ALN precursors which divide during embryogenesis, and the Q.a and Q.p precursors which divide during the first larval stage (Cordes et al., 2006). Synergistic interactions between mutations in *pig-1* and the cell death gene *ced-3* were also observed in four of the lineages: HSN/PHB, Q.p, I2 and PLM/ALN. In each lineage the *pig-1 ced-3* double mutants had a dramatically stronger duplication phenotype than either single mutant and exceeded the expectations from the additive effects. Furthermore, mutations in *pig-1* were reported to be epistatic to mutations in *ham-1* in the HSN/PHB and PLM lineages. Where it was seen that a mutation in *pig-1* was masking the phenotypic effect of a the *ham-1* mutation. Mutations in both *pig-1* and *ham-1* disrupt the cell size asymmetry of the HSN/PHB neuroblast daughters. Strong *ham-1* mutations reverse the relative sizes of the daughters (Frank et al., 2005), while mutants for *pig-1* and *pig-1 ham-1* double mutants cause the neuroblast to divide more symmetrically (Cordes et al., 2006). These results suggest *ham-1* is a negative regulator of *pig-1.*

By using chromatin immunoprecipitation coupled with high-throughput DNA sequencing (CHIP-seq) HAM-1 was found to bind to the promoter region of the *pig-1* gene. To study the significance of the HAM-1 binding site in the *pig-1* promoter, the

binding sire was deleted from a functional P*pig-1::pig-1::gfp* plasmid. This completely abolished *pig-1::gfp* expression in the Q.a cell (Feng et al., 2013). An expression study of P*pig-1::pig-1::gfp* was performed in WT and *ham-1* mutants. The PIG-1::GFP fluorescence was visible in all the WT Q.a cells, but was significantly reduced in *ham-1* mutants (Feng et al., 2013). This result is opposite to that seen previously, where now HAM-1 is a positive regulator of *pig-1* expression during Q.a cell asymmetric division through the binding site in the *pig-1* promoter region.

1.2.7. Hypothesized Models of HAM-1 Function

It is evident HAM-1 has a role in the asymmetric division of many neuronal lineages that produce apoptotic cells (Frank et al., 2005). The mechanism by which HAM-1 regulates ACDs in these lineages is still unknown. In *ham-1* mutants, the HSN/PHB, PLM and Q cell lineages all share anterior-posterior cell fate transformations. In the HSN/PHB and Q.a lineages a *ham-1* mutation causes neuronal duplications indicating the transformation of normally apoptotic daughter cells to their wildtype sister cells. However, in the PLM/ALN lineage *ham-1* mutations lead to losses of the terminal neurons, indicating a transformation to the apoptotic cell fate. The role of HAM-1 has been suspected of being a cell fate determinant, however this is unlikely. In the HSN/PHB precursor HAM-1 is asymmetrically localized to posterior cortex during division, indicating it is likely inherited in the posterior daughter cell (Guenther & Garriga, 1996). However, it is the anterior apoptotic daughter cell whose fate may be transformed to that of its sister. In the PLM lineage double mutants with the cell death gene *ced-4* in suppresses the neuronal loss phenotype of *ham-1* mutants. This indicates that *ham-1* is not required to specify PLM neuron fate and may instead function to inhibit cell death (Leung et al., 2016). The leading models of HAM-1 function suggest it may function as something other than a cell fate determinant.

HAM-1 could act as a Tether of Cell Fate Determinants

In wild-type animals, the HSN/PHB neuroblast is polarized along the AP axis, with an anteriorly displaced cleavage plane and posteriorly localized determinants of neural precursor fate (Fig. 1-11) (Cordes et al., 2006). In 1996, Guenther and Garriga suggested that HAM-1 restricts cell fate determinants to the posterior periphery of the dividing HSN/PHB neuroblast to ensure that only the posterior daughter cell adopts the

specified fate. In this model, a wildtype neuroblast divides to produce a smaller anterior apoptotic daughter that inherits no determinants, and a larger posterior daughter that inherits the determinants, which becomes a neural precursor. In the absence of HAM-1, the cell fate determinants would distribute equally to both daughter cells causing both cells to adopt the HSN/PHB precursor fate (Guenther & Garriga, 1996). This model could support the phenotypes seen in the HSN/PHB lineage of *pig-1* mutants (Feng et al., 2013). Wherein neuroblasts of *pig-1* mutants a lack of proper polarization causing a symmetrically localized cleavage plane and equally distributed determinants. Both daughters would inherit an equal dose of determinants resulting in two cells of the same fate. In *ham-1* mutants, neuroblast polarity is partially inverted along the AP axis causing a posteriorly displaced cleavage plane and an anteriorly asymmetric distribution of cell fate determinants. Overall neuronal duplications would occur when a sufficient concentration of determinants enters both neuroblast daughters and neuronal losses would occur when the anterior daughter undergoes apoptosis, and the posterior daughter receives an insufficient concentration of determinants to develop properly. This is supported by the larger cell death corpse seen in *ham-1* mutants (Guenther & Garriga, 1996)(Frank et al., 2005). However, this model was proposed before it was known that HAM-1 is localized to the nucleus, and that its nuclear localization is required for function.

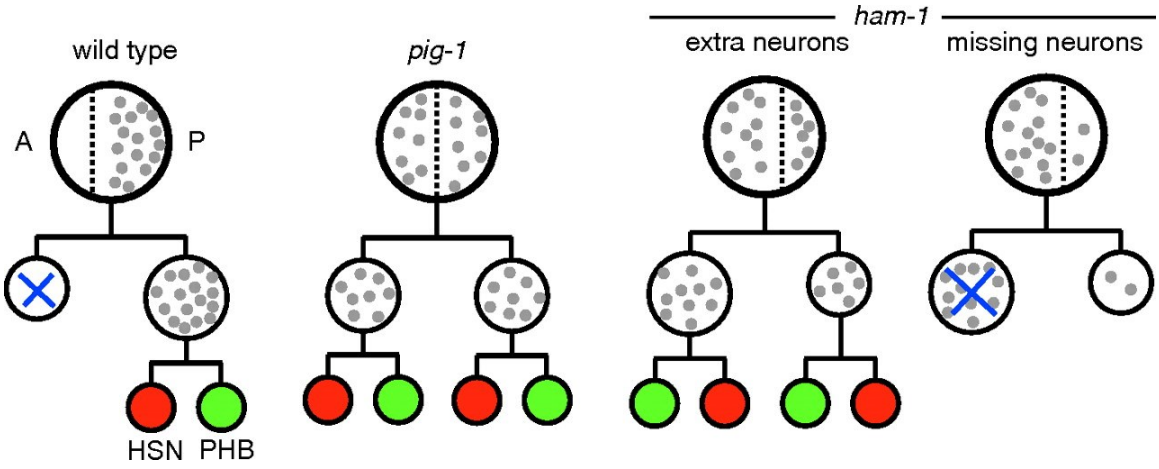

Figure 1-11 Modeling the HSN/PHB lineage in *pig-1* and *ham-1* mutants.
In wild-type animals, the HSN/PHB neuroblast is polarized along the AP axis, with an anteriorly displaced cleavage plane (vertical dotted line) and posteriorly localized determinants of neural precursor fate (gray circles). (Cordes et al., 2006)

HAM-1 Polarization Affects Cleavage Plane Positioning

Another early hypothesis proposed HAM-1 may localize to posterior pole in the HSN/PHB precursor neuroblast to restrict the position of the mitotic spindle to the anterior of the cell, along with the cleavage plane (Fig. 1-12) (Frank et al., 2005). This asymmetric spindle position would cause anterior positioning of the cleavage plane, generating a smaller anterior daughter and a larger posterior daughter. The reversal of the HSN/PHB neuroblast cleavage plane in *ham-1* mutants, and the generation of the larger cell death corpse, suggests that there could be a mechanism that antagonizes the activity of HAM-1. In the absence of HAM-1, this second activity pushes the spindle to the posterior of the neuroblast.

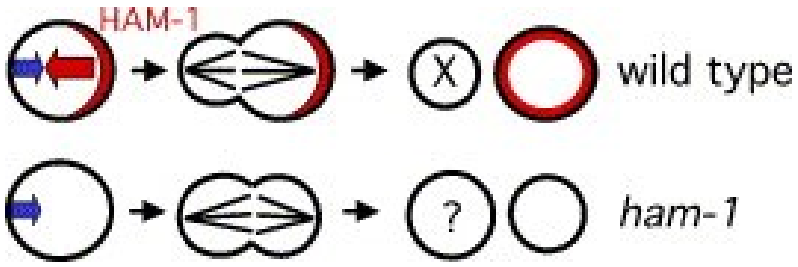

Figure 1-12. Mitotic Spindle Positioning Model for the role of HAM-1 in neuroblast division.

HAM-1 (red) restricts the spindle to the anterior part of the cell (red arrow), leading to an anterior bias of the cleavage plane. In *ham-1* mutants, an opposing activity (blue) of unknown origin overcomes the absence of HAM-1, leading to a posterior bias of the cleavage plane. As a result, the anterior daughter is much larger than normal and often fails to express its normal cell death fate (? instead of X). (Frank et al., 2005)

This model doesn't quite explain the phenotypes identified in the Q lineage in *ham-1* mutants. Time-lapse imaging of the Q.a and Q.p divisions previously revealed spindle-independent and myosin II (NMY-2) dependent mechanisms to generate daughter cell size asymmetry. The Q.a neuroblast divides by a spindle-independent, NMY-2 dependent mechanism to establish the generation of a small Q.aa and a large Q.ap (Ou et al., 2010).In *ham-1* mutants, 62% of QR.a properly positioned their spindles, but myosin was evenly distributed in the contractile ring, producing two equal daughter

cells; for the remaining 38% of QR.a, the spindle was shifted towards the posterior and myosin symmetrically distributed, producing a large QR.aa and a small QR.ap. By contrast, the Q.p neuroblast divides by a spindle-dependent, myosin independent mechanism producing a larger anterior daughter and smaller apoptotic posterior daughter, and *ham-1* is required for the Q.p division. Therefore, another possibility is that HAM-1 regulates cleavage plane positioning in spindle-independent, myosin-dependent asymmetric divisions.

All models so far rely on the polarization of HAM-1 during asymmetric cell division. So, another question at hand is: what is the mechanism by which HAM-1 becomes polarized? Furthermore, are there independent roles for HAM-1 localized to the cell cortex as opposed to HAM-1 localized in the nucleus? Could the cortical localization of HAM-1 be a mechanism to control its own inheritance? In *C. elegans* the Wnt pathway specifies the fate of posterior daughter cells in many cell divisions, raising the interesting possibility that Wnt genes might have a function in regulating *ham-1* cell fates and organizing daughter cell size asymmetry along the AP axis.

1.3. Wnt Signalling

Wnt signalling is an evolutionarily conserved extracellular signalling pathway required for cellular communication during organism development. Wnt signals guide many cues in development including cell proliferation, fate specification, polarity, and migration (Polakis, 2000). Wnts are a large family of secreted, cysteine-rich secreted glycoproteins that regulate several intra-cellular signal transduction cascades. The name Wnt comes from the fusion of the *Drosophila* segment polarity gene *wingless* (*wg*) and original vertebrate homolog, *integrated* (*int-1*) (Wodarz & Nusse, 1998). The study of the Wnt pathway is significant as it affects the maintenance and metastasis of cancer stem cells (Zhan et al., 2017). Research in vertebrates and invertebrates like *Drosophila melanogaster* has shown there are two distinct major signaling cascades downstream of the Fz receptor, a canonical or Wnt/β-catenin dependent pathway and the non-canonical or β-catenin-independent pathway (Komiya & Habas, 2008).

1.3.1. Canonical Wnt Signalling Pathway

Wnt proteins initiate the canonical (β-catenin-regulated) signaling cascade by binding to seven-transmembrane spanning receptors of the Frizzled (Fzd) family together with the coreceptors LRP5 and -6, members of the low-density lipoprotein receptor-related protein family (LRP) (Fig. 1-13) (Komiya & Habas, 2008). The major effector molecule of the canonical Wnt signalling pathway is β-catenin. During an absence of a Wnt ligand, cytoplasmic B-catenin interacts with the destruction complex, consisting of Casein Kinase 1 (CKIα), Glycogen Synthase Kinase 3-B (GSK3β,) Adenomatous Polyposis Coli (APC) and Axin. In this complex, Axin binds β-catenin, acting as a scaffold for the other components of the destruction complex. APC assists in the stabilization of β-catenin such that the kinases CK1 and GSK3-B can phosphorylate β-catenin, making it a target for ubiquitination and therefore degradation by a proteosome. This ultimately leads the Wnt responsive genes remaining inactive (Wodarz & Nusse, 1998). Upon binding of a Wnt ligand the Fzd forms a heterodimeric co-receptor complex with LRP5/6. This recruits the scaffolding phosphoprotein Dishevelled (Dsh/DVL) to the membrane where it binds to the cytoplasmic domain of Fzd. This signals phosphorylation of the cytoplasmic domain of LRP5/6 by CK1 and GSK3-B, recruiting Axin to the membrane causing the inactivation of the destruction complex (Wodarz & Nusse, 1998). This leads to the stabilization of β-catenin in the cytoplasm, allowing for its translocation to the nucleus where it functions as a transcriptional co-activator with the TCF family transcription factors. β-catenin binding to a TCF protein provides a transcription activation domain such that Wnt responsive genes are activated.

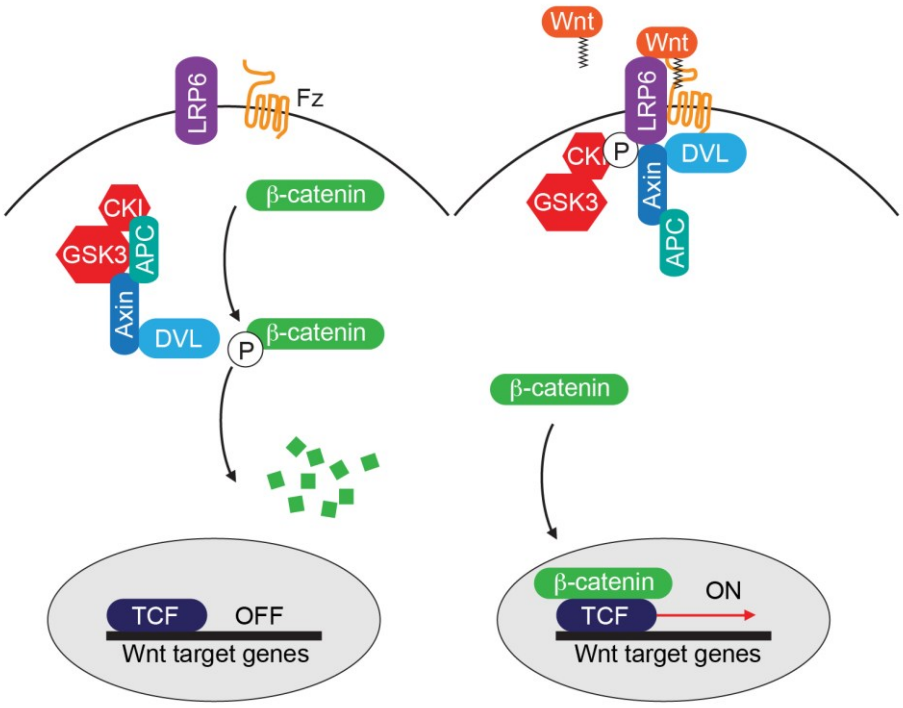

Figure 1-13. Canonical Wnt Signaling Pathway

A schematic representation of the canonical Wnt signal transduction cascade. Left, in the absence of Wnt ligand, the complex of Axin, APC, GSK3-β, CK1 and β-catenin is in the cytosol. β-catenin is phosphorylated by CK1 and GSK3-β and targeted for degradation. Right, with Wnt stimulation, signaling through the Fz receptor and LRP5/6 co-receptor complex induces DVL recruitment to the membrane. DVL binds to Fz and Axin leading to the phosphorylation of LRP6 by CK1 and GSK3-β. This complex causes the stabilization of β-catenin allowing it to translocate into the nucleus where it complexes with Lef/Tcf family members to mediate transcriptional induction of target genes. Adapted from (Sawa and Korswagen, 2013).

1.3.2. Non-canonical Wnt Signalling Pathways

Non-canonical Wnt signalling pathways in *Drosophila* and vertebrates are characterized by β-catenin independent signalling, and regulate processes in vertebrate gastrulation, the polarity of bristle, hair and ommatidia in *Drosophila* (Polakis, 2000). The non-canonical Wnt signalling pathways include the Wnt/Planar Cell Polarity (PCP) Pathway, the Wnt/Ca^{2+} Pathway, and the Ror and Ryk dependent pathways.

In *Drosophila* the Wnt/Planar Cell Polarity (PCP) Pathway controls the polarity of cells in alignment with the plane of the epithelial sheet and establishes the orientation of bristles and hairs (Maung & Jenny, 2011). The key feature of this pathway is the asymmetric distribution of the transmembrane signalling components to specific cell compartments of a patterned tissue. This directs the orientation of cell behaviours by influencing cytoskeletal structures and cell adhesions (Butler & Wallingford, 2017).This pathway is controlled by a conserved set of proteins called the PCP genes, that are responsible for coordinating development signalling cues with individual cell behaviors (Wallingford, 2012). This pathway is well characterized during *Drosophila* wing blade development and where it is dependent on the asymmetric localization of the transmembrane proteins Frizzled (Fz), transmembrane proteins Van Gogh (Vang), Flamingo (Fmi) and the cytoplasmic proteins Dishevelled (Dsh), Prickle (Pk) and Diego (Dgo). Initially these components are symmetric but a gradient of Wnts disturbs the plane of organization, leading to the asymmetric accumulations of Fz, Dsh, and Dgo opposite to Vang, and Pk. This controls the positioning and orientation of an actin-based trichome in each cell of the wing epithelium (Butler & Wallingford, 2017).

The Wnt/Ca^{2+} pathway emerged from finding that some Wnts and Fz receptors can stimulate intracellular Ca^{2+} release from ER activate and calcineurin and the kinases calcium/calmodulin-dependent kinase II (CAMKII) and protein kinase C (PKC) in a G-protein dependent manner (Kühl et al., 2000). The Wnt/Ca^{2+} pathway is seen to control dorsoventral axis formation during gastrulation in *Xenopus* (Komiya & Habas, 2008) (Wallingford et al., 2001). In *Xenopus* a ventral signal is established by Wnt5a activation of CaMKII and calcineurin. Activation of calcineurin dephosphorylates its target transcription factor NFAT, where it translocates from the cytosol to the nucleus. In the nucleus NFAT target gene expression inhibits the dorsalizing signal of the canonical Wnt pathway by suppression of the GSK3-β-catenin-degradation complex (Saneyoshi et al., 2002).

Both Receptor tyrosine kinase-like orphan receptor (Ror) and the receptor tyrosine kinase Ryk contain a Wnt binding domain and play important roles in Wnt signaling. Binding of Wnt to Ror can trigger many responses including inhibition of the canonical Wnt signalling pathway, and the stimulation of cell motility (Green et al., 2008). Active WNT/ROR signalling is linked to drivers of tumor development and progression, making them an important interest in cancer research (Menck et al., 2021). Ryk-family

members are required for Wnt signaling in many contexts as well. In the *Drosophila* embryonic nervous system Ryk ortholog *drl* mutants display incorrect axonal guidance across the midline, where instead of crossing into the anterior commissure they crossover and project into the posterior commissure (Bonkowsky et al., 1999). This the same phenotype also observed in *Wnt5* mutants in *Drosophila* (Fradkin et al., 2004).

1.4. Wnt Signaling in *C. elegans*

In *C. elegans* the canonical Wnt pathway is evolutionarily conserved, where it uses the β-catenin BAR-1 to turn on transcription factors for Wnt responsive genes. Its main use is to guide polarization and migration of neurons along the anterior-posterior axis. Unique to *C. elegans* is the Wnt/β-catenin asymmetry pathway, a variation of the canonical Wnt pathway that controls asymmetric cell divisions in both embryonic and post embryonic stages.

1.4.1. Wnt Pathway Components in *C. elegans*

C. elegans has a complement of the canonical Wnt pathway components found in flies and vertebrates, and except for LRP6/Arrow, most of the components are conserved. The orthologs include five Wnt ligands and four Frizzled receptors, four β-catenin's, and one TCF. There are also clear orthologs of the noncanonical Wnt signalling pathway components, Vangl and Prickle of the PCP pathway, and the receptor tyrosine kinases Ror and Ryk. An overview of the Wnt pathway components and their *C. elegans* orthologs are summarized in Table 1-A. *C. elegans* also has a variation of the canonical Wnt/ β -catenin pathway, called the Wnt β-catenin asymmetry pathway dependent on the unique regulation of pathway components by polarization rather than the stabilization of β-catenin to activate Wnt target genes.

Table 1-1. Wnt Pathway Components

Adapted from (Jackson & Eisenmann, 2012)

Component	***C. elegans* Ortholog**	**Component**	***C. elegans* Ortholog**
Wnt Production and Secretion		**Wnt/β-Catenin Pathway Components**	
Porcupine	*mom-1*	CK1	*kin-19*
Wntless	*mig-14*	Dishevelled	*mig-5*
Retromer complex	*vps-26, vps-29, vps-35, snx-3*		*dsh-1*
Wnt Ligands			*dsh-2*
	mom-2	GSK3β	*gsk-3*
	lin-44	Axin	*pry-1*
	egl-20		*axl-1*
	cwn-1	APC	*apr-1*
	cwn-2	βTrcp	*lin-23*
Wnt Receptors		Nlk	*lit-1*
Frizzled	*mom-5*	Tak1	*mom-4*
	lin-17	Tab1	*tap-1*
	mig-1	β-catenin	*bar-1*
	cfz-2		*sys-1*
LRP6/Arrow	*?*		*wrm-1*
Ror	*cam-1*		*hmp-2*
Ryk	*lin-18*	TCF	*pop-1*
Secreted Wnt Inhibitors		Groucho	*unc-37*
Sfrp	*sfrp-1*	**PCP Pathway Components**	
		Vangl	*vang-1*
		Prkl	*prkl-1*
		Flamingo	*fmi-1*

1.4.2. Wnt/β-catenin (BAR-1) Signalling Pathway

Like vertebrates and *Drosophila,* the canonical Wnt signaling pathway in *C. elegans* is activated when a Wnt ligand binds a Frizzled receptor, which activates Disheveled, ultimately resulting in the accumulation of the B-catenin BAR-1. BAR-1 then translocates into the nucleus where it functions as a co-activator to the TCF ortholog

POP-1 mediate target gene activation. The Wnt/β-catenin (BAR-1) signalling pathway is required during larval development for Q neuroblast migration, P12 fate specification and the formation of rays from seam cells in the male tail. In each of these processes the main targets of the pathway are the Hox genes *lin-39, mab-5, and egl-5* (Korswagen et al., 2000). The Wnt/β-catenin signaling pathway also plays a role in vulval precursor cell (VPC) fate specification through the regulation of the Hox gene *lin-39* (Eisenmann et al., 1998)(Gleason et al., 2002). It was also found that mutants for *bar-1*(β-catenin) and *apr-1*(APC) had low *lin*-39(Hox) expression and caused the over-induction of VPCs to an 'F' cell fate within the pattern, which fuse with the neighbouring syncytium (Gleason et al., 2002). Finally, the axin *pry-1* was found to be a negative regulator of Wnt signalling in the VPCs, where hyperactivation of the Wnt pathway through loss-of-function *pry-1* mutants also lead to this over-induction to the "F' phenotype (Gleason et al., 2002).

1.4.3. Wnt/β-catenin Asymmetry Pathway

In *C. elegans* both embryonic and post embryonic asymmetric cells divisions are patterned by the Wnt/β-catenin asymmetry pathway, a variant of the canonical Wnt signaling pathway. This pathway functions in numerous asymmetric cell divisions such as the EMS blastomere, the T cell of the tail, the seam cells, Z1 and Z4 the somatic L1 gonad (Jackson & Eisenmann, 2012).The Wnt/Beta-catenin asymmetry pathway is uniquely characterized by the asymmetric distribution of pathway components in both mother cells and daughter cells. Prior to cell division, Frizzled and Dishevelled are located on the opposite side of the cell cortex to APR-1, PRY-1, LIT-1 and WRM-1. After cell division, these proteins are seen to be asymmetrically inherited by the daughter cells. In this pathway the activity of the transcription factor POP-1 is regulated through two beta-catenins, WRM-1 and SYS-1 (Lin et al., 1998)(Zacharias et al., 2015). In an un-signalled daughter cell nuclear SYS-1 levels are low, and conversely nuclear POP-1 levels are high. This leads to the inactivation of target gene transcription. In a signalled daughter cell, there are two downstream pathways that are activated. One pathway localizes SYS-1 to the nucleus, while the other uses the beta-catenin WRM-1 and the nemo-like kinase LIT-1 to phosphorylate POP-1, targeting it for nuclear export. This leads to high nuclear SYS-1 and low nuclear POP-1. SYS-1 and POP-1 then form a complex, leading to target gene activation (Jackson & Eisenmann, 2012).

1.4.4. Wnt Ligand Secretion

The C. elegans genome contains five genes encoding functionally redundant Wnt ligands, *lin-44, egl-20, mom-2, cwn-1,* and *cwn-2*. Wnts are lipid modified glycoproteins which require a dedicated pathway to be secreted from producing cells. Wnt proteins are known to be acylated, a conserved mechanism for control during extracellular transport. The murine Wnt-3a was found to be acylated with a palmitoleic acid at serine residue (Ser209), a modification determined to be required for secretion from the endoplasmic reticulum (Takada et al., 2006). In *Drosophila* the protein *porcupine (porc),* and in *C. elegans* its ortholog *mom-1*, encode ER bound acyltransferases that mediate this lipid modification of Wnts. The lipid modified Wnts are then transported from the Golgi to the cell surface for secretion by the Wnt sorting receptor *Wntless*/*mig-14*. After secretion *mig-14* is returned to the Golgi via endocytosis through a specialized retromer complex reliant on the sorting nexin *snx*-3 for retrograde transport (Tian et al., 2021).

1.4.5. Biological Roles and Phenotypes of Wnt Ligands

The Wnt glycoprotein family regulates many developmental processes. EGL-20, CWN-1, and CWN-2 have been shown to direct cell migrations (Harris et al., 1996) (Maloof et al., 1999)(Pan et al., 2006) and even act as guides for ALM process growth (Hilliard & Bargmann, 2006a). MOM-2 is known to be required for the asymmetric division of EMS which produces a daughter cell that produces endoderm (Rocheleau et al., 1997)(Thorpe et al., 1997). LIN-44 was found to control the polarity of asymmetric cell divisions in the tail (Herman & Robert Horvitz, 1994)(Herman et al., 1995). There is also evidence of the five Wnts demonstrating functional redundancy in vulval development. A single mutation in any of the five Wnt ligands does not cause strong defects in vulval precursor cell fate specification alone. However, each of the five Wnts do influence vulval precursor cell fate specification, with the strongest defects observed in a *lin-44; cwn-1; egl-20* triple mutant (Gleason et al., 2006a). The Wnt proteins LIN-44, MOM-2 and CWN-2 have also been identified to function redundantly in the patterning of the vulval lineage (Inoue et al., 2004).

lin-44

lin-44 (abnormal cell LINeage) was discovered during an investigation into mutants abnormal in the development of the *C. elegans* male tail. Alignment of *lin-44*

cDNA found LIN-44 is most similar to DWnt-2 (32.5% sequence identity) from *Drosophila melanogaster* and to Wnt7a (30.3% sequence identity) and Wnt7b (30.7% sequence identity) from the mouse (Herman et al., 1995). A transcriptional fusion of *lacZ* to the *lin-44* upstream region identified expression only in the tail, beginning at the 1.5-fold stage (430min) of embryogenesis. Expression was seen in the hypodermal cells (hyp8-hyp11) and in the T cells of the tail. *lin-44* was determined to affect the asymmetric cell divisions of the B, U, F and T cell. These lineages are not related linearly but instead share their position in the tail of the animal (Herman et al., 1995). These divisions are all polarized to produce two different daughter cells. In *lin-44* mutants the polarity of each division is reversed. By mosaic analysis *lin-44* was found to act cell non-autonomously. This correlates with its function as a signaling molecule. Its influence on cells near its expression in the tail infer *lin-44* may act in orienting the polarities of asymmetric cell divisions nearby. Additionally, the length of the anterior and posterior processes of the PLM neuron is known to be optimized by a high concentration of Wnt ligand LIN-44 through its receptor LIN-17 in the tail region of the worm. In wild type worms, the PLM cell body is in the tail where its processes develop posteriorly, and its axon extends anteriorly towards the head. In the absence of either *lin-17* or *lin-44*, the polarity of the PLM neuron is reversed, with its small posterior process growing longer and making ectopic synapses in the tail region (Puri et al., 2021).

egl-20

egl-20 (EGg Laying abnormal) was found in a screen for mutants that are defective in egg laying. Commonly these mutations are found to affect neurons that directly innervate the sex muscles of the vulva such as the HSN (hermaphrodite specific neuron) neurons. *egl-20* mutants are also seen to disturb the migration of the Q neuroblasts through the activation the Hox gene, *mab-5* (Harris et al., 1996).In the late stage of embryogenesis, the two Q neuroblasts QL and QR are born on bilateral sides of the embryo (Sulston & Horvitz, 1977). These neuroblasts generate identical daughter cells that eventually migrate in opposite directions. In the post-embryonic stage, the QL neuroblast is polarized such that it migrates towards the posterior of the larva, and the QR neuroblast is polarized such that it migrates towards the anterior of the larva. After migration both Q neuroblasts divide symmetrically, each giving rise to Q.a and Q.p cells that migrate in the same direction as their respective neuroblasts. In the QL descendants' activation of the canonical Wnt/β-catenin dependent signaling by EGL-20

results in expression of the Hox gene *mab-5* which maintains posterior migration (Maloof et al., 1999) (Korswagen et al., 2000). The QR descendants in contrast require the lack of *mab-5* activation to control anterior migration. EGL-20/Wnt signaling is also known to affect the polarization of an asymmetrically dividing epidermal cell division called V5. In this post-embryonic lineage six epidermal V cells (V1-V6), also called seam cells, are polarized along the A/P axis to develop cuticle and sensory structures. Loss of function *egl-20* mutations causes reversal of the polarity of V5, and overexpression of egl-20 via a 5-minute pulse in a *egl-20* heat shock promoter strain suppressed this reversal. With a 10-minute heat shock, all six V cells were seen to have their polarities disrupted, with their divisions occasionally becoming symmetric. By laser ablation of the neighboring V6 and T cells, it was determined that the V5 division polarity is reversed in *egl-20* mutants due to V5 receiving 'polarity-reversing' signals via direct cell-cell contact or short-range signals from the V6 and T cells (Whangbo et al., 2000).

cwn-1 and cwn-2

cwn-1 was identified by looking for *C. elegans* genes with DNA homology to the *Drosophila* Wnt genes and was found to share sequence with the *Drosophila* ligand *int-1* (now known as *wnt-1*)(Kamb et al., 1989). *cwn-2* was found during screen of clones in a CDNA library by the Caenorhabditis Genome Project (Shackleford et al., 1993). Both *cwn-1* and *cwn-2* null mutations have been found to affect Q, Canal-associated neuron (CAN), ALM cell migrations through one or both Frizzled receptors *cfz-2* and *mom-5* (Zinovyeva & Forrester, 2005). Previously I've discussed EGL-20 acts via a canonical Wnt pathway to activate MAB-5 in QL and its descendants, preventing them from adopting a QR-like fate (Maloof et al., 1999). In the Q lineage, a mutation in *cwn-1* has been seen to suppress the QL anterior migration defect of *egl-20* mutants that irregularly migrate like QR. This suggests that CWN-1 and EGL-20 act antagonistically in QL migration such that *cwn-1* enhances the cell migration defect of QR like cells. *cwn-2* has been found to signal through the Ror receptor tyrosine kinase *cam-1* and the Frizzled receptor *lin-17* in the *C. elegans* nervous system. *cwn-2* modulates synaptic transmission by regulating the translocation of acetylcholine receptors (AChRs) to synapses. Mutations in *cwn-2*, *lin-17*, *cam-1*, or the downstream effector *dsh-1,* all caused similar subsynaptic accumulations of AChRs in motor neurons, leading to diminished synaptic currents and less thrashing of the worm. Use of a heat shock-driven CWN-2 signaling in mutants was able to rescue the accumulations of AChRs, and this

was reflected in the increase of a thrashing phenotype (Jensen et al., 2012). *cwn-2* is also found to act primarily through the Wnt receptor *cam-1* (Ror), together with the Frizzled protein *mig-1* at the time of nerve ring formation. In wild-type animals, the nerve ring is more posterior, centered around the isthmus of the pharynx. In *cwn-2* mutants, all neuronal structures around the nerve ring are shifted to an anterior position, nearer the metacorpus of the pharynx (Kennerdell et al., 2009).

mom-2

mom-2 (*mom* for MOre Mesoderm) was identified while studying the induction of cell polarity in the 4-cell stage embryonic cell blastomere called EMS (Thorpe et al., 1997)(Rocheleau et al., 1997). In a wild-type embryo a signal from the EMS sister cell, called P2, polarizes EMS causing the two daughters E and MS to adopt different fates. MS produces the mesoderm which eventually forms the pharynx and body wall muscle, and E produces the endoderm, which eventually forms the intestinal cells of the worm. In a study by Thorpe et al., 1997 a genetic screen identified six recessive, maternal-effect embryonic lethal *mom* mutants wherein both daughters of the EMS blastomere adopt an MS fate and produce excess mesoderm. Embryos produced by homozygous *mom* mutant mothers failed to hatch and exhibit severe abnormalities in morphogenesis. The MOM-2/Wnt protein is 363aa in length and a BLASTp search indicates that the predicted MOM-2 protein is most closely related to human and *D. melanogaster Wnt4*.

Further investigation into *mom-2* interactions during endoderm specification found that mutation of the transcription factor *pop-1*, had the opposite phenotype, with both EMS daughters adopting E fates. POP-1 is known to be asymmetric, found higher in the anterior MS nucleus than the posterior E nucleus. However, in *mom-2* mutant embryos asymmetric levels of POP-1 in MS and E is lost, and they are instead symmetric (Lin et al., 1995). Additionally, *pop-1; mom-2* double mutants resemble that of a *pop-1* single mutant, placing *mom-2* function upstream of *pop-1.* This revealed that *mom-2*/Wnt signaling from P_2 at the 4-cell stage polarizes the blastomere EMS downregulating POP-1 in the posterior daughter, thereby distinguishing endoderm from mesoderm. Both endoderm specification and proper EMS spindle orientation require Wnt signaling from P_2. Along with the lack of endoderm *mom-2*/Wnt and *mom-5/Fz* mutant embryos are defective in orienting the mitotic spindle of the 4 cell stage

EMS and the 8-cell stage blastomere called Abar. In wild-type embryos the EMS centrosomes align along the left–right axis and the EMS nucleus/centrosome complex rotates to form the spindle along the anterior-posterior axis. The spindle then elongates, with the posterior daughter of EMS touching P_2. In a *mom-2; mom-1* double mutant strains and *mom-5*Fz strains the mitotic spindle in EMS is misaligned leading to division along the left-right axis, or the dorsal-ventral axis (Thorpe et al., 1997)(Schlesinger et al., 1999).

The embryonic AB lineage is also affected by *mom-2* mutations. In a wild-type embryo, ABar divides along the left–right axis, perpendicular to the other AB descendants that divide along the anterior-posterior axis. In *mom-2*/Wnt and *mom-5/Fz* mutant embryos, ABar division is misaligned, and instead parallel to the other AB descendants (Rocheleau et al., 1997)(Thorpe et al., 1997). Interestingly, *mom*-2/Wnt mutants instead show polarity reversal, rather than polarity loss, of the transcription factor POP-1 in the AB lineage. After the fourth division, and up until the 28-cell stage, POP-1 is high in the anterior sister and low in the posterior sister of a sister cell pair (Lin et al., 1995). In *mom-2* mutants the AB^8 stage has a loss of POP-1 asymmetry between sister pairs of AB^8 cells.(Park & Priess, 2003).

1.4.6. Functional Redundancy of Wnt Ligands

Evidence of the five Wnts demonstrating functional redundancy occurs in multiple cell lineages. During vulval development six VPCs must be induced to adopt correct fates in a correct pattern to generate the vulva opening. In this process all five Wnt ligands were found to be functionally redundant. Strains containing null or strong loss-of-function mutations in a single Wnt gene did not have strong defects in VPC fate specification, with the *cwn-1(ok546)* strain having the highest under-induced phenotype at 7%. After analysis of double Wnt mutant strains, the strongest defect was observed in the *cwn-1(ok546); egl-20(n585)* double mutant, where 87% of worms had either an under-induced or vulvaless phenotype (Gleason et al., 2006a). Functional redundancy is also seen in the requirement for Wnt receptors during VPC specification, as combinations of *lin-17, mig-1* and *mom-5* double mutant strains also cause an under-induced phenotype (Gleason et al., 2006a). CWN-1, CWN-2, and EGL-20 have been found to act redundantly for specific cell migrations (Zinovyeva & Forrester, 2005). Animals mutant for both *cwn-1* and *cwn-2* had dramatically enhanced ALM, BDU, CAN,

HSN, and QR descendant migration cell migration defects. Similarly, in *egl-20* and *cwn-1* double mutants, HSN and QR descendant cell migration defects were enhanced relative to either single mutant.

Wnts have also been found to function redundantly during the asymmetric cell division that generates the cholinergic interneuron AIY neuron (Kaur et al., 2020). In wild-type embryos the neuronal SMDD/AIY progenitor divides asymmetrically along the anterior-posterior axis after the expression of the transcription factor TTX-3. After division TTX-3 is seen to be expressed in the posterior AIY daughter and absent in the anterior SMDD. Using transcriptional reporters of the five Wnt ligands, it was found that the three most posterior ligands in the embryo CWN-1, CWN-2 and MOM-2 were transcribed at higher levels at the time of SMDD/AIY division. In addition, the Frizzled receptor MOM-5 is transiently enriched at the posterior side of the mother cell. After analysis of multiple loss and gain of function mutations of these Wnt ligands only the triple *mom2; cwn-1; cwn-2* mutants caused a loss of TTX-3 expression in the SMDD/AIY neuroblast. Furthermore, overexpression of CWN-2 via a heat shock promoter caused a duplication of the AIY fate, with TTX-3 expression occurring in the sister SMDD neuron (Kaur et al., 2020).

1.4.7. Wnt Ligand Expression and Inhibition

The expression patterns of the five Wnt genes of *C. elegans* have been extensively studied using traditional transgenic reporter gene-based assays. A study using transcriptional reporters of the five Wnt ligands, consisting of the *cis*-regulatory elements of the Wnt ligands placed upstream of a nuclear GFP, found CWN-1, CWN-2 and MOM-2 were expressed in posterior cells of the embryo during the epidermal enclosure stage (Fig. 1-14). LIN-44 and EGL-20 expression did not occur until later stages during elongation but was also seen in posterior cells of the embryo (Kaur et al., 2020).

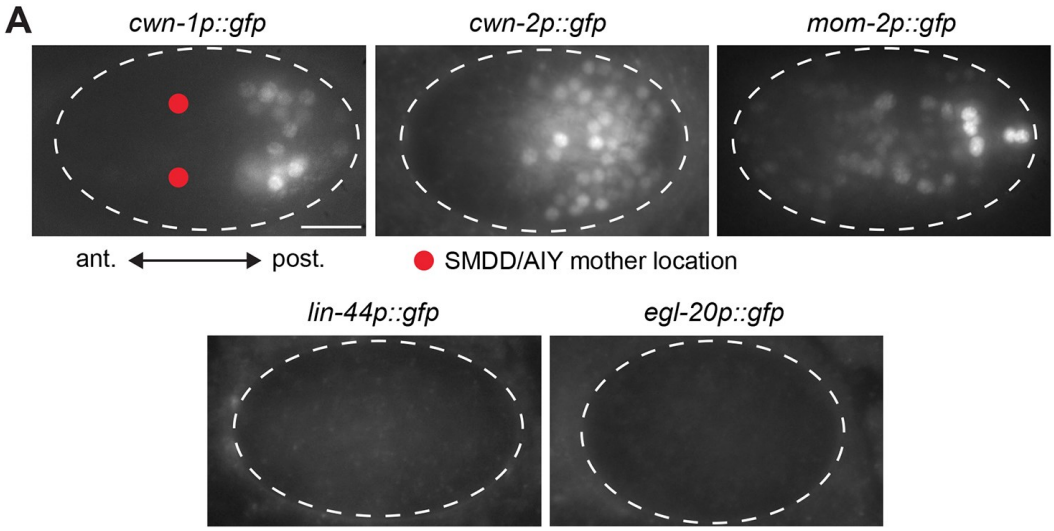

Figure 1-14. Effect of Wnt mutants and overexpression on AIY fate.
(A) Expression of Wnt ligands in the embryo at epidermal enclosure stage. Transcriptional reporters with the cis-regulatory regions of the Wnt genes driving the expression of a nuclear gfp Ventral view, red dots indicate the location of the SMDD/AIY mothers. Adapted from (Kaur et al. 2020)

In a major undertaking (Zacharias et al., 2015) identified all cells expressing transcriptional reporters for each Wnt ligand at single cell resolution throughout embryonic cleavage by 4D imaging and automated cell tracking and reporter quantification (Fig. 1-15). This study revealed *mom-2* is expressed maternally in descendants of the P1 and P2 blastomeres, with transient zygotic activity of the *mom-2* promoter in MS, E and several posterior AB sublineages. The *cwn-2* promoter was activated in a partially overlapping set of AB sublineages and the *cwn-1* promoter expression is limited to the C and D lineages. The reporters for *egl-20, lin-44* and *mom-2* are expressed much later, just prior to the final round of embryonic divisions, in cells in the tail. These findings are consistent FISH analysis performed by (Harterink et al., 2011).

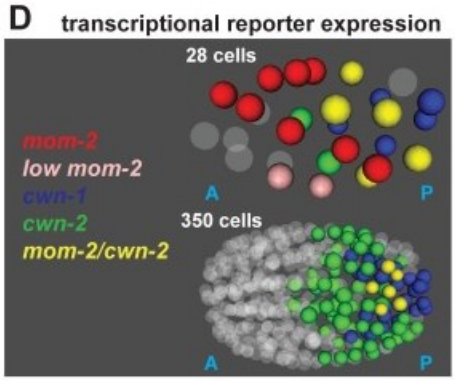

Figure 1-15 Wnt Transcriptional Reporter Expression
Location of the nuclei expressing the 3 earliest Wnt ligands at the 28 and 350 cell stages. Adapted from (Zacharias et al., 2015)

The spatio-temporal expression patterns of the five C. elegans Wnt genes were determined in another study by using single molecule mRNA FISH to measure endogenous transcript levels in staged L1 larvae and during embryonic development (Harterink et al., 2011). Of the five Wnt transcripts, *lin-44*, *egl-20* and *cwn-1* were mostly localized to the posterior half of L1 larvae, a pattern already seen at the comma stage of embryonic development (Figure 1-16). The theme that emerges from these studies is the predominantly posterior expression of the five Wnt ligands during embryonic development that results in a series of partially overlapping expression domains. It has been well characterized in *Drosophila* and vertebrates that Wnts can act as morphogens, that can form long-range concentration gradients providing positional information to cells in developing tissues. This overlapping Wnt expression is proposed to act as a mechanism for providing positional cues or specification along the primary anterior-posterior axis.

Wnt protein activity is mediated by secreted Wnt inhibitory proteins. These include Dickkopf (Dkk) (Glinka et al., 1998), Wnt inhibitory factor (WIF) (Hsieh et al., 1999), and the secreted Frizzled related proteins (SFRPs). The orthologs of Dkk and WIF are absent, however *C. elegans* does contain the SFRP ortholog *sfrp-1*(Harterink et al., 2011). A single molecule mRNA FISH analysis found *sfrp-1* to be expressed in the four head muscle quadrants of the L1 larvae and in the anterior of embryo by the 100-cell stage of development. This anterior expression alludes to the counteraction of the posteriorly expressed Wnts by SFRP-1. This was confirmed, as SFRP-1 was seen to

repress the activity of CWN-1 and CWN-2 in the anterior region of the body as a mechanism to control the migration of the CAN and ALM neurons (Harterink et al., 2011). This opposing expression of Wnts and Wnt inhibitors is again proposed to be a significant evolutionarily conserved mechanism of specification along the primary body axis.

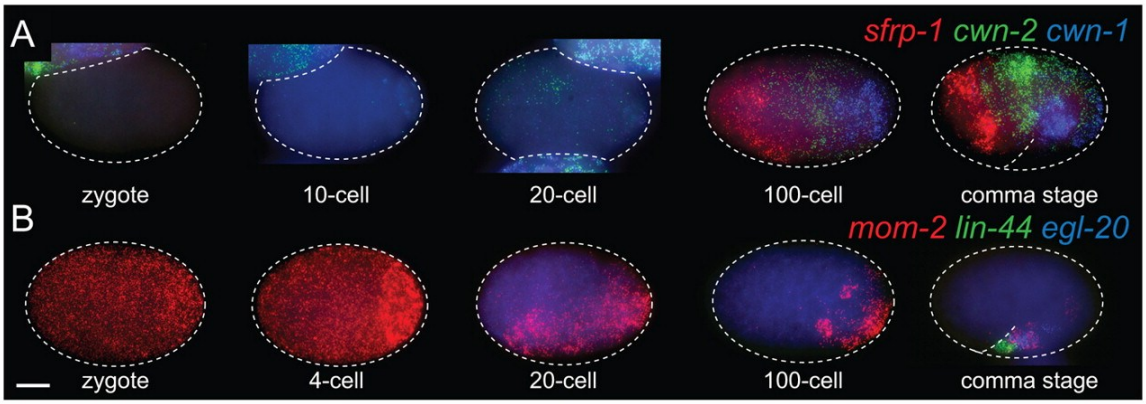

Figure 1-16 Single molecule mRNA FISH analyses of the *C. elegans* Wnt genes and *sfrp-1* during embryonic development

Images are maximum intensity projections of lateral z-stacks. Detection of (**A**) sfrp-1, cwn-1 and cwn-2, and (**B**) mom-2, lin-44 and egl-20 transcripts. Embryos were staged using DIC microscopy and DAPI staining of nuclei. (Harterink et al., 2011).

1.5. Hypothesis and Aims

We hypothesize that the asymmetric polarization of HAM-1 may be a mechanism of ACD to ensure direct inheritance by the daughter cells, where it can enter the nucleus and regulate transcription. In addition, as Wnts are the primary signaling pathway in *C. elegans* controlling anterior-posterior polarization we hypothesize they may have a functional relationship with HAM-1. Therefore, to further characterize HAM-1 dynamics within asymmetrically dividing cells, I have narrowed my research to two experimental aims.

AIM 1: Follow the localization of GFP::HAM-1 in asymmetrically dividing cells to investigate the relationship between HAM-1 polarization during mitosis and its distribution in daughter cells.
AIM 2: Investigate the requirement for Wnts in two asymmetrically dividing cell lineages known to be dependent on *ham-1* function using RNAi.

Chapter 2. Materials and Methods

2.1. Strains and Alleles

Strains were grown on Easiest Worm Media plates seeded with *Escherichia coli* strain OP50 and incubated at 20°C or 15°C (Brenner, 1974). Strains used in this study are included in Table 2-A.

Table 2-1. Strain List

Strain	Genotype
NN795	*zdIs5[mec-4::GFP] I; hkIs39[unc-119p-GFP::HAM-1 unc-122::GFP]*
NN535*	*zdIs5[mec-4::GFP] I; hkIs39[unc-119p-GFP::HAM-1 unc-122::GFP]*
NN907*	*zdIs5[mec-4::GFP] I; hkIs39[unc-119p-GFP::HAM-1 unc-122::GFP]; cwn-1(ok546) II; cwn-2(ok895) IV*
NN903*	*zdIs5[mec-4::GFP] I; hkIs39[unc-119p-GFP::HAM-1 unc-122::GFP]; cwn-1(ok546) II*
NN908*	*zdIs5[mec-4::GFP] I; hkIs39[unc-119p-GFP::HAM-1 unc-122::GFP]; cwn-2(ok895) IV*
NN904*	*zdIs5[mec-4::GFP] I; cwn-1(ok546) II; cwn-2(ok895) IV*
NN905*	*zdIs5[mec-4::GFP] I; cwn-1(ok546) II*
NN906*	*zdIs5[mec-4::GFP] I; cwn-2(ok895) IV*
NN140	*cwn-1(ok546) II; cwn-2(ok895) IV*
NN532	*hkIs39 [unc-119p-GFP::HAM-1 unc-122::GFP]*
SK4005	*zdIs5 [mec-4::GFP] I*
NG4532	*zdIs5[lin-15(+) mec-4::GFP] I; ham-1(gm279) IV*
NN840	*ham-1(gm279) IV*
NG2958	*gmIs12(srb-6::GFP) III; ham-1(gm279)*
NG2693	*gmIs12(srb-6::GFP) III*

*Strain generated as a part of this study

2.2. Live Embryo Mounting and Imaging

Worms were mounted following a protocol adapted from (Hardin, 2011). On a cover slip adult hermaphrodite worms were suspended in a drop of M9 buffer and sliced open using the edge of two needles to release early-stage embryos. Embryos were then mounted on a slide prepared with a 5% agarose pad, and the coverslip was inverted and sealed with VALAP (Hardin, 2011). The slide was allowed to rest for at least 20 minutes before imaging to allow the VALAP and agarose pad to set, aiding in the prevention of focal drift. Live embryo imaging was performed using Harald Hutter's Spinning Disc Microscope and a Hamamatsu 1394 ORCA-ERA camera. Acquisition was performed via Volocity 6.5.1 software (https://www.volocity4d.com/). Embryos were imaged every 30 seconds in z-stacks at a maximum depth of 15µm in 0.5µm slices, for up to 2 hours. The embryos were imaged using a 63x oil immersion objective with a 1.6x optivar in two channels GFP (525nm), and Nomarski.

2.3. Genetic Cross for the Generation of Wnt Mutant strains

Genetic crosses were performed to incorporate *cwn-1(ok546) and/or cwn-2(ok895)* deletion alleles into backgrounds containing a GFP reporter for the PLM neurons (*zdIs5 [mec-4::GFP])* and/or the GFP::HAM-1 overexpression transgene (*hkIs39 [unc-119p-GFP::HAM-1 unc-122::GFP]*. The schematic for the cross between NN140 (*cwn-1(ok546) II; cwn-2(ok895)*) and NN795 (*zdIs5[mec-4::GFP] I; hkIs39[unc-119p-GFP::HAM-1 unc-122::GFP] IV*) is outlined in Fig A5-1. Progeny carrying *zdIs5* were identified by *mec-4::GFP* expression in the six touch neurons (AVM, ALM_L, ALM_R, PVM, PLM_L, PLM_R). Progeny carrying *hkIs39* were identified by *unc-122::GFP* expression in the six coelomocytes. The *cwn-1* and *cwn-2* deletion alleles were identified in clonal populations using a pooled or single worm lysis genotyping PCR on parental or progeny worms (Table A5-D). N2 males were mated to *zdIs5; hkIs39* hermaphrodites then heterozygous cross progeny males were selected to mate with *cwn-1(ok546) II; cwn-2(ok895)* hermaphrodites. 24 cross progenies carrying both *zdIs5 and hkIs39* were cloned and PCR was used to genotype *cwn-1 and cwn-2.* From wells heterozygous for *zdIs5, hkIs39, cwn-1 and cwn-2,* 120 hermaphrodites were cloned to generate six strains: NN900 (*zdIs5[mec-4::GFP] I; hkIs39[unc-119p-GFP::HAM-1 unc-122::GFP]; cwn-1(ok546) II; cwn-2(ok895) IV)*, NN901 (*zdIs5[mec-4::GFP] I; hkIs39[unc-119p-*

GFP::HAM-1 unc-122::GFP]; cwn-1(ok546) II), NN902 (*zdIs5[mec-4::GFP] I; hkIs39[unc-119p-GFP::HAM-1 unc-122::GFP]; cwn-2(ok895) IV*), NN903 (*zdIs5[mec-4::GFP] I; cwn-1(ok546) II; cwn-2(ok895) IV*), NN904 (*zdIs5[mec-4::GFP] I; cwn-1(ok546) II),* and NN905 *(zdIs5[mec-4::GFP] I; cwn-2(ok895) IV*).

2.4. Standard Micro-injection

Micro-injections were accomplished by using N_2 gas (pressure controlled by Tritech Research microinjector System MINJ-1) to expel the injection mix through a pulled capillary needle mounted on a Narishige Three-axis Motorized Micromanipulator (MN-151, SN:02042). The process was observed through a microscope. Worms were placed onto a NGM plate and glazed with halo-carbon oil to protect the osmotic integrity of the worms prior to injection. Worms were then picked off the plate and placed onto a dried 2% agarose pad. They were then injected in both gonads and removed off the pad by floating them in a small drop of M9 buffer. Worms were placed on a EWM agar plate seeded with OP50 *E.coli* and left at room temperature for about an hour to recover.

2.5. Molecular Biology

2.5.1. Worm Lysis

Worms were lysed for PCR genotyping using a Lysis Buffer (10 mM Tris pH 8.2, 50 mM KCl, 2.5 mM $MgCl_2$, 0.5% Tween 20, 0.05% gelatin) containing 3 µL of 20 mg/mL Proteinase K per 1 mL of buffer. For single worm lysis, 7.5 µL lysis buffer was used, and for ten worms, 20 µL of lysis buffer was used. Tubes were centrifuged at 13,000 rpm for 2 minutes. Tubes were then placed at -80°C for 15 minutes, then thawed and stored on ice before the lysis PCR. The following Lysis PCR program was run in a thermocycler: 60°C for 90 minutes, 15°C for 15 minutes, 4°C hold. 1 µL of each ten-worm lysis and 2 µL of each single worm lysate used in PCR.

2.5.2. Standard PCR Protocol

Standard PCR Conditions and Thermocycling program, 95ºC 3min, [95ºC 30sec, 58ºC 20sec, 72ºC 1:20min] x35 cycles 72ºC 3min, 4ºC Hold, performed in a Thermo-Fisher Scientific MiniAmp Plus Thermal Cycler, adapted as necessary.

Table 2-2. Standard PCR Conditions

Working Stocks	PCR Vol Used (µL)	Final Concentration
5uM Primer L	2.5	0.5µM
5uM Primer R	2.5	0.5µM
2mM dNTP mix	2.5	200µM
10xPFU Buffer (20mM MgSO4)	2.5	1x
Template DNA	2	Unknown (0.1 – 1µg)
PFU (2.5U/µL)	0.5	0.05U/µL
ddH20	12.5	/
Final Reaction:	25	/

2.5.3. Primer Design

Primers (Table A5-B) were designed using Primer 3 (https://primer3.ut.ee/).

2.5.4. Generation of a Dendra2::HAM-1 Expressing Worms

Bacterial Transformation

Prior to electroporation, and equal volume of water was added to the ligation mixes and 1µl of each sample was added to 200 µL of DH5α cells and transferred o a pre-chilled electroporation cuvette and electroporated. Cells were recovered in 1mL of LB media and incubator at 37C for 45 minutes. 100µl of the experimental and the control sample were spread plated onto LB Ampicillin (100mg/mL) plates. The remaining 900 µL of sample was pelleted by centrifugation at 5000rpm resuspended in 100 µL and spread onto a LB Ampicillin (100mg/mL) plate and incubated at 37ºC overnight.

STET Prep

Individual colonies were incubated overnight at 37ºC in 3mL of LB Ampicillin (100mg/mL) and plasmid isolated using a STET prep. Cells were pelleted by adding 1.5mL of each sample into a sterile Eppendorf tube and centrifuged at 5000 rpm for 5 minutes. Supernatant was discarded and the remaining 1.5mL of each sample was pelleted on top of the existing pellet. The supernatant was then discarded, and pellets

were resuspended in 350 µl of STET Buffer [8% sucrose, 50 mM Tris-HCl pH 8.0, 50 mM EDTA pH 8.5, 5% Triton X-100]. To each tube 30 µl of 10 mg/mL Lysozyme was added, and then immediately vortexed and placed in a 95ºC water bath for 3 minutes. After 3 minutes, tubes were immediately spun at 13,000rpm for 15 minutes and the snotty pellet was removed using a sterile toothpick. 30µl of ice-cold isopropanol was added to each sample and placed on ice for 30 minutes. Samples were then spun at 13,000rpm for 8 minutes, supernatant was removed and 1mL of 70% ethanol was added to each sample. Samples were mixed by inversion and re-spun for 1 minute if the pellet was disturbed. The supernatant was decanted, and any remaining ethanol was removed with a pipette. Samples were left to air dry completely before being dissolved in 100 µl TE Buffer [10mM Tris pH 8.0, 1mM EDTA pH 8.0] with RNase (10mg/mL) and stored at -20ºC.

Micro-injection and Worm passaging

The initial injection mix contained 50ng/µl Dendra-2::HAM-1 Plasmid, along with 30ng/µl of *dpy30::dsRed* (from Hamida Safi), the co-injection marker. Dr. Hawkins injected at least 20 N2 worms, and they were allowed to recover for 1 hour. After recovery they were re-plated in groups of 3 and transferred every 24 hours. After 2-3 days plates were checked for *dpy-30::dsRed* fluorescence, which would indicate a successful injection. Worms were also assessed for Dendra-2 fluorescence in the green channel.

2.5.5. Synthesis of N-terminal 3xMYC::HAM-1 Repair Templates for CRISPR/Cas9

Primers (Table A5-C) were designed using sequences for the 3xMyc tag, provided by Hamida Safi, *ham-1* sourced from GenBank (GenBank: Z73908.2) and WormBase (Sequence: F53B2.6), and the *unc-54* 3'UTR from the plasmid pPD95.77 (Addgene plasmid # 1495 ; http://n2t.net/addgene:1495 ; RRID:Addgene_1495),.

PCR Synthesis of the 3xMYC::HAM-1 Repair Template

Primers Dm1 and Dm2 were designed to PCR amplify 3xMyc dsDNA from a synthetic G-Block of 3xMyc dsDNA provided by Hamida Safi. They contain 35 base pairs (bp) of *ham-1* homology arms, including the *ham-1* start site in the forward primer Dm1. The 25bp sequence used to amplify the 3xMyc sequence was previously used and

validated by Hamida Safi in an experiment where she generated a W04A8.6::3xMyc tag. The final product was purified using a Monarch DNA Gel Extraction Kit (#T1020L) and products were eluted in DEPC treated nuclease free water. 1ul of each sample was then run on a 1.3%(w/v) agarose gel for quantification.

Stitch PCR Synthesis of the Negative Control 3xMYC::TAG::UNC-54 3'UTR Repair Template

The experimental schematic is outlined in (Fig 3-17). A Stitch PCR was performed to generate a negative control made of the 3xMyc sequence, a TAG stop codon, the *unc-54* 3'UTR and flanking *ham-1* homology arms containing a mutant PAM site. The mutated PAM sequence is made to prevent the CRISPR/Cas9 system from binding and cutting the donor dsDNA. The original PAM sequence was GGA for Glycine, however there is no available silent mutation for Glycine. Instead, the sequence was changed in the second position to GCA for another nonpolar amino acid Alanine. This insert introduces a stop codon in the *ham-1* sequence.

The first PCR was performed using 1ng of the synthetic G-Block of 3xMyc dsDNA using forward primer Dm1 and reverse primer Dm5. The standard PCR protocol was used with the following thermocycling parameters: 3 minutes at 95 °C for the initial denaturation, followed by 35 cycles of 30 s at 95 °C for denaturation, 30 s at 64 °C for annealing, 1 minute at 72 °C for extension, and 3 min at 72 °C for the final extension. The PCR product was examined by gel electrophoresis on a 1.2%(w/v) agarose gel and confirmed to be the expected band size of 141bp. The amplified 3xMyc product was then purified using a GeneJet PCR Purification Kit and eluted in the provided elution buffer.

The second PCR used 1ng of the plasmid pPD95.77, primers Dm6 and Dm7, and the same protocol as PCR 1. These primers were designed to amplify the *unc-54* 3'UTR from the plasmid pPD95.77 with a 5' 3xMyc homology arm followed by a TAG stop codon and a 3' HAM-1 homology arm. The PCR product was examined by gel electrophoresis on a 1.2%(w/v) agarose gel, evaluated against a FroggaBio 100bp DNA Ladder and confirmed to be the expected band size of 378bp. The amplified *unc-54* 3'UTR product was then purified using a GeneJet PCR Purification Kit and eluted in the provided elution buffer.

To find an even molar ratio and to match the number of available ends for priming between the 3xMyc fragment and the *unc-54* 3'UTR fragment in the stitch PCR, I performed a 2-fold dilution series of the purified product from PCR 2 and gel quantified the dilutions along with the product from PCR 1. From this I determined that I would require a ⅙ dilution of PCR product 2 to obtain the same concentration as PCR product 1. The third and final Stitch PCR utilized the purified products from PCR 1 and PCR 2, with primers Dm1 and Dm7 to generate a final construct consisting of 35 bp of HAM-1 homology, the 3xMyc sequence, a stop codon, the *unc-54* 3'UTR and a final 35 bp HAM-1 homology arm with the mutant PAM site. The PCR followed the same thermocycle program as PCR 1 and PCR 2. The product was then evaluated on a 1.2%(w/v) agarose gel and confirmed to be the expected band size of 490bp. Primers Dm20 and Dm21 were then used in an additional PCR to extend the length of the existing *ham-1* homology arms by 15bp, increasing the length of the homology arms from 35bp to 50bp. This was performed to increase the likelihood of achieving HDR and producing an edit. The final product was purified using a Monarch DNA Gel Extraction Kit (#T1020L) and products were eluted in DEPC treated nuclease free water. 1ul of each sample was then run on a 1.3%(w/v) agarose gel for quantification.

3xMYC::HAM-1 CRISPR Guide RNA Design

The entirety of F53B2.6 *ham-1* Wormbase coordinates IV: 12542183..12545737 was used to generate a list of guide RNAs in a region of the *C. elegans* genome. The *ham-1* guide RNA [TACTTAGCCGTTGTGCTCAA] used was selected using the CRISPR Guide RNA Selection Tool (http://genome.sfu.ca/crispr/) maintained by Harald Hutter.

Repair Template Injection Mix Preparation

Injection mixes were prepared by following the Ghanta., K.S. and Mello, 2020. To a tube of Cas9, tracrRNA and then crRNA was added. The tube was then mixed by pipetting up and down gently three times, and incubated at 37 for 15min, to allow the ribonucleoprotein time to form. During this time, an aliquot of the dsDNA donor was melted from 95°C to 4°C using the Melt PCR Program in a thermocycler. When this was complete the melted dsDNA donor was added to the tube containing the ribonucleoprotein complex, along with PRF4::rol-6(su1006) plasmid. Finally, DEPC-Treated nuclease free water was added to a final volume of 20uL (see Tables 4 and 5).

The injection mix was then centrifuged for 15 minutes at 13,000rpm and kept on ice until use.

Micro-injection and Worm Passaging for CRISPR/Cas9 edits

Micro-injections were performed by Dr. Hawkins by following the standard micro-injection protocol. Worms were placed on a NGM agar plate seeded with OP50 *E.coli* and left at room temperature for about an hour to recover. Recovered worms were then singled into 6 wells and stored at 15°C or 20°C for 72 hours. Two wells with the highest number of F1 rolling progeny were then selected and from those wells 48 non-rolling younger progeny were cloned. Ten F2 worms from each F1 clone were then lysed to isolate DNA. Primers Dm3, Dm4, and C-Myc-R were designed to be a three-primer system to detect any negative, heterozygous, and homozygous edits in the worm lysates. C-Myc-R was provided by Hamida Safi and was designed as a poison primer inside the 3xMyc sequence. Dm3 was designed in Primer3 using +/- 400bp sequence of *ham-1* around the PAM site, using C-Myc-R as the right primer. Dm4 was then subsequently designed using Dm3 as the left primer.

2.5.6. Synthesis of Wnt dsRNA for RNAi by Injection

For four of the Wnt genes I used plasmids containing the respective cDNAs subcloned into the vector L4440 as template for in vitro transcription reactions: *lin-44*(yk120c7) *egl-20* (yk1183alo) *cwn-1*(yk236alo) *cwn-2 (a fragment of exon2-4)* in L4440 in DH5α. For *mom-2* a genomic fragment containing the first two exons was PCR amplified from genomic N2 DNA. The cDNA fragments in each plasmid were validated by restriction mapping and then linearized by restriction digest. The first PCR uses the standard PCR protocol, the linearized plasmid template and primers F1 and R1 to amplify ~400bp of exonic sequence. Product from each initial PCR was purified in a PCR clean up column and then used as a template in the second round of PCR (Primers in Table A5-C). In the case of *mom-2* an initial PCR was performed off N2 lysate to amplify a slightly larger product which was then used as a template to nest with T7 containing primers. The second round of PCR uses the same protocol to add T7 sequences to the 5’ or the 3- ends of the amplified Wnt sequence. Primer pairs used were: wntT7F + R1, and F1 + wntT7R with each purified Wnt template to generate both strands. Products were validated on a 1.3% agarose gel using a 100bp DNA ladder (FroggaBio) and then

purified (GeneJet PCR Purification Kit). 400 ng of each purified product was used in a in vitro transcription reaction (T7 Mega script Kit) to generate ssRNA. To generate dsRNA, equimolar rations of respective Wnt ssRNA pairs were incubated at 72ºC for 10 minutes, and then cooled slowly to room temperature. Successful annealing was determined by dsRNA shifting upward compared to its respective ssRNA on a 1.6% agarose gel. All products were stored at -20ºC.

Micro-injection and worm passaging for RNAi by Injection

dsRNA was prepared in varying concentrations and diluted with nuclease free water. Worms were injected following the standard micro-injection protocol. After injection worms were placed on a EWM plate seeded with OP50 *E.coli* and left at room temperature for about an hour to recover. Injected worms were then place onto a new plate and transferred every 24 hours for 3 days at 20ºC.

2.6. Dye Filling Assay

Worms were washed off 10mL plates into and Eppendorf tubes using 1mL of M9. The tube was centrifuged at 2000rpm for one minute and the supernatant was removed. This wash was repeated once, and then worms were finally resuspended in 1mL of M9 and 4µl of a 2mg/mL DiI solution. Tubes were then covered in aluminum foil and placed on a rocker for 3 hours. After 3 hours, tubes were centrifuged at 2000rpm for one minute, the supernatant was removed and then worms were washed twice in M9. After the final wash worms were resuspended in 1mL of M9. Worms were finally transferred to a plate and allowed to dry before visualization in the red channel.

2.7. Statistics

Statistics were performed using a Chi Square test in JMP17 software after consultation with Ian Bercovitz, Director of Statistical Consulting Services.

Chapter 3. Results

3.1. Investigation of GFP::HAM-1 Localization by 4D Microscopy

In embryos, GFP::HAM-1 is seen to localize both in the nucleus of cells and in a tight crescent to the posterior pole during mitosis (Leung et al., 2016). However, a complete analysis has not been performed to follow the distribution of GFP::HAM-1 to daughter cells. Thus, the fate of the asymmetrically localized protein is still unknown during cell division. Is the anterior-posterior polarization of HAM-1 a mechanism to control inheritance of itself or cell fate determinants to daughter cells? Is localization at the cell cortex a mechanism to influence nuclear localization? As HAM-1 may function differently in each asymmetric cell lineage, will we see a similar pattern of localization across all asymmetrically dividing cells? An investigation into GFP::HAM-1 localization over time can provide insights into the relationship between HAM-1 polarization and its distribution during mitosis and in daughter cells.

Visualization was performed in transgenic *hkIs39* (GFP::HAM-1) embryos using 4D microscopy. Embryos were removed from adult hermaphrodites, mounted onto an agarose pad and visualized over 1- 1.5 hours. Z-stacks were taken in both the Nomarski and GFP channels and were limited to a 15μm depth from the top of the embryo.

3.1.1. GFP::HAM-1 Localizes to the Posterior Cell Cortex during Mitosis in all expressing cells

The GFP::HAM-1 in embryos was consistent with previously published results (Leung et al., 2016). GFP::HAM-1 expression was observed broadly across many cells during embryogenesis, both within the nucleus and at the cortex (Fig 3-1). Timelapse imaging provided qualitative observations of GFP::HAM-1 localization (Fig. 3-2, 3-3). Due to limitations of the recordings with respect to quality and quantity the findings observed should be interpreted as preliminary. The small size of the daughter cells along with their movement as other divisions occur in the embryo limited my ability to further follow the localization of GFP::HAM-1 after mitosis. Of 19 embryonic cell divisions observed, I was only able to follow four in which I could see both daughter cells immediately after division in the same plane of division. Of those four divisions, only the

division in Fig 3-3 was I able to observe both daughter cells for up to 15 min after division. From these recordings I observed that prior to mitosis GFP::HAM-1 is localized at both the cell cortex and in the nucleus. The start of mitosis is marked by a loss of GFP::HAM-1 fluorescence in the nucleus, likely during the breakdown of the nuclear envelope. GFP::HAM-1 at the cortex is then seen to be expressed highly as crescent at the posterior cell cortex. During division GFP::HAM-1 remains highly expressed at the posterior cell cortex, and after division GFP::HAM-1 appears brighter and diffuse around the cortex in the posterior daughter cell compared to the anterior daughter cell. In Fig. 3-3, after division GFP::HAM-1 is seen to be present within both post-mitotic nuclei and at the cortex of both daughter cells. Immediately after division GFP::HAM-1 first appears within the anterior daughter cell nucleus one minute before the posterior daughter cell. Concurrently, GFP remains brighter at the crescent within the posterior daughter than in the cortex of the anterior daughter cell. The posterior crescent in the posterior daughter cell then begins to appear more diffuse around the entire cell cortex. Over time expression of GFP::HAM-1 is identical in both daughter cells. Across all nineteen cell divisions recorded the GFP crescent remained bright within in the posterior daughter cell cortex immediately after division.

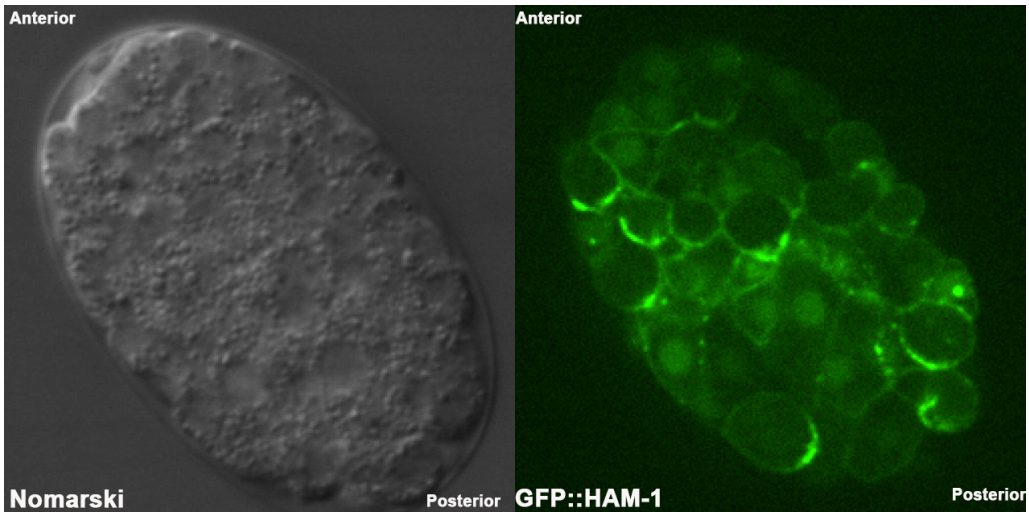

Figure 3-1. GFP::HAM-1 expression in a *hkIs39* embryo

Nomarski (left) GFP::HAM-1 fluorescence (right). GFP::HAM-1 is seen in the nucleus and diffuse at the cell cortex of all cells. In dividing cells GFP::HAM-1 is localized in a crescent at the posterior cell cortex.

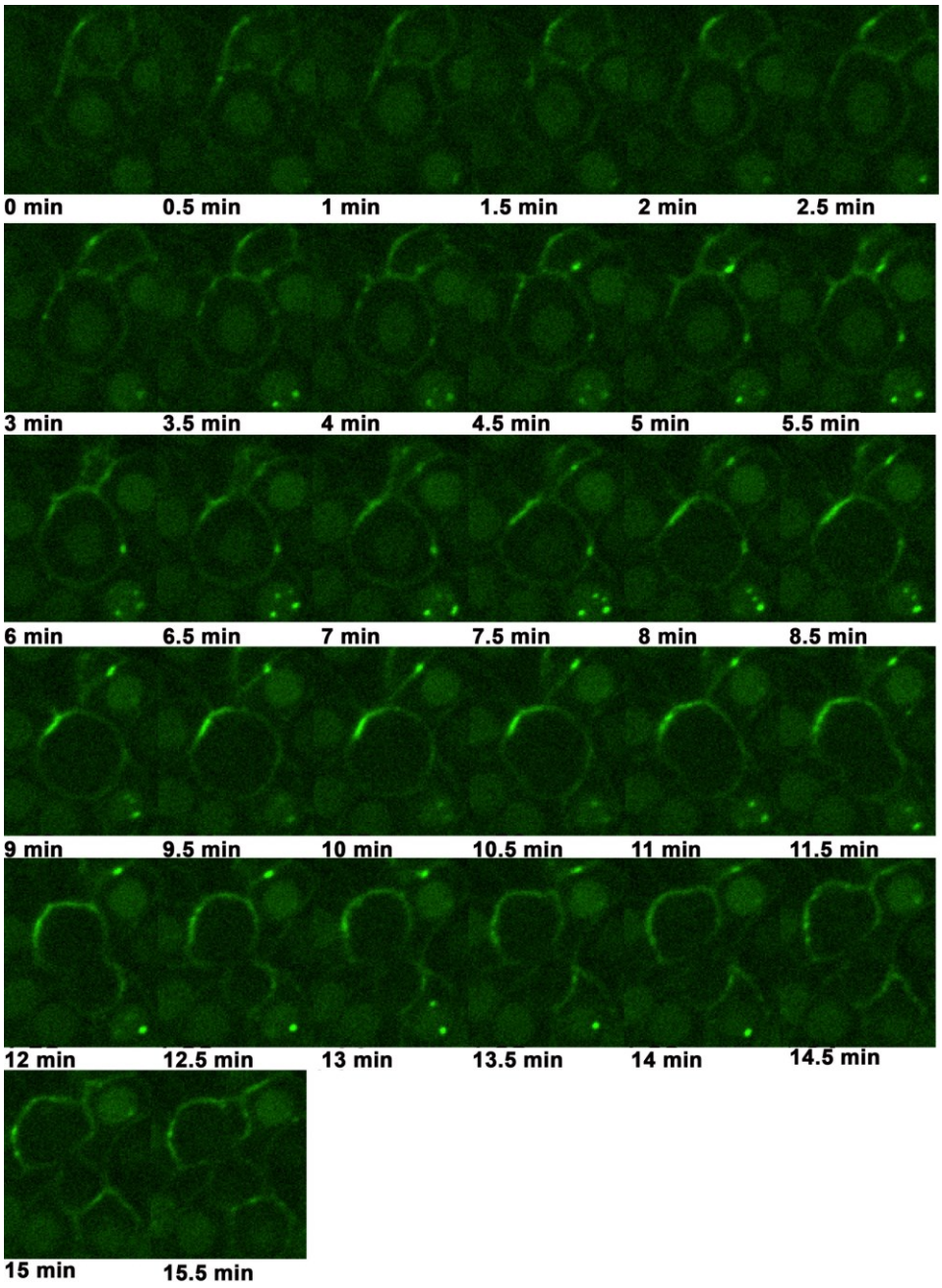

Figure 3-2. Timeseries 1 of a dividing cell expressing GFP::HAM-1 in *hkIs39*

Timeseries in a single z-slice of a single cell division occurring over 15.5 minutes in an *hkIs39* embryo. The GFP signal at the posterior cortex increases about 5–7 minutes before the cell divides, with no discernible changes in the nuclear GFP. Then the nuclear GFP declines and the cortical GFP rises continues to increase. The nuclear GFP vanishes during cell division (11–15 min) because of the breakdown of the nuclear envelope, and the cortical GFP diffuses throughout the posterior cell's cortex, reaching an almost uniform distribution right after cell division is finished (15 min).

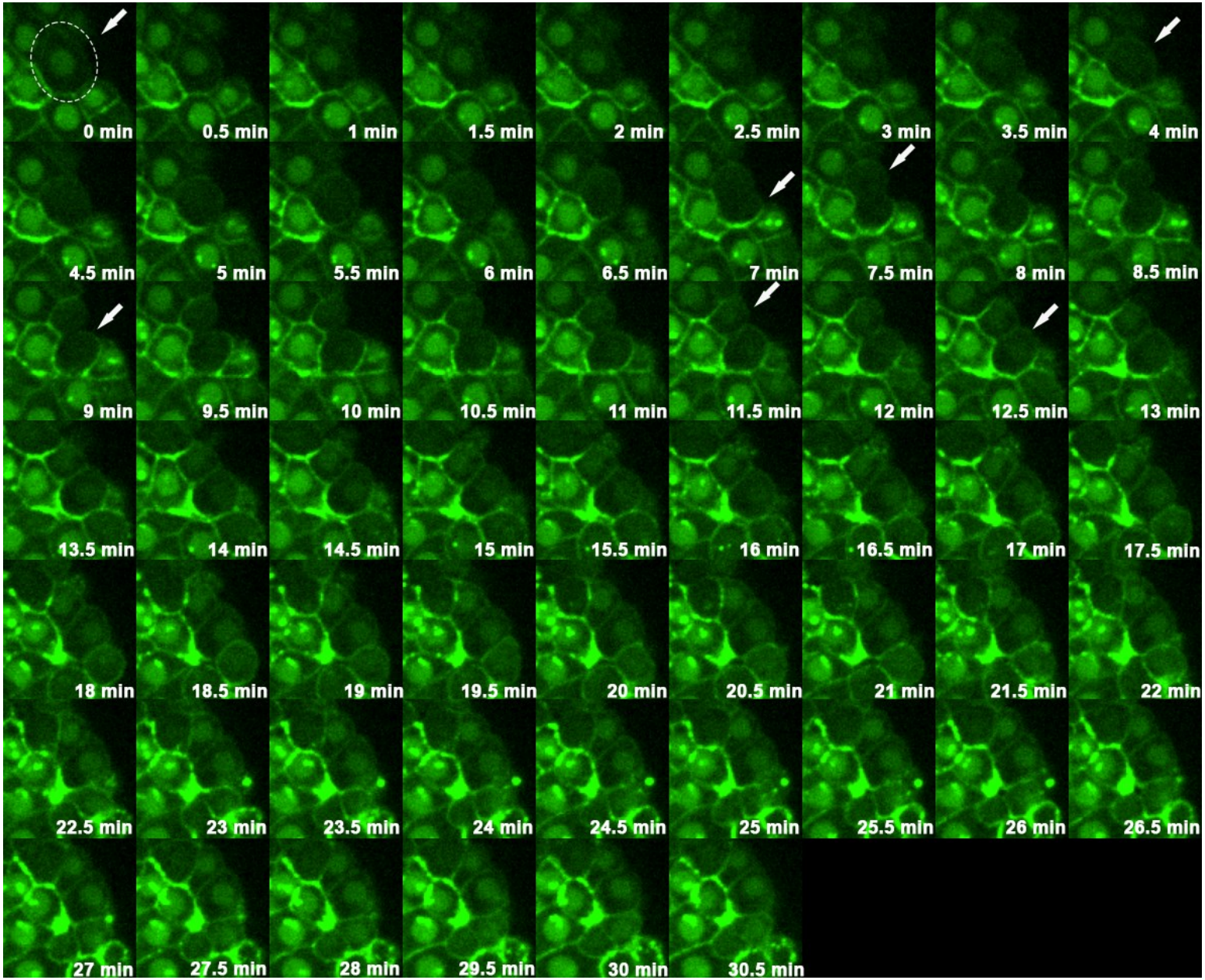
0 min
0.5 min
1 min
1.5 min
2 min
2.5 min
3 min
3.5 min
4 min
4.5 min
5 min
5.5 min
6 min
6.5 min
7 min
7.5 min
8 min
8.5 min
9 min
9.5 min
10 min
10.5 min
11 min
11.5 min
12 min
12.5 min
13 min
13.5 min
14 min
14.5 min
15 min
15.5 min
16 min
16.5 min
17 min
17.5 min
18 min
18.5 min
19 min
19.5 min
20 min
20.5 min
21 min
21.5 min
22 min
22.5 min
23 min
23.5 min
24 min
24.5 min
25 min
25.5 min
26 min
26.5 min
27 min
27.5 min
28 min
29.5 min
30 min
30.5 min

Figure 3-3 Timeseries 2 of a dividing cell expressing GFP::HAM-1 in *hkIs39*

Timeseries in a single z-slice of a single cell division occurring over 30.5 minutes in an *hkIs39* embryo. GFP::HAM-1 is present at both the nucleus and uniformly around the cell cortex. The GFP signal at the posterior cortex increases 7 minutes before the cell divides, then the nuclear GFP declines (4 min) and the cortical GFP rises continues to increase. The nuclear GFP vanishes during cell division (7 min) because of the breakdown of the nuclear envelope, and the cortical GFP diffuses throughout the posterior cell's cortex (9 min), reaching an almost uniform distribution right after cell division is finished (>15 min). Immediately after division GFP appears brighter first within the anterior daughter cell nucleus (11.5 min) than in the posterior daughter cell (12.5 min). GFP expression does return to be both nuclear and uniformly cytoplasmic in each daughter cell after division.

3.1.2. Generating a Dendra2::HAM-1 Transgenic Strain

A limitation to assessing inheritance of GFP::HAM-1 during cell division is the inability to distinguish inherited protein from newly synthesized GFP::HAM-1 in daughter cells. A solution would be to use a photo-convertible fluorescent tag such as Dendra2. Dendra2 can be irreversibly photoconverted from a green to a red fluorescent state by excitation of the chromophore with 405 nm light emission. The purpose is to photo-convert, the cortical Dendra2::HAM-1 in dividing cells which will allow me to observe the difference between inherited red Dendra2::HAM-1 and newly synthesized green Dendra2::HAM-1 in the daughter cells. This approach should allow us to characterize any possible preferential inheritance of cortical HAM-1 into the nucleus of either daughter cell.

Therefore, my goal was to generate a Dendra2::HAM-1 transgenic strain. A Dendra2::HAM-1 construct was generated by a two step subcloning process. A previous student had replaced the GFP::HAM-1 sequence in the plasmid pNH144 [UNC-119p::GFP::HAM-1::LET-858 3'UTR] with Dendra2 to generate the intermediate construct [UNC-119p::Dendra-2::EcoR1 cut site::LET-858 3'UTR]. The HAM-1 open reading frame was then ligated into a unique EcoR1 site downstream of Dendra2. I transformed this final ligation mix that had been generated by a previous student (Kasey Stirling) and performed minipreps to isolate plasmid from transformants. Plasmids were then digested with ApaI (NEB). This enzyme was selected as its cut site was asymmetric in the fragment. If HAM-1 was in the forward orientation the digest would generate a 739bp fragment and a 5438 bp fragment. If HAM-1 was in the reverse orientation the digest would generate a 1449bp fragment and a 4728 bp fragment. 'Colony 13' was identified to have HAM-1 ligated in the forward orientation. The plasmid was then miniprepped (Purelink Quick Plasmid Miniprep Kit), concentrated and digested with EcoRV (Invitrogen) to linearize the plasmid. The plasmid was sent for Sanger sequencing (Azenta) using multiple primers (Table 5-2) to validate the entirety of the unc-119 promoter, the unc-119p::Dendra-2 junction, and the Dendra-2::HAM-1 junction. Sequencing results revealed there were no mutations in the construct and that Dendra2 was in frame with *ham-1* (Figure 3-3). This plasmid was injected at a concentration of 50 ng/µl along with a co-injection marker dpy30::dsRed injected at a concentration of 30

nu/µl. These are the same concentrations used in the generation of GFP::HAM-1 transgenic strains (Leung et al., 2016).

Of 21 injected worms, only one transgenic line was obtained. This line produced L1s with morphology defects, that appeared lumpy. However, there was little or no Dendra2::HAM-1 expression except for a few fluorescent puncta in later stage embryos, and a few fluorescent puncta in the tail of L1s. The experiment was repeated using 10 ng/µl plasmid, 30 ng/µl dpy30::dsRed, and 50 ng/µl of a stuffer L4440 plasmid DNA. This yielded five transgenic lines with the same lumpy morphology defect and the same distribution of fluorescent puncta. In both experiments there was no expression that resembled GFP::HAM-1, even though the same promoter was used to drive expression. Since there were also no sequence errors in the construct, there is no explanation for the lack of expression. This experiment was consequently abandoned as we could not discern a method to fix it.

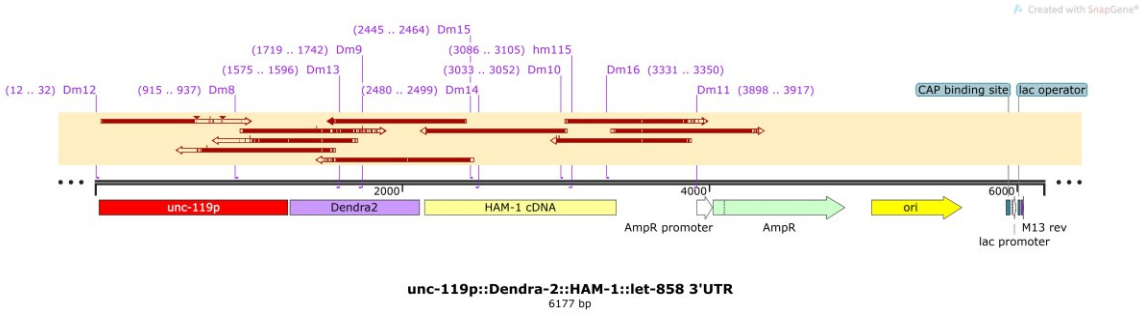

Figure 3-4. Dendra-2::HAM-1 construct and Sequencing Alignment

Alignment of sanger sequencing results (red arrows) from each primer (purple) against the designed UNC-119::Dendra-2::HAM-1::let-858 3'UTR below in Snapgene.

3.2. Investigation of the Requirement for Wnts in HAM-1 dependent Cell Lineages

I have chosen to investigate this requirement in two different cell lineages: the HSN/PHB lineage and the ALN/PLM lineage. These lineages have both been previously used to extensively to study *ham-1* function. Both neuronal lineages divide asymmetrically and produce both apoptotic and neuronal daughter cells. In *ham-1* mutants, there is a predicted anterior to posterior cell fate transformation in both lineages. In the HSN/PHB lineage this results in neuronal duplications while in the PLM

lineage this results in neuronal losses. In each lineage a mutation in *ham-1* causes a cell fate transformation however fates are affected differently, meaning they may have different requirements for *ham-1.* We hypothesize HAM-1 may function to tether cell fate determinants in the HSN/PHB neuroblast causing them to be inherited by the posterior HSN/PHB precursor cell and not the anterior daughter cell which dies. Therefore, to assess if division of the ALN/PLM lineage and the HSN/PHB lineage is dependent on Wnt signalling I can disturb the function of Wnts in a *ham-1* mutant background and score the number of neurons using transcriptional reporters. The PLM lineage can be observed by using the *zdIs5* (mec4::GFP) transgenic reporter strain, which expresses GFP in the PLM neuron. The PHB lineage can be observed by using the *gmIs12* (srb-6::GFP) transgenic reporter strain, which expresses GFP in the PHA/PHB neurons. From these experiments I aimed to determine if loss of Wnt function can enhance or suppress the neuronal fate transformations seen using the transgenic reporters in *ham-1* or GFP::HAM-1 overexpression backgrounds. To accomplish this aim I used a combinations of deletion alleles and RNAi knockdown by micro-injection.

3.2.1. Generation and Validation of Wnt Knockdown by RNAi

To generate the dsRNA for each Wnt I PCR amplified approximately 500 bp of exonic sequence from genomic DNA for each gene using primers with the T7 promoter incorporated at either end. Single stranded RNA was then synthesized, and dsRNA generated by annealing of the two single strands. The yield and integrity of the RNA was assayed by running on an agarose gel. To determine efficacy of knockdown, dilutions of dsRNA were tested by injection into worms followed by scoring of the F1 progeny for phenotypes associated with the null allele (Fig. 3-4).

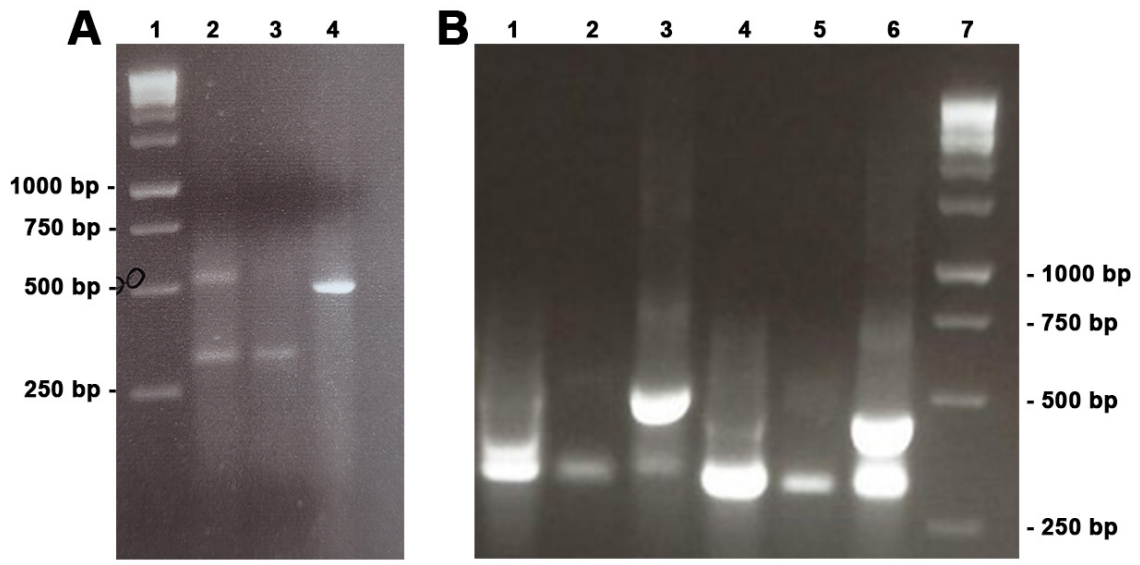

Figure 3-5. Wnt ssRNA shifted upon after annealing to dsRNA as seen on a Agarose Gel

To evaluate synthesis and integrity ssRNA and annealed dsRNA products were compared on a1.8% (w/v) agarose gel against a Generuler 1KB DNA Ladder. (A) Lane 1: Generuler 1KB DNA Ladder, 2: *mom-2* T7F ssRNA, 3: *mom-2* T7R ssRNA, 4: *mom-2* dsRNA. (B) Lane 1: *egl-20* T7F ssRNA, 2: *egl-20* T7R ssRNA, 3: *egl-20* dsRNA, 4: *lin-44* T7F ssRNA, 5: *lin-44* T7R ssRNA, 6: *lin-44* dsRNA, 7: Generuler 1KB DNA Ladder.

mom-2 RNAi

The complete loss of *mom-2* is maternal effect embryonic lethal, however I needed to score both PLM and PHB neurons in L1 larvae. As RNAi knockdown by injection is concentration dependent, I performed multiple injections to find a dilution of the *mom*-2 dsRNA that yielded approximately to 90% embryonic lethality and 10% of animals that hatched into L1s. The 10% “squeakers” that survive can then be scored. My *mom-2* dsRNA was highly effective at causing embryonic lethality. I needed to dilute my stock *mom-2* dsRNA 1/900 before I reliably obtained a low percentage of L1 escapers. Lesser dilutions all yielded 100% lethality in the progeny and a very low brood size indicating *mom-2* knockdown caused some sterility in the parent (Fig. 3-5).

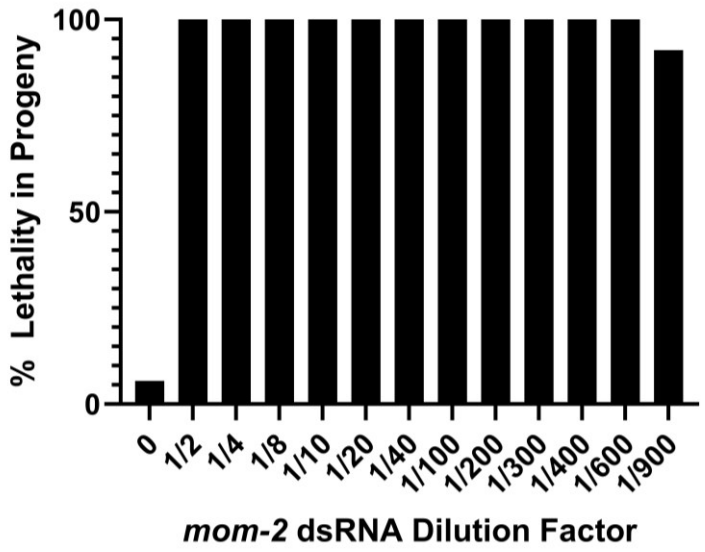

Figure 3-6. A 1/900 dilution of *mom-2* dsRNA is required for 10% viability of progeny in *zdIs5 animals (n<20)*.

Each dilution injected into 10-15 *zdIs5* worms and n progeny scored for percentage of lethality. Control *zdIs5* 6% (n=285), 1/2 100% (n=18), 1/4 100% (n=11), 1/8 100% (n=16), 1/10 100% (n=22), 1/20 100% (n=13), 1/40 100% (n=14), 1/100 100% (n=14), 1/200 100% (n=23), 1/300 100% (n=15), 1/400 100% (n=21), 1/600 100% (n=15), 1/900 92% lethality (n=151).

lin-44 RNAi

I measured *lin-44* knockdown by performing a Dye Fill assay. The T cell in *C. elegans* is one of the seam cells in the tail that divides asymmetrically. The anterior daughter (T.a) produces hypodermal cells, and the posterior daughter (T.p) generates neural cells (Sulston and Horvitz, 1977). The polarity of the T cell is regulated by lin-44/Wnt and lin-17/Fz (Herman et al., 1995, Sawa et al., 1996). In *lin-44*/Wnt, *lin-17*/Fz, *wrm-1*/β-catenin, or *lit-1*/MAPK mutants, both daughters of the T cell adopt the normal hypodermal fate of T.a, resulting in the loss of phasmid socket cells derived from T.p (Mizumoto & Sawa, 2007). In wildtype worms these phasmid socket cells in the tail are open to the environment and so when worms are soaked with dye they will be filled. If *lin-44* is sufficiently knocked down, we see a failure of the phasmid socket cells to fill (Fig 3-6). Because the undiluted dsRNA is so concentrated there is a propensity for the RNA to clog the injection needles. Therefore, I tested two different dilutions of my dsRNA stock into *zdIs5*; 1/3 (85%, n = 120) and 1/5 (62%, n = 88). Both dilutions resulted in a

highly penetrant dye filling defect indicating robust knockdown of *lin-44*. This assay proved that there is a dsRNA concentration dependent effect on *lin-44* knockdown. All subsequent injections of *lin-44* dsRNA occurred at an 1/3 dilution of the new dsRNA stock.

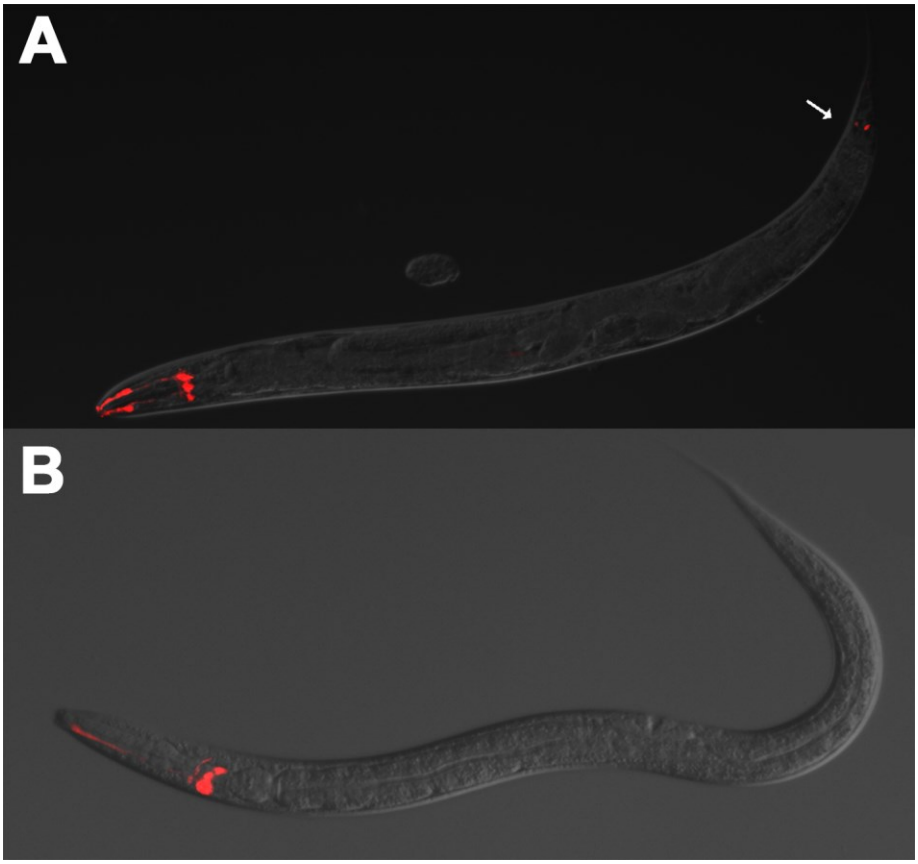

Figure 3-7. Dye filling of wild-type and *lin-44* knockdown *zdIs5*
Double exposure of bright-field and fluorescence images of Dye (DiI) filling of (A) a *zdIs5* hermaphrodite and (B) a *zdIs5* hermaphrodite after *lin-44* knockdown by RNAi. The fluorescence in the anterior shows dye-filling of the amphids. The fluorescence in the posterior of the hermaphrodite shows dye-filling of the phasmids (arrow). The phasmids of *lin-44* knockdown hermaphrodites do not fill while the amphids still do.

egl-20 RNAi

Like *lin-44,* knockdown of EGL-20 was able to be validated by phenotype, as *egl-20* worms display an EGL egg laying defective phenotype (Fig. 3-7). This phenotype occurs when the animal is defective in egg laying and retains its eggs (Trent et al., 1983). A dilution 1/3 of the new preparation of *egl*-20 dsRNA was sufficient to achieve at

least 80% (n = 106) egg laying defective worms in the progeny of injected worms into *zdIs5.*

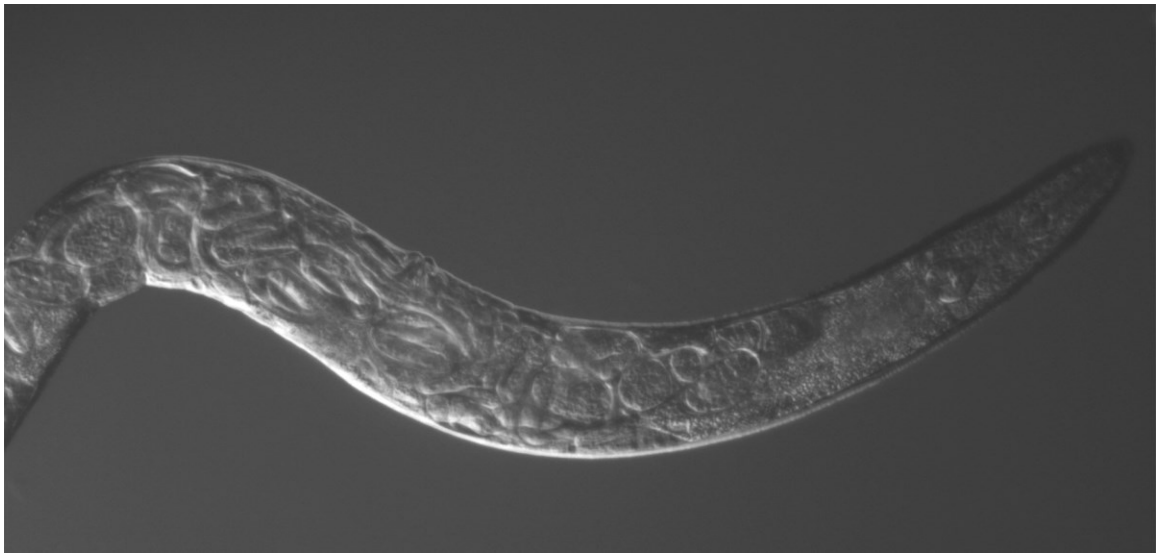

Figure 3-8. Egg laying defective phenotype of a *zdIs5* worm after *egl-20* knockdown by RNAi

Brigh-tfield image at 20x magnification of a *zdIs5* hermaphrodite displaying an egg laying defective phenotype after *egl-20* knockdown using RNAi. Posterior is left, anterior and head is right. Build up of developed embryos seen in mid-body of worm.

3.2.2. Analysis of the requirement for Wnts in the generation of the PLM neuron

To determine if Wnts are required for asymmetric division in the PLM lineage I used the *mec-4::GFP* reporter transgene *zdIs5* to visualize the PLM neuron. There is an 80% PLM neuronal loss in *ham-1* mutants. I wanted to determine if loss of Wnt function also resulted in a change in the number of PLM neurons. Overexpression of *ham-1* from the integrated array *hkIs39*[GFP::HAM-1] results in the opposite phenotype; PLM duplication. Thus, I also tested if loss of Wnt function could suppress or enhance this overexpression phenotype. Finally, I tested whether loss of Wnt function could enhance of suppress a *ham-1* null mutation.

Analysis of Wnt Requirement for Asymmetric Cell Division in Wildtype PLM Lineage

To achieve Wnt knockdown 1/3 dilutions of *egl-20* and *lin-44* along with 1/900 *mom-2* were individually microinjected into healthy young adult worms. The efficacy of each injection was monitored by scoring their associated dissecting scope phenotypes in the progeny. As there are no assays or dissecting scope phenotypes for loss of *cwn-1* or *cwn-2*, I performed genetic crosses to generate *hkIs39*[GFP::HAM-1]; *zdIs5*[mec4::GFP], and *zdIs5*[mec4::GFP] strains containing *cwn-1* and/or *cwn-2* deletion alleles. I then scored the strains for PLM neuronal duplication or losses. I determined that the loss of any each Wnt or even *cwn-1* and *cwn-2* together does not affect production of the PLM neuron in the *zdIs5* background (Fig. 3-8).

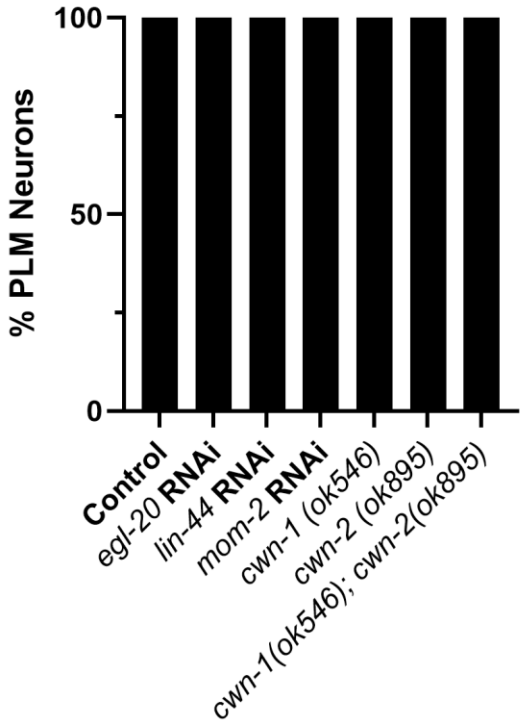

Figure 3-9. Wnt RNAi or Deletion Allele strains have no significant effect on PLMs in *zdIs5*

No RNAi control strain *zdIs5* 100% PLM (n=100), 1/3 *egl-20* RNAi 100% PLM (n=111), 1/3 *lin-44* 100% PLM (n=102), 1/900 *mom-2* RNAi 100% PLM (n=103), *zdIs5; cwn-1(ok546*) 100% PLM duplication (n=104), *zdIs5; cwn-2(ok895)* 100% PLM duplication (n=110). All experimental results were not significant (P > 0.05) by Chi Square analysis.

Analysis of Wnt Requirement for the HAM-1 PLM Overexpression Phenotype

All individual Wnt knockdowns or deletion alleles in the *zdIs5; hkIs39* HAM-1 overexpression background had no significant effect on the PLM duplication phenotype. (Fig. 3-9).

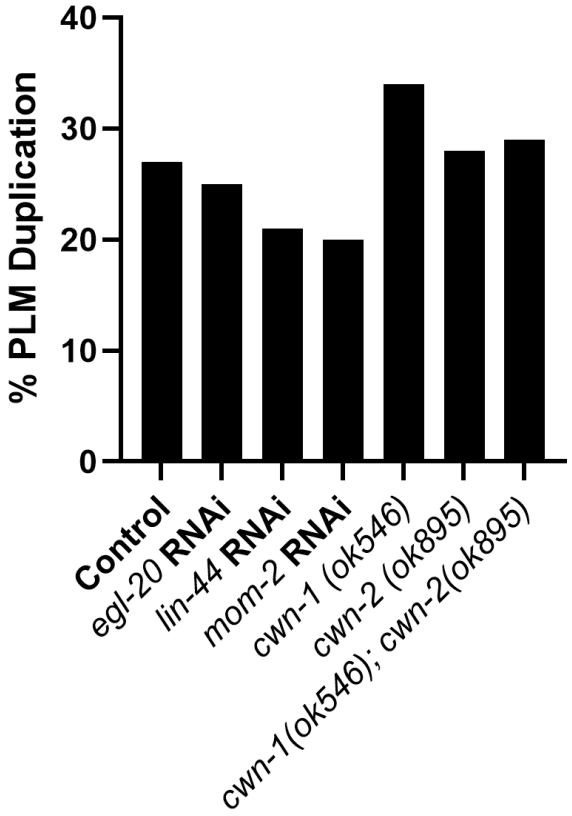

Figure 3-10. Wnt RNAi or Deletion Allele strains have no significant effect on PLM duplication in *zdIs5; hkIs39*

No RNAi control strain *zdIs5; hkIs39* 27% PLM duplication (n=100), 1/3 *egl*-20 RNAi 25% PLM duplication (n=120), 1/3 *lin-44* 22% PLM duplication (n=101), 1/900 *mom-2* RNAi 20% PLM duplication (n=100), *zdIs5; hkIs39; cwn-1(ok546*) 34% PLM duplication (n=100), *zdIs5; hkIs39; cwn-2(ok895)* 28% PLM duplication (n=100). All experimental results were not significant (P > 0.05) by Chi Square analysis.

Multiple Wnt knockdown was achieved by performing RNAi into the *cwn-1(ok546)* and *cwn-2(ok895)* null backgrounds. The data revealed Wnt knockdown combinations with *egl-20* and *lin-44* are cause the greatest effect on the PLM overexpression phenotype. Knockdown of *egl-20* and *lin-44* individually, into the *cwn-1; cwn-2* deletion background both rescue the overexpression phenotype to 18% and 12%, respectively (Fig 3-10, 3-11). Surprisingly, our hypothesis was that reducing function of *cwn-1, cwn-2* and *mom-2* together could show the greatest effect on the PLM duplication phenotype, as they are expressed in the embryo at the same time as many *ham-1* related cell divisions are occurring (Kaur et al., 2020). However, knockdown of *mom-2* in the *cwn-1; cwn-2* null background did not significantly change the overexpression phenotype (Fig 3-12).

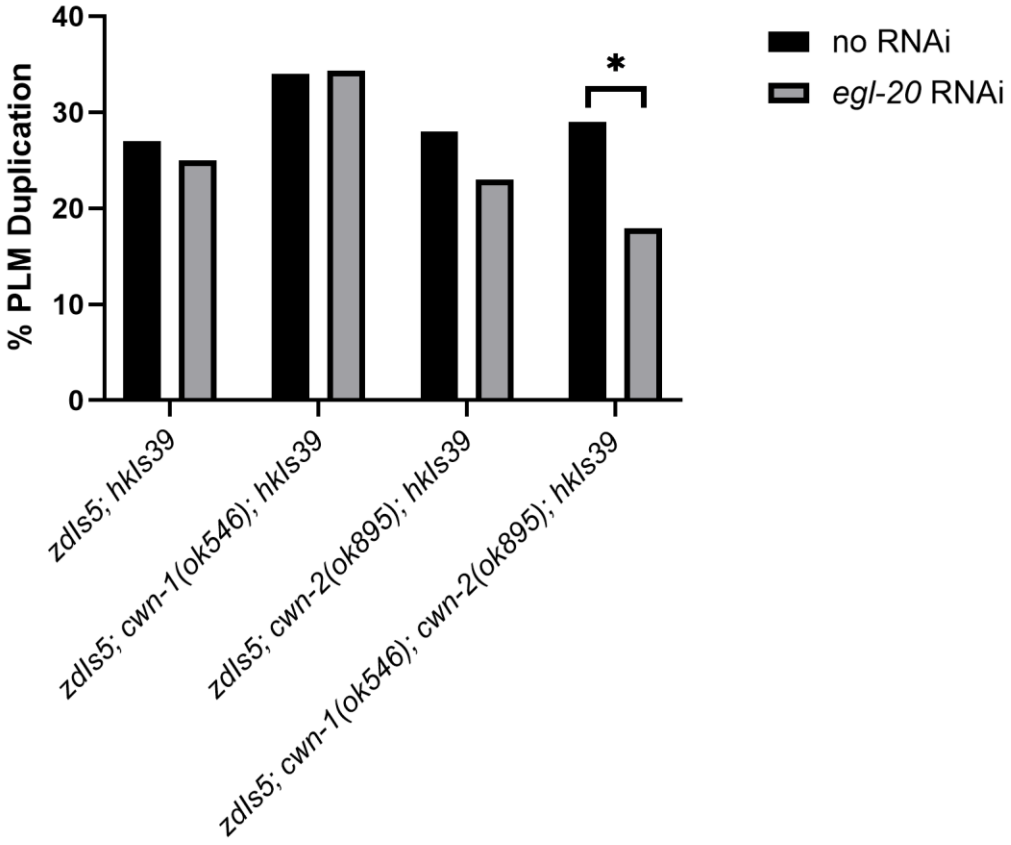

Figure 3-11. *egl-20* RNAi effect on PLM Phenotype in *zdIs5; hkIs39*

No RNAi control *zdIs5; hkIs39* 27% PLM duplication (n=100) and experimental 1/3 *egl-20* RNAi 25% PLM duplication (n=120). Control *zdIs5; hkIs39; cwn-1(ok546*) 34% PLM

duplication (n=100) and experimental 1/3 *egl-20* RNAi 34% PLM duplication (n=108). *zdIs5; hkIs39; cwn-2(ok895)* 28% PLM duplication (n=100) and experimental 1/3 *egl-20* RNAi 23% PLM duplication (n=100). *zdIs5; hkIs39; cwn-1(ok546); cwn-2(ok895)* 29% PLM duplication (n=100) and experimental 1/3 *egl-20* RNAi 18% PLM duplication (n=128). Not significant (ns = P > 0.05) and * P ≤ 0.05 by Chi Square analysis.

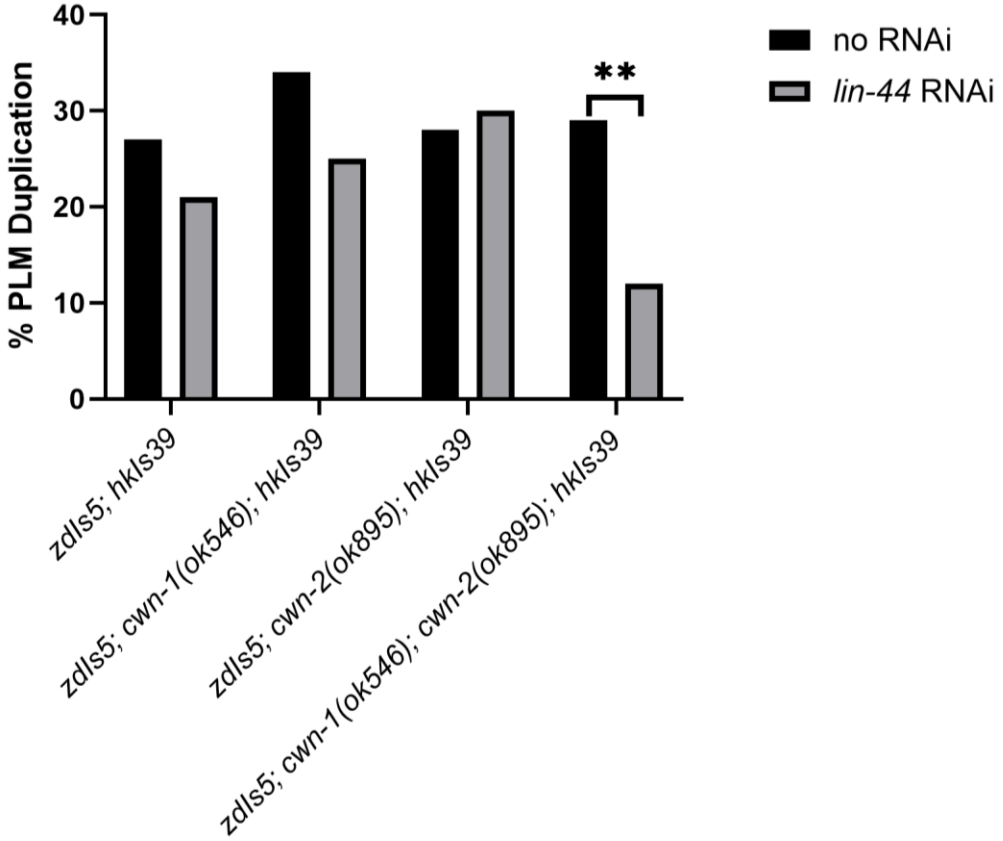

Figure 3-12. *lin-44* RNAi effect on PLM Phenotype in *cwn-1(ok546) and cwn-2(ok895)* backgrounds

No RNAi control strain *zdIs5; hkIs39* 27% PLM duplication (n=100) and experimental 1/3 *lin-44* RNAi 22% PLM duplication (n=101). Control *zdIs5; hkIs39; cwn-1(ok546*) 34% PLM duplication (n=100) and experimental 1/3 *lin-44* RNAi 26% PLM duplication (n=127). *zdIs5; hkIs39; cwn-2(ok895)* 28% PLM duplication (n=100) and experimental 1/3 *lin-44* RNAi 31% PLM duplication (n=100). *zdIs5; hkIs39; cwn-1(ok546); cwn-2(ok895)* 29% PLM duplication (n=100) and experimental 1/3 *lin-44* RNAi 12% PLM

duplication (n=100). not significant (ns = P > 0.05) and ** P ≤ 0.01 by Chi Square analysis.

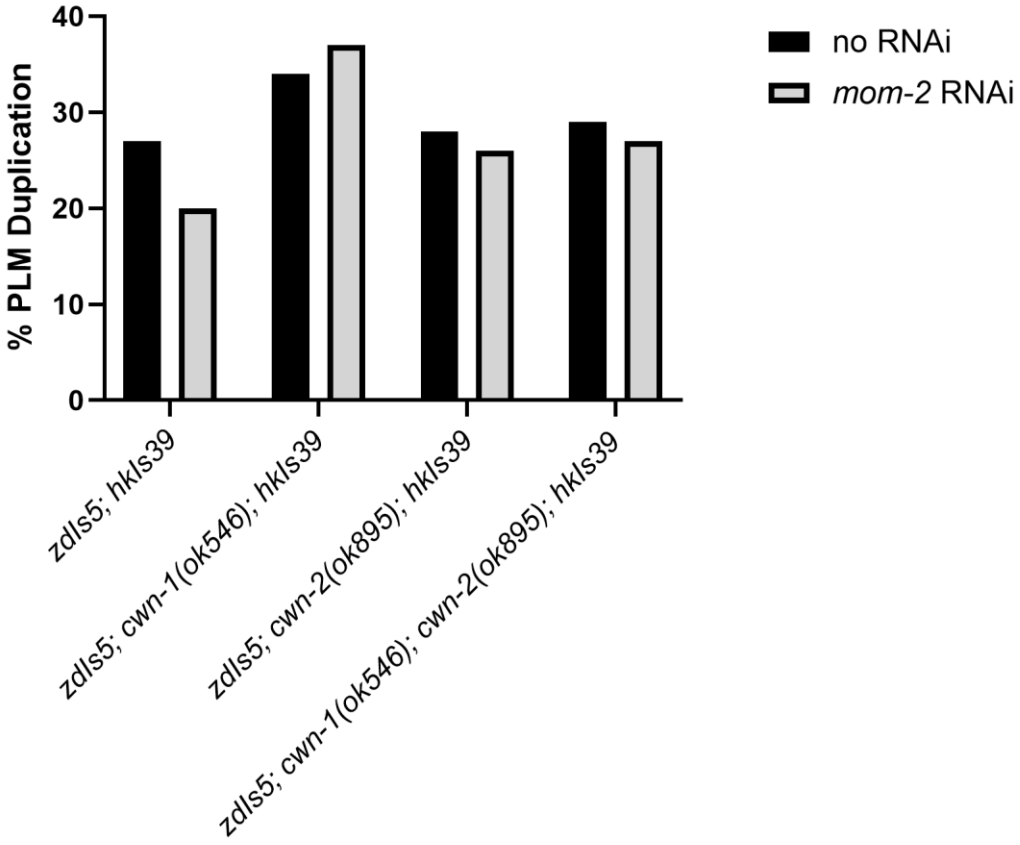

Figure 3-13. *mom-2* RNAi effect on HAM-1 overexpression PLM Phenotype
No RNAi control strain *zdIs5; hkIs39* 27% PLM duplication (n=100) and experimental 1/900 *mom-2* RNAi 20% PLM duplication (n=100). Control *zdIs5; hkIs39; cwn-1(ok546*) 34% PLM duplication (n=100) and experimental 1/900 *mom-2* RNAi 37% PLM duplication (n=116). *zdIs5; hkIs39; cwn-2(ok895)* 28% PLM duplication (n=100) and experimental 1/900 *mom-2* RNAi 26% PLM duplication (n=100). *zdIs5; hkIs39; cwn-1(ok546); cwn-2(ok895)* 29% PLM duplication (n=100) and experimental 1/900 *mom-2* RNAi 27% PLM duplication (n=100). All experimental results were not significant (P > 0.05) by Chi Square analysis.

Analysis of Wnt Requirement for PLMs in a ham-1 null mutant

In a *ham-1* null background we see a penetrant 86% loss of the PLM neurons (Fig. 3-13). Knockdown of *egl-20, lin-44* and *mom-2* by RNAi into a *ham-1(gm279)* null background revealed that *mom-2* significantly rescues the PLM loss phenotype to 75%. However, the knockdown of either *egl-20* or *lin-44* had no significant effect on the PLM loss phenotype.

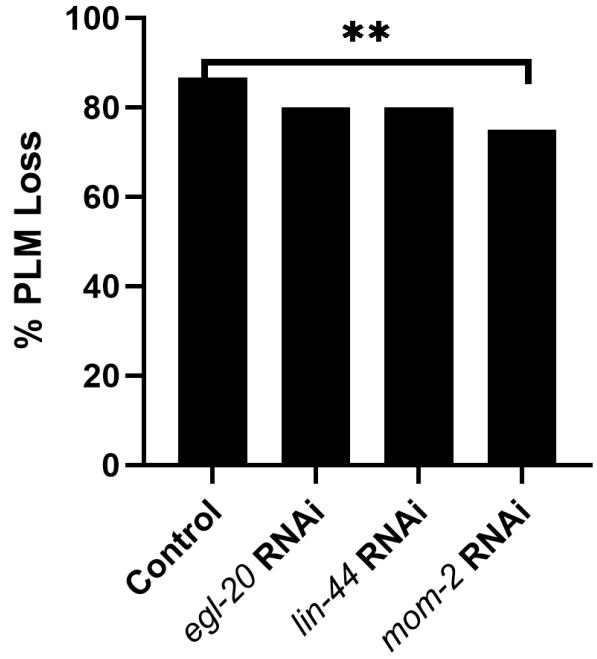

Figure 3-14. Single Wnt RNAi in *zdIs5; ham-1 (gm279)*

No RNAi control strain *zdIs5; ham-1(gm279)* 86% PLM loss (n=188), 1/3 *egl-20* RNAi 80% PLM loss (n=118), 1/3 *lin-44* RNAi 80% PLM loss (n=114), 1/900 *mom-2* RNAi 75% PLM loss (n=186). ** P ≤ 0.01 by Chi Square analysis.

Double Wnt Injection Mix is Ineffective by Phenotype

As combinations with *egl-20* or *lin-44* RNAi had the greatest effect on the PLM duplication phenotype, achieving knockdown of both together was the obvious next step. To evaluate the effects of both *lin-44 and egl-20* knockdown together I tried to mix the two dsRNA stocks to perform a simultaneous knockdown. I prepared mix containing a final dilution of 1/3 for each *lin-44* and *egl-20* and then performed injections into *zdIs5; hkIs39.* I then assayed *egl-20* knockdown and *lin-44* dye fill phenotypes in the progeny.

Injected progeny produced minimal egg laying defective phenotypes and dye fill defective worms compared to control injections of the independent 1/3 dsRNA dilutions (Fig 3-14). It appears that mixing dsRNA for injection unfortunately had an inhibitory effect and could not be used.

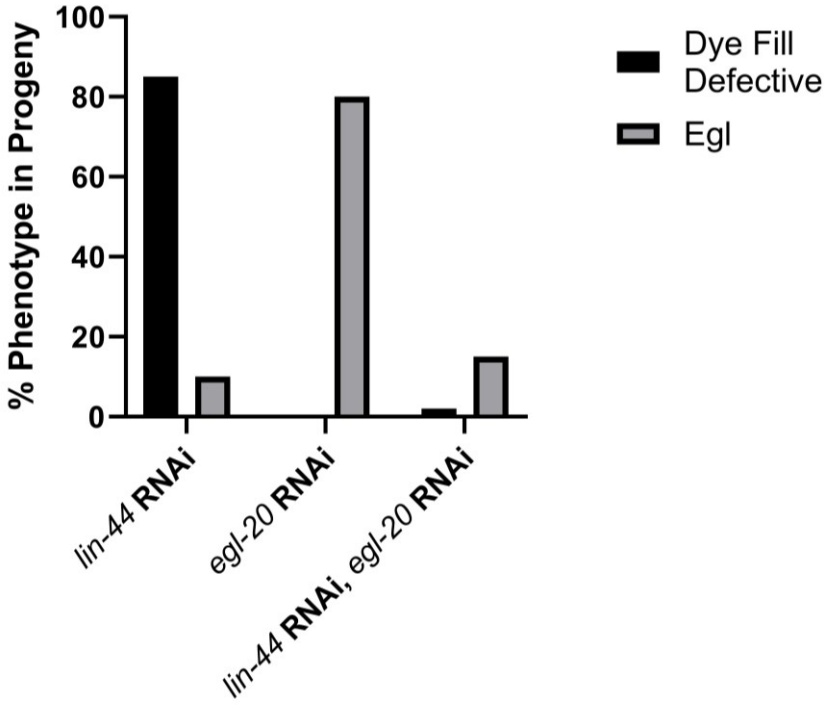

Figure 3-15. Mixed *lin-44* and *egl-20* dsRNA injections into *zdIs5; hkIs39* are ineffective at causing knockdown, as assessed by phenotypic analysis

zdIs5; hkIs39 with validated 1/3 *lin-44* dsRNA produces 85% dye fill defective progeny and 10% egl progeny (n=112). *zdIs5; hkIs39* with validated 1/3 *egl20* dsRNA produces 0% dye fill defective progeny and 80% egl progeny (n=86). *zdIs5; hkIs39* with validated mixed 1/3 *lin-44 and egl-20* dsRNA produces 2% dye fill defective progeny and 15% egl progeny (n=126).

3.2.3. Analysis of the requirement for Wnts in the generation of the PHB neuron

Analysis of Wnt Requirement for Asymmetric Cell Division in Wildtype PHB Lineage

To assess the Wnt requirement in the PHB lineage I investigated the effects of Wnt knockdown in two available strains: the wildtype *gmIs12* and *gmIs12; ham-1* null strain. Loss of *ham-1* results in an asymmetric division defect in the lineage that generates the PHB sensory neuron. The PHB neuron can be visualized in the transgenic strain *gmIs12* [srb-6::GFP]. This strain expresses GFP in both the PHA and PHB neurons. The PHA neuron is derived from an unrelated lineage to the PHB neuron and is unaffected in a *ham-1* mutant. Thus, wild type animals have two GFP expressing neurons on each side of the animal. In a *ham-1* mutant 1 cell indicates a PHB loss while 3 cells indicate a duplication of the PHB cell. I determined that the loss of any each Wnt does not affect production of the PHB in a *gmIs12* background (Fig. 3-15).

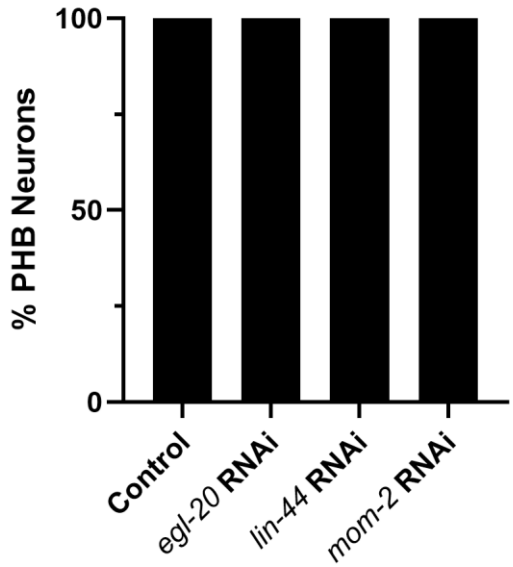

Figure 3-16. Wnt RNAi or Deletion Allele strains have no significant effect on PHBs in *gmIs12*

No RNAi control *gmIs12(srb-6::GFP)* 100% PLM (n=100), 1/3 *egl*-20 RNAi 100% PLM (n=100), 1/3 *lin-44* 100% PLM (n=100), 1/900 *mom-2* RNAi 100% PLM (n=96). All experimental results were not significant (P > 0.05) by Chi Square analysis.

Analysis of Wnt Requirement for Asymmetric Cell Division in ham-1 null PHB Lineage

Finally, RNAi by injection was also used to knock own the function of *lin-44*, *egl-20* and *mom-2* in *gmIs12; ham-1(gm279)*. Like previously published results, loss of *ham-1* resulted in a 33% duplication of a phasmid neuron as well as a small percentage of neuronal loss (Frank et al., 2005). Knockdown of both *mom-2* and *lin-44* resulted in a suppression of the *ham-1* loss phenotype (Fig. 3-16). In contrast, knockdown of *egl-20* did not have a significant effect on the *ham-1* loss phenotype.

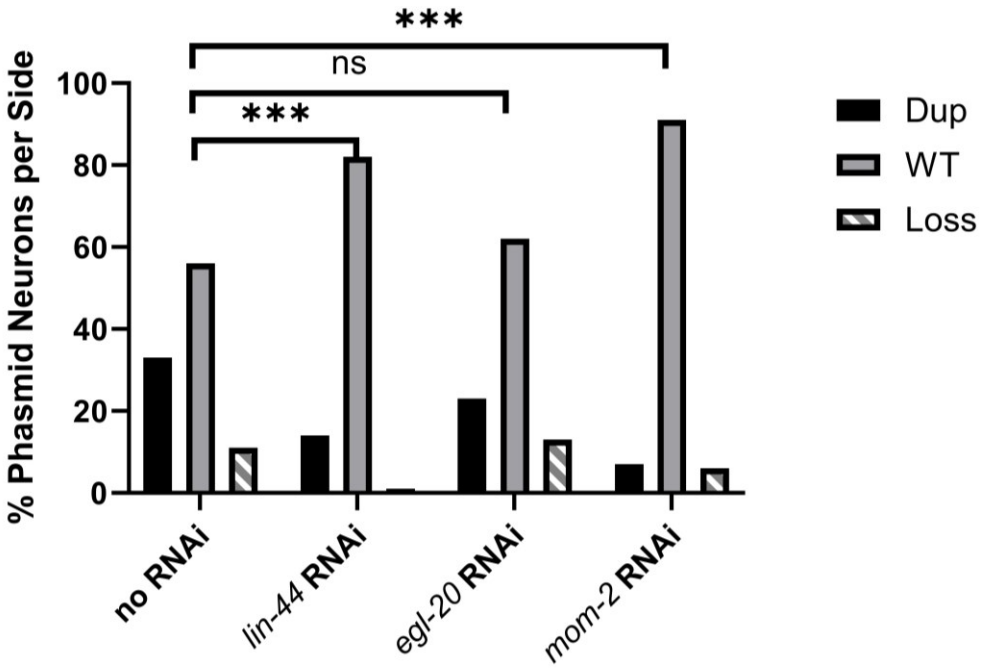

Figure 3-17. Single Wnt Knockdown in *gmIs12; ham-1(gm279)*

No RNAi control *gmIs12(srb-6::GFP); ham-1(gm279)* 33% Duplication, 56% WT, 11% loss of PHBs n=100, 1/3 *lin-44* RNAi 14% Duplication, 82% WT, 4% loss of PHBs n=136, 1/3 *egl-20* RNAi 24% Duplication, 63% WT, 13% loss of PHBs n=134, 1/900 *mom-2* RNAi 9% Duplication, 90% WT, 4% loss of PHBs n=100. Not significant (ns = $P > 0.05$) and *** $P \leq 0.001$ by Chi Square analysis.

3.3. Approach to Investigate HAM-1 Interacting Proteins

The function of HAM-1 is largely unknown. The identification of interacting proteins could lend insight into how HAM-1 is asymmetrically localized at the cell cortex, and the transcriptional machinery it may interact with in the nucleus. I designed a coimmunoprecipitation approach to identify interacting proteins. For this approach the goal was incorporate a 3xMYC tag into the N-terminus of *ham-1* by a CRISPR/Cas9 method. The 3xMYC::HAM-1 fusion protein would be immunoprecipitated using Chrom-Tek's Myc trap and the interacting proteins identified by mass spectrophotometry in collaboration with Dr. Bingyun Sun.

3.3.1. Insertion of N-Terminal 3xMYC tag in HAM-1 by CRISPR/Cas9 for Co-IP

The biochemist Jennifer Doudna and microbiologist Emmanuelle Charpentier co-invented the gene-editing system CRISPR-Cas9 in 2012. Krishna Ghanta and Craig Mello adapted the effective precision genome editing technique in *C. elegans.* Their adapted protocol takes advantage of homology-directed repair (HDR), a natural process that requires cells to use exogenously supplied DNA templates to repair targeted double-strand breaks. The N-terminal 3xMYC repair template was made by PCR of a 3xMYC Geneblock using primers to add 35 bp flanking *ham-1* homology arms containing a mutant PAM site. The mutant PAM site is necessary to prevent cutting of the fragment by the Cas9 protein. The flanking homology arms included 5' triethylene glycol (TEG) modifications, that have been found to consistently increase the frequency of precision editing (Ghanta et al., 2021). The repair template was made using PCR to include *ham-1* homology arms upstream and downstream of the *ham-1* ATG start site. A Stitch PCR was performed to generate a negative control made of the 3xMyc sequence, a stop codon, the *unc-54* 3'UTR and flanking *ham-1* homology arms containing the mutant PAM site and 5'TEG modifications. This acts as a negative control by introducing a stop codon in the *ham-1* sequence followed by the *unc-54* 3'UTR to create a *ham-1* null phenotype. The experimental Stitch PCR schematic is outlined in (Fig. 3-17).

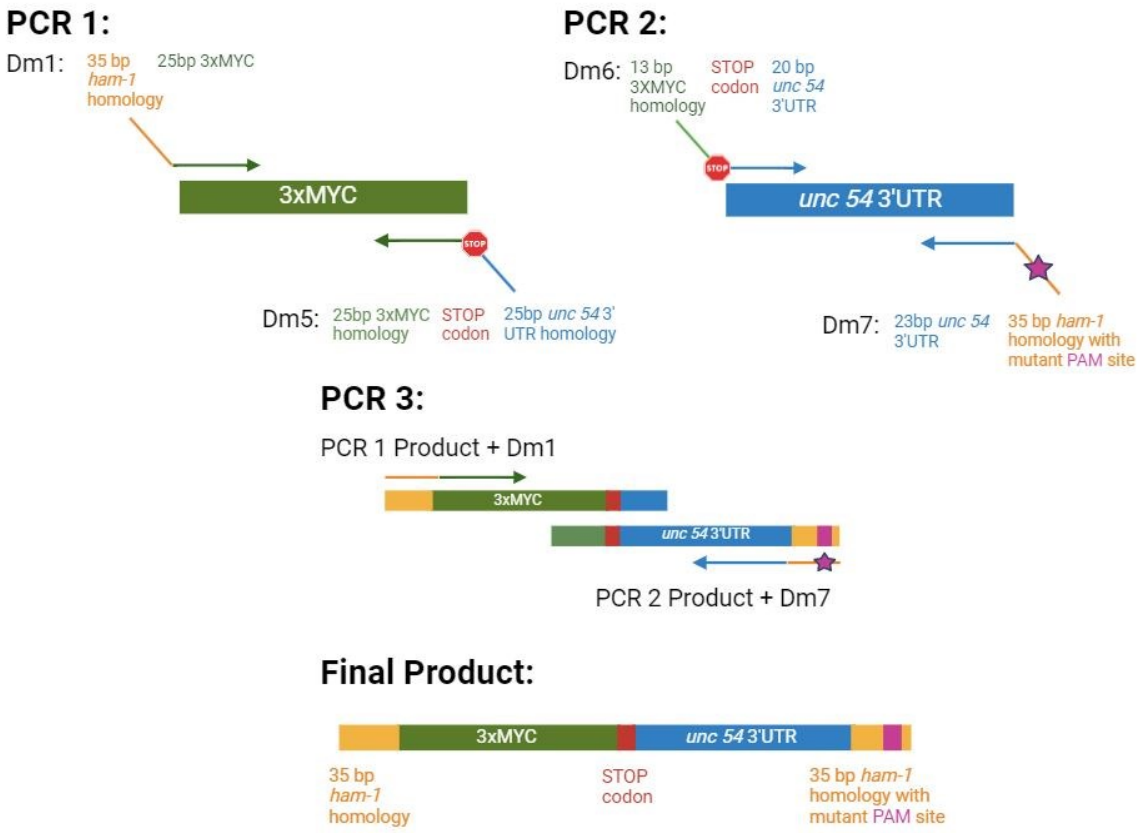

Figure 3-18. Stitch PCR Schematic for Generation of a Negative Control
A stitch PCR was performed to "stitch" two PCR products together to synthesize the negative control repair template containing a 3xMYC tag, a TAG stop codon, and the *unc-54* 3'UTR with flanking *ham-1* homology arms.

Micro-injections were performed in young adult N2 worms by Dr. Hawkins. The injection mix contained the repair template, Cas9, the guide RNA and a co-injection marker *rol*-6. The repair template was melted and re-annealed before use as it has been shown to increase CRISPR-mediated homology directed repair to as high as 50% in the post-injection progeny (Ghanta & Mello, 2020). As most insertions are found to occur later in the brood, wells of injected worms producing the highest number of rolling progeny were used to clone 48 F1 non-rolling younger progeny (Ghanta & Mello, 2020). Ten F2 worms from each F1 clone were then lysed to isolate DNA. A three-primer PCR system was used to detect any negative, heterozygous, and homozygous edits in the worm lysates. No CRISPR edits were found by PCR, however eight F2 wells displayed a slight egg laying defective phenotype or notched tail phenotype which are known *ham-1* mutant phenotypes. DNA from each of these wells was sent for Sanger sequencing

along with N2 DNA (Fig. 3-18). While none of these worms had the intended repair template integrated, they did have small 1-3 amino acid deletions at the intended Cas9 cut site. In the case of sample 8 there was a larger insertion of unknown origin. Its sequence did not align to any repair template or sequence within *ham-1*. Samples 2, 3, 4 shared the same (CTC >G--) mutation. Worms from sample 3 were frozen and added to the Hawkins worm collection as the strain had no other point mutations. These deletions and insertions demonstrated that while the experiment was not successful, the guide selected and the Cas9 enzyme were at least effective. After troubleshooting, it was determined that the concentration of the repair template was 100x too low.

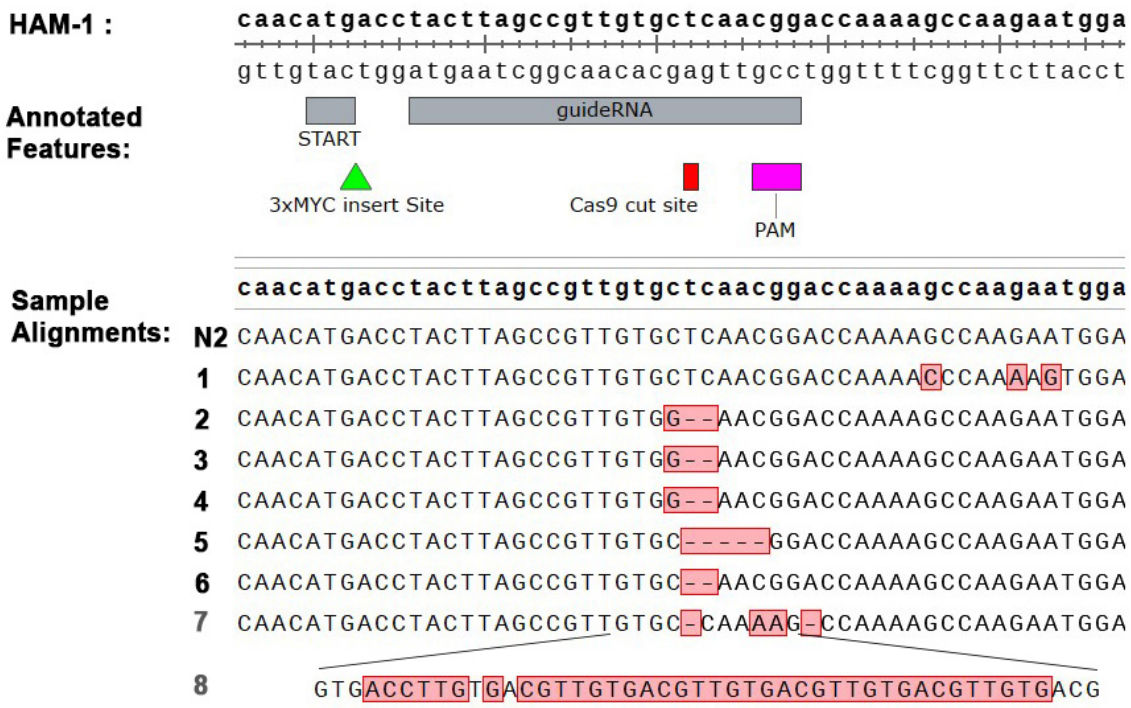

Figure 3-18. Sequencing DNA alignments from eight CRISPR Progeny against *ham-1*.

Samples sequenced using forward primer DM3 aligned to *ham-1* sequence. Features labeled in *ham-1* sequence. Alignment data of eight mutant progeny from CRISPR/Cas9 experimental repair template injections, mutations highlighted in red. Viewed using Snapgene (https://www.snapgene.com/).

Chapter 4. Discussion

4.1. HAM-1 is in the nucleus and becomes asymmetrically localized during cell division

My first aim was to visualize the localization of HAM-1 by following GFP::HAM-1 expression in transgenic embryos using 4D microscopy on a spinning disc microscope. The purpose of this aim was to further characterize HAM-1 dynamics during mitosis. Using anti-HAM-1 antibodies the protein is detected around the cell cortex in interphase cells. During mitosis it is detected in a crescent at the posterior cell cortex. In addition to the cortical localization, nuclear expression was detected from a GFP::HAM-1 transgene (Leung et al., 2016). However there have been no experiments performed to monitor HAM-1 inheritance after division. My work determined that GFP::HAM-1 is within the nucleus of cells prior to division, becomes asymmetrically localized to the posterior cell cortex during division and appears to remain brighter in the cortex of the posterior daughter after division. Therefore, my findings build on the previously published work. This pattern suggests that the localization of GFP::HAM-1 to the posterior cortex before division could be a mechanism to ensure its greater inheritance to the posterior daughter cell. Ultimately, I would have liked to ascertain an understanding of the relationship between cortical and nuclear HAM-1. With a greater number of acquisitions, I would have liked to identify if cortical HAM-1 eventually translocates to the nucleus of the daughter cell, or if it remains at the cell cortex. Perhaps the cortical localization is a mechanism to keep HAM-1 out of the daughter cell nucleus. These different localization patterns may reveal more about HAM-1 and it's potential for function in both the nucleus and the cell cortex.

There are limitations to be learned about HAM-1 localization by using the GFP::HAM-1 construct. The transgenic strain *hkIs39(unc-119p:GFP::HAM-1*) was created by integration of an extrachromosomal array expressing a functional GFP::HAM-1 fusion protein. The construct consists of GFP fused to the N-terminus of the full-length HAM-1 open reading frame. At the time the *ham-1* promoter was not identified, and so the *unc-119* promoter was used to regulate expression. UNC-119 is a promoter, its expression is known to begin at the 60-cell stage of embryogenesis and is observed broadly throughout many neuronal lineages (Maduro, 2015). Due to these properties it is

fair to question if GFP::HAM-1 localization is an artifact of overexpression due to it being an integrated array. However, GFP::HAM-1 cortical expression was consistent with previous immunostaining performed and a sub cellular nuclear fractionation study confirmed its presence in both the cytoplasm and nucleus (Leung et al., 2016). The strain containing GFP::HAM-1 driven by the *ham-1* promoter from (Feng et al., 2013b) could be ordered to observe its proposed endogenous expression. However, a construct containing the potential promoter region of HAM-1 (3kb region upstream of the HAM-1 start site) was tested to replicate known HAM-1 antibody staining in the Hawkins lab. This construct did not provide consistent expression with what was seen previously (Hawkins, unpublished).

Initial 4D acquisitions performed using *hkIs39* embryos were challenging due to several factors. Focal drift would occur over the course of acquisition due to evaporation of the agarose pad over time. To correct this a new mounting protocol from (Hardin, 2011) was followed, which uses VALAP and provides a better seal for the coverslip. VALAP is a mix of equal parts by volume of Vaseline, lanolin, and paraffin that is heated until homogenized and when cools acts as a non toxic sealant. The total length of the acquisition was limited by the integrity of the embryo and fluorophore, which would degrade and photo-bleach with exposure to higher laser power as time went on. The actual acquisition of the dividing cells and their daughters was limited by cell size and the plane of cell division. GFP::HAM-1 fluorescence is first expressed in early gastrulation while cells are still large however the resolution quickly decreased as division occurred and cell sizes decreased. This limited resolution also proved to pose a challenge in discerning GFP::HAM-1 fluorescence between cells that appear to be touching. To have time to observe two acquisitions per minute the depth of the z-stack was limited to 15 µm. This limited depth meant that during division daughter cells with an uneven plane of division would often fall out of the range of acquisition. To work around these factors, multiple acquisitions were performed to increase the chance of catching a division that occurred within the limited depth. In the future more imaging can be performed with the improved protocol.

The GFP::HAM-1 strain allowed us to follow HAM-1 during mitosis, however it does not allow us to differentiate newly synthesized HAM-1 from inherited HAM-1 in the daughter cell. One approach you could take to discern this is to photo bleach the GFP::HAM-1 crescent at the posterior cortex and then monitor GFP::HAM-1

fluorescence within the daughter cells. However, the better option to discern inherited GFP::HAM-1 from newly synthesized GFP::HAM-1 is to use a photoconvertible fluorescent tag, like Dendra2. Dendra2 is a fluorescent protein that shifts from green to red upon photoactivation with violet light. It has been previously used in studies to track study intracellular protein dynamics (Chudakov et al., 2007). Using a Dendra2::HAM-1 construct, one could photoconvert the cortical portion such that after mitosis newly synthesized protein (green) would be easily discernable from inherited protein (red) in the daughter cell. This specific inheritance information would help to further characterize the role of HAM-1 function both at the cell cortex and within the nucleus during mitosis. Therefore, I generated a Dendra2::HAM-1 construct and injected it into N2 worms to generate transgenic lines. This construct was identical to the GFP::HAM-1 construct except GFP was replaced with Dendra2. However transgenic progeny did not share a GFP fluorescence pattern similar to GFP::HAM-1 expressed under the same UNC-119 promoter. Multiple sanger sequencing alignments revealed no mutations within the UNC-119 promoter, Dendra2 sequence or the HAM-1 sequence. Going forward, this would still be the most ideal experiment to study HAM-1 inheritance. Another way to continue it would be to use a CRISPR/Cas9 approach to insert Dendra2 into the endogenous HAM-1 locus. This would be a useful tool to tell us both the endogenous expression patterns of HAM-1 and discern the inheritance of HAM-1.

The only other transcription factor that shares a similar localization pattern to the cell cortex is Prospero, in *Drosophila*. Prospero was determined to alter its subcellular localization in a cell-cycle dependent manner via an immunofluorescence experiment (Hirata et al., 1995). During interphase Prospero is faintly detected within the cytoplasm. During mitosis Prospero is tethered to the basal cortex and becomes inherited by basal daughter of mitotic CNS neuroblasts. Within the basal daughter Prospero translocates to the nucleus and where it is necessary for differentiation. However, there are several differences between HAM-1 and Prospero. In the lineage the generates the HSN and PHB neurons, HAM-1 is asymmetrically localized to the posterior cell cortex of the HSN/PHB neuroblast. However, it is not the fate of the posterior daughter that is affected, but the fate of the anterior daughter that does not inherit the protein (Guenther & Garriga, 1996). Additionally, there is no evidence that Prospero affects positioning of the mitotic spindle.

The N-terminus of HAM-1 shares 33% sequence similarity to the human transcription factor STOX1 (Storkhead box 1) (Leung et al., 2016). STOX1 has been implicated in early onset pre-eclampsia, and late onset Alzheimer's, where its expression was found to correlate with the severity of the disease (Van Dijk et al., 2010). STOX1 has two isoforms, STOX1A and STOX1B. STOX1A is the full-length isoform, including the DNA-binding domain and a transactivating domain. It is involved in transcriptional regulation across various biological contexts such as autoimmune diseases and cancer (Jin et al., 2021)(Ducat et al., 2020). It plays a critical role in trophoblast cell proliferation and migration and has also been seen to influence the PI3K/Akt signaling pathway, which impacts apoptosis (Li et al., 2019). Conversely, STOX1B is a shorter variant that contains only the DNA- binding domain of STOX1A (Ducat et al., 2020). A ChIP-Seq study of STOX1A in the neuroblastoma cell-line SK-N-SH identified thirteen genes of which STOX1A was positioned directly in known promoter regions (van Abel et al., 2011). Notably these genes included the human Wnt ligand WNT2B. STOX1A has been seen in both the cytoplasm and the nucleus of brain and placenta cells (van Dijk et al., 2010). Unlike HAM-1 STOX1A has not been observed at the cell cortex or to be polarized during division. STOX2, is not as well studied as its human paralogue STOX1. It is primarily studied in placental development, with its abnormal expression linked to preeclampsia and even oral squamous cell carcinoma progression (Sasahira et al., 2016) (Fenstad et al., 2010).

4.2. Wnt function is required in lineages affect by HAM-1

The Wnt/β-catenin asymmetry pathway is known to regulate many asymmetric cell divisions during *C.elegans* development (Mizumoto & Sawa, 2007). Because HAM-1 also regulates asymmetric division along the A/P axis of many cells during embryogenesis, and the HAM-1 protein is polarized to the posterior cortex in dividing cells, we wanted to explore if there was a connection between HAM-1 and Wnt signaling. Expression studies using transcriptional Wnt reporters of the five Wnt ligands found that that *cwn-1*, *cwn-2* and *mom-2* are expressed in the embryo during the time many *ham-1* controlled asymmetric divisions are occurring (Cordes et al., 2006) (Kaur et al., 2020). These three Wnts were determined to be transcribed at higher levels at the posterior of the embryo and play a role in regulating the asymmetric division of the SMDD/AIY neural progenitor.

Therefore, to start looking for a connection between HAM-1 and Wnt signaling, my first step was to determine if Wnts were required for asymmetric division in lineages that require HAM-1. I chose to look at two lineages specifically, the HSN/PHB lineage and the PLM/ALN lineages that develop in posterior of the embryo. The ALMs and PLMs are two pairs of mechanosensory neurons that project a long anterior neurite (ALM) or a short (PLM) posterior neurite. During PLM neuron development posteriorly enriched LIN-44 is known to act as a repellant to drive anterior neurite outgrowth (Prasad & Clark, 2006). CWN-1 and EGL-20 are known to act together to polarize the ALMs (Hilliard & Bargmann, 2006b). These signals contribute to the localization of the PLM in the tail, and the ALM in the mid-body of the worm. Similarly, the HSN motor neuron is found within the mid-body of the worm, and the chemosensory phasmid neuron PHB is found in the tail of the worm. The HSN motor neurons control vulval muscle contraction and their dysfunction contribute to an egg laying defective (egl) phenotype. These lineages have both been previously used to extensively to study *ham-1* function. Both neuronal lineages divide asymmetrically and produce both apoptotic and neuronal daughter cells. In *ham-1* mutants, there is a predicted anterior to posterior cell fate transformation in both lineages however, fates are affected differently. This means each lineage may have different requirements for *ham-1.* Based on other Wnt studies it was likely that there would be functional redundancy and so I anticipated needing to knockdown the function of multiple Wnts to see a phenotype.

In the wildtype background of both lineages' knockdown of each Wnt produced did not produce a phenotype. However, there were significant results in the PLM lineage when multiple Wnts were knocked down in a HAM-1 overexpression strain. Knockdown of *cwn-1, cwn-2* and *egl-20* or with *cwn-1, cwn-2* and *lin-44* was sufficient to significantly rescue HAM-1 overexpression neuronal duplication phenotype in the PLM lineage. This indicates that these Wnts are required to produce the HAM-1 overexpression phenotype in the PLM lineage. This may place Wnt signalling upstream of HAM-1, however because this is a modification of an overexpression phenotype, alone it is not sufficient to make this conclusion. I also observed that individual Wnt knockdown or use of deletion allele had no significant effect on the duplication phenotype, which was not surprising given their known functional redundancies (Gleason et al., 2006b). From these results I predict that knockdown of *cwn-1, cwn-1, egl-20* and *lin-44* together would even more strongly suppress the duplication phenotype. I attempted a mixed *egl-20* and

lin-44 dsRNA injection, however this ineffective. The mixed dsRNAs had an inhibitory effect and knockdown was not successful, as assessed using a dye fill assay for *lin-44* knockdown and scoring for egg laying defective worms in the progeny. Instead, in the future, a triple mutant strain carrying *cwn-1 (ok546); cwn-2 (ok895); lin-44 (n1792)* along with the over expressing GFP::HAM-1 transgene *hkIs39* could be constructed, and *egl-20* function then knocked down using RNAi.

Individual Wnt knockdown of *egl-20, lin-44 or mom-2* in the wildtype PHB lineage produced no phenotype. However, in the lineage a *ham-1* null mutation is known to cause both neuronal losses and duplications. The severity of this phenotype was seen to be significantly reduced after knockdown either *lin-44* or *mom-2.* The loss of Wnts causing suppression of a *ham-1* null mutant phenotype indicates that Wnts function as a bypass suppressor or HAM-1 in the HSN/PHB lineage. Here we can conclude that when the Wnt pathway is deregulated it bypasses the need for HAM-1. This means that Wnts and HAM-1 likely belong to different but functionally related pathways during asymmetric cell division.

My data suggests a connection between Wnts and HAM-1 in the HSN/PHB and the PLM/ALN lineage. If this is the case, could we determine a direct link between Wnts and HAM-1? In the SMDD/AIY neural progenitor its knows that Wnts function through the transmembrane MOM-5 Frizzled receptor enriched at the posterior pole and the APC protein APR-1 enriched at the anterior pole of the mother cell (Kaur et al., 2020). APC is a cytoplasmic protein that gets recruited to the cell cortex during cell division. *C. elegans* only has one, APC, APR-1, that is known to regulate cell shape through microtubule organization and cell fate through β-catenin (Mizumoto & Sawa, 2007). In the SMDD/AIY mother cell, loss of APR-1 caused both loss and duplications of AIY fate in the daughter cell (Kaur et al., 2020).

Another protein of the Wnt β-catenin pathway known to localize to the cell cortex are the Dishevelled paralogs. Activation of Wnt signaling results in the Dishevelled scaffold protein binding to a Frizzled receptor. In *C. elegans* DSH-2 and MIG-5 are known to redundantly regulate cell fate in hypodermal seam cells (Baldwin et al., 2016). While DSH-1 has not been directly implicated in WβA signaling, experiments in the Hawkins lab found DSH-1 in a yeast two-hybrid with HAM-1 (Nancy Hawkins, unpublished). A *dsh-1* mutant was evaluated, and no phenotypes were observed in HSN

lineage that resembled a *ham-1* phenotype (data not shown). With this information in mind, it is worth looking at available Frizzled and Dishevelled mutant strains in the collection. We could even go back and use the *dsh-1* mutant background in the same Wnt knockdown experiments to determine if there is a direct link between HAM-1 and Wnts through DSH-1 presumably at the cell cortex.

There are currently no known HAM-1 interacting proteins. To pursue this one could perform a co-immunoprecipitation of HAM-1 from embryonic extracts, followed by mass spectrophotometry to identify interacting proteins. To accomplish this, I designed and synthesized the experimental and control repair templates necessary for a CRISPR/Cas9 method to insert a 3xMYC tag at the N-terminal endogenous locus of HAM-1.

Following the *C. elegans* specific CRISPR/Cas9 methods developed by (Ghanta & Mello, 2020) I was able to generate eight mutant lines that displayed known *ham-1* mutant phenotypes. However, upon sequencing it was determine there were no successful CRISPR edits using the template injected. The sequencing revealed that all eight mutant lines were cut by Cas9 in the same predicted location, indication the guide RNA and CRISPR/Cas9 complex were effective. A retrospective analysis determined the concentration of the repair template used was inaccurate and I was unable to achieve any edits. This is still a viable experiment to continue. Furthermore, this CRISPR/Cas9 technique and the guide RNA I selected can also be used to insert Dendra2 into endogenous HAM-1 locus. In a protein interacting screen, the validation steps would include an analysis for genes with known expression or function during embryogenesis. Identified candidates can be tested using an RNAi approach and I would look for an enhancement or suppression of known *ham-1* phenotypes. Direct interactions between HAM-1 and its binding partners could be tested in a GST-Pull down experiment. The eluted proteins can then be detected by SDS-PAGE followed by a western blot analysis.

As Wnts are the primary signaling pathway in *C. elegans* controlling anterior-posterior polarization, we hypothesize they may have a functional relationship with HAM-1. Preliminary analysis indicates that GFP::HAM-1 localizes in a tight crescent to the posterior pole during mitosis of asymmetrically dividing cells. If Wnt signalling is required for HAM-1 function it is possible that normal GFP::HAM-1 cortical polarization may be perturbed with loss of Wnt function. To investigate this we could follow GFP::HAM-1

localization in embryos after knockdown of *lin-44* and *egl-20* into the *zdIs5; cwn-1 (ok546); cwn-2 (ok895) ;hkIs39* strain by RNAi. This combination was found to cause a significant reduction in the PLM duplication phenotype of HAM-1 overexpressing embryos. This would be performed with the intention to analyze the degree of any change of the GFP::HAM-1 cortical crescent in a cell in relation to the anterior-posterior axis of the embryo. Future injections in this strain would be ideal if we could achieve multiple Wnt knockdowns by injection, leading with combinations of *egl-20* and *lin-44,* as lethality caused by *mom-2* knockdown slows data acquisition. However, upon testing a mixed *lin-44* and *egl-20* injection mix was ineffective. Another approach to continue with this would be to generate the triple Wnt mutant strain *zdIs5; cwn-1 (ok546); cwn-2 (ok895); lin-44 (n1792); hkIs39* and achieve knockdown of *egl-20* function by RNAi.

4.3. HAM-1 functions in asymmetric lineages that produce a neuron and an apoptotic daughter

In *C. elegans* multiple asymmetrically dividing cell lineages require *ham-1* function, all (except one CEPso) produce a neuron and an apoptotic daughter (Frank et al., 2005). In *ham-1* mutants, the HSN/PHB, PLM and Q cell lineages all share polarized anterior-posterior cell fate transformations. The function of *ham-1* is unknown; however, we do know it is not likely a cell fate determinant itself. It is hypothesized that HAM-1 polarization may be part of an antagonistic mechanism that controls the positioning of the cleavage plane along the A/P axis. In the Q lineage polarized NMY-2 dependent cleavage plane positioning is seen to be affected in HAM-1 mutants, where NMY-2 becomes more symmetric throughout the cortex (Teuliere et al., 2018). This leads to a common *ham-1* phenotype, which is a daughter cell size asymmetry perturbation. This is also seen in the HSN lineage, where the cleavage plane is inverted possibly due to an anterior-posterior positioning defect in *ham-1* mutants. It is also theorized that a disturbance in the cleavage plane in *ham-1* mutants could lead to a change in the dosage of cell fate determinants inherited between daughter cells (Cordes et al., 2006). In this model *ham-1* could have different functions at the nucleus and at the cell cortex, as supported by GFP::HAM-1 localization patterns (Leung et al., 2016). At the cortex HAM-1 may act as a tether for the determinants. HAM-1 polarization may also be a mechanism to control its own inheritance to daughter cells. This was also seen in my GFP::HAM-1 localization study where in a small subset of available daughter cells

captured HAM-1 was brighter in the cortex of the posterior daughter cell. HAM-1 may be asymmetrically inherited to a daughter cell so that it may enter the nucleus and act as a transcription factor. This is inferred as HAM-1 is found is predominantly localized to the nucleus, and shares sequence similarity to the transcriptional factor STOX-1 (Feng et al., 2013).

The posterior polarization of HAM-1 during mitosis could also be due to Wnt signaling. During embryogenesis Wnts are expressed in the posterior of the embryo at same time *ham-1* lineages are affected (Kaur et al., 2020). My study found knockdown of several Wnt ligands in the PLM lineage was sufficient to significantly reduce the duplication phenotype seen in a HAM-1 overexpression background. A study into the direct effect of Wnt knockdown of GFP::HAM-1 polarization dynamics during mitosis can easily be performed to understand this further. The polarization of HAM-1 to two distinct locations during mitosis suggests it may have two distinct functions at the nucleus and at the cortex. A deletion analysis determined that there are regions of HAM-1 specifically required for both nuclear and cortical localization (Leung et al., 2016). Furthermore, there were alleles of HAM-1 determined to have differing phenotypes on PLM neuronal defects. It was discovered that *ham-1(n1811),* a point mutation in the N terminus, is defective in cortical localization but only a very low penetrance of PLM neuronal losses (Leung et al., 2016). Other mutations in *ham-1* that disrupt cortical localization have defects in the HSN/PHB lineage but not the PLM lineage. This suggests that cortical localization not important in the PLM lineage. This can suggest that *ham-1* may have two separate and independent functions. A function at the cell cortex, perhaps to position the mitotic spindle, and a different function in the nucleus as a transcription factor. Another protein that displays a dual function is cytochrome *c.* Cytochrome *c* is commonly known as the soluble electron carrier from the oxidative phosphorylation complex III to complex IV in the electron transport chain. However, upon release from the mitochondria it has been shown to stimulate apoptosome assembly (Vempati et al., 2007).

HAM-1 has been seen to uniquely affect lineages that produce an apoptotic daughter. The only known downstream effector of HAM-1 is PIG-1 kinase. In HSN/PHB lineage, *pig-1* mutations cause cleavage plane defects were reported to be epistatic or masking the effects of a *ham-1* mutation. Indicating HAM-1 may be a negative regulator of PIG-1 in the HSN/PHB lineage. However, in the Q cell lineage HAM-1 was suspected of acting as a positive regulator of PIG-1. The contrasting information makes it difficult to

glean a clear relationship between the two. A common phenotype in HAM-1 and PIG-1 mutants is that they may influence apoptotic cells. PIG-1 affects proteins associated with the cell cycle and asymmetric cell division, and influences proteins regulating myosin distribution and spindle positioning (Offenburger et al., 2017). A large mass spectrometry-based proteomics approach was undertaken to identify proteins and pathways that are affected by loss of the PIG-1 kinase (Offenburger et al., 2017). It was determined that *pig-1* mutation leads to an overall decrease of proteins related to actomyosin processes, locomotion, and metabolism and to an overall increase of proteins connected to the cell cycle, embryo development, apoptosis, and microtubules. Interestingly, Wnt signaling receptors MOM-5 and DSH-2, showed higher abundance in *pig-1* mutant embryos. The apoptosis proteins CED-3 and CED-4 and the corpse engulfment proteins CED-2 and CED-12, all show increased abundance in *pig-1* mutant embryos (Offenburger et al., 2017). This finding is in notable as PIG-1 has also been seen to function in a mechanism for apoptotic cell elimination distinct from that of canonical programmed cell death by caspases (Denning et al., 2012). ABplpappap normally undergoes programmed cell death but in *ced-3* mutants it is eliminated by being extruded or shed from the developing embryo into the extra-embryonic space of the egg (Denning et al., 2012). Genetic studies determined PIG-1 to promote shed-cell detachment by endocytosis-mediated removal of cell-adhesion molecules from the cell surface of the ABalapapaa cell (Denning et al., 2012). This cell extrusion process utilizes a kinase pathway involving PAR-4, STRD-1 and MOP-25.1/2, the *C. elegans* homologs of the mammalian tumor suppressor kinase LKB1 and its binding partners STRADα and MO25α. Therefore in *C. elegans* programmed cell death can be achieved by both a canonical caspase-mediated apoptotic pathway and a caspase independent shedding pathway. These two mechanisms are also found to be functionally redundant, as ABplpappap survives only in mutants in which both pathways are disrupted (Denning et al., 2012). These studies tell us the only known downstream effector of HAM-1, PIG-1 kinase, affects proteins associated with the cell cycle and asymmetric cell division, and influences proteins regulating myosin distribution and spindle positioning.

Chapter 5. Conclusion

The purpose of this project was to determine the requirement for Wnt Signaling in HAM-1 regulated asymmetric cell divisions. HAM-1 is a putative transcription factor that is seen to both localize in the nucleus and become polarized to the posterior cell cortex of diving cells. HAM-1 affects asymmetrically dividing cell lineages that produce a neuron and an apoptotic daughter. HAM-1 loss in the HSN/PHB, PLM/ALN, and Q cell lineages have led to cell fate transformations during the process of asymmetric cell division. The role of HAM-1 and the mechanism for asymmetric cell division is still not well understood. In *C. elegans* the main signalling pathway that controls asymmetric cell divisions is the Wnt β-catenin Asymmetry pathway. Wnt ligands have been found to be expressed in posterior cells of the embryo during the time many HAM-1 regulated asymmetric cell divisions are occurring. This study determined that perturbation of Wnt ligands in two HAM-1 affected lineages can rescue HAM-1 loss and HAM-1 over expression associated phenotypes. This study highlighted the previously reported functional redundancy of Wnts seen in various cell lineages. Future experiments into this relationship can continue to sift through these functional redundancies to narrow down the genetic interactions between HAM-1 and Wnt signalling. The study of HAM-1 localization in this project helped characterize the role of HAM-1 in existing functional models. The 4D microscopy study identified a potential mechanism for HAM-1 polarization to aid in an asymmetric pattern of inheritance. A combination of these experimental techniques used in this study can be applied to better understand the requirement of Wnt signalling on HAM-1 polarization during asymmetric cell division.

References

Baldwin, A. T., Clemons, A. M., & Phillips, B. T. (2016). Unique and redundant β-catenin regulatory roles of two Dishevelled paralogs during *C. elegans* asymmetric cell division. *Journal of Cell Science*, *129*(5), 983–993. https://doi.org/10.1242/jcs.175802

Bonkowsky, J. L., Yoshikawa, S., O'Keefe, D. D., Scully, A. L., & Thomas, J. B. (1999). Axon routing across the midline controlled by the Drosophila Derailed receptor. *Nature*, *402*(6761), 540–544. https://doi.org/10.1038/990122

Brenner, S. (1974). The genetics of Caenorhabditis elegans. *Genetics*, *77*(1), 71–94. https://doi.org/10.1093/GENETICS/77.1.71

Butler, M. T., & Wallingford, J. B. (2017). Planar cell polarity in development and disease. *Nature Reviews Molecular Cell Biology*, *18*(6), 375–388. https://doi.org/10.1038/nrm.2017.11

Chao, S., Yan, H., & Bu, P. (2024). Asymmetric division of stem cells and its cancer relevance. *Cell Regeneration*, *13*(1), 5. https://doi.org/10.1186/s13619-024-00188-9

Chudakov, D. M., Lukyanov, S., & Lukyanov, K. A. (2007). Tracking intracellular protein movements using photoswitchable fluorescent proteins PS-CFP2 and Dendra2. *Nature Protocols*, *2*(8), 2024–2032. https://doi.org/10.1038/nprot.2007.291

Cordes, S., Frank, C. A., & Garriga, G. (2006). The C. elegans MELK ortholog PIG-1 regulates cell size asymmetry and daughter cell fate in asymmetric neuroblast divisions. *Development (Cambridge, England)*, *133*(14), 2747–2756. https://doi.org/10.1242/dev.02447

Denning, D. P., Hatch, V., & Horvitz, H. R. (2012). Programmed elimination of cells by caspase-independent cell extrusion in C. elegans. *Nature*, *488*(7410), 226–230. https://doi.org/10.1038/nature11240

Desai, C., Garriga, G., McIntire, S. L., & Horvitz, H. R. (1988). A genetic pathway for the development of the Caenorhabditis elegans HSN motor neurons. *Nature*, *336*(6200), 638–646. https://doi.org/10.1038/336638a0

Ducat, A., Couderc, B., Bouter, A., Biquard, L., Aouache, R., Passet, B., Doridot, L., Cohen, M.-B., Ribaux, P., Apicella, C., Gaillard, I., Palfray, S., Chen, Y., Vargas, A., Julé, A., Frelin, L., Cocquet, J., San Martin, C. R., Jacques, S., … Vaiman, D. (2020). Molecular Mechanisms of Trophoblast Dysfunction Mediated by Imbalance between STOX1 Isoforms. *IScience*, *23*(5), 101086. https://doi.org/10.1016/j.isci.2020.101086

Eisenmann, D. M., Maloof, J. N., Simske, J. S., Kenyon, C., & Kim, S. K. (1998). The β-catenin homolog BAR-1 and LET-60 Ras coordinately regulate the Hox gene *lin-39* during *Caenorhabditis elegans* vulval development. *Development*, *125*(18), 3667–3680. https://doi.org/10.1242/dev.125.18.3667

Feng, G., Yi, P., Yang, Y., Chai, Y., Tian, D., Zhu, Z., Liu, J., Zhou, F., Cheng, Z., Wang, X., Li, W., & Ou, G. (2013a). Developmental stage-dependent transcriptional regulatory pathways control neuroblast lineage progression. *Development (Cambridge)*, *140*(18), 3838–3847. https://doi.org/10.1242/DEV.098723

Feng, G., Yi, P., Yang, Y., Chai, Y., Tian, D., Zhu, Z., Liu, J., Zhou, F., Cheng, Z., Wang, X., Li, W., & Ou, G. (2013b). Developmental stage-dependent transcriptional regulatory pathways control neuroblast lineage progression. *Development (Cambridge, England)*, *140*(18), 3838–3847. https://doi.org/10.1242/dev.098723

Fenstad, M. H., Johnson, M. P., Loset, M., Mundal, S. B., Roten, L. T., Eide, I. P., Bjorge, L., Sande, R. K., Johansson, A. K., Dyer, T. D., Forsmo, S., Blangero, J., Moses, E. K., & Austgulen, R. (2010). STOX2 but not STOX1 is differentially expressed in decidua from pre-eclamptic women: data from the Second Nord-Trondelag Health Study. *Molecular Human Reproduction*, *16*(12), 960–968. https://doi.org/10.1093/molehr/gaq064

Fradkin, L. G., van Schie, M., Wouda, R. R., de Jong, A., Kamphorst, J. T., Radjkoemar-Bansraj, M., & Noordermeer, J. N. (2004). The Drosophila Wnt5 protein mediates selective axon fasciculation in the embryonic central nervous system. *Developmental Biology*, *272*(2), 362–375. https://doi.org/10.1016/j.ydbio.2004.04.034

Frank, C. A., Hawkins, N. C., Guenther, C., Horvitz, H. R., & Garriga, G. (2005). C. elegans HAM-1 positions the cleavage plane and regulates apoptosis in asymmetric neuroblast divisions. *Developmental Biology*, *284*(2), 301–310. https://doi.org/10.1016/j.ydbio.2005.05.026

Gallaud, E., Pham, T., & Cabernard, C. (2017). *Drosophila melanogaster Neuroblasts: A Model for Asymmetric Stem Cell Divisions* (pp. 183–210). https://doi.org/10.1007/978-3-319-53150-2_8

Ghanta, K. S., Chen, Z., Mir, A., Dokshin, G. A., Krishnamurthy, P. M., Yoon, Y., Gallant, J., Xu, P., Zhang, X.-O., Ozturk, A. R., Shin, M., Idrizi, F., Liu, P., Gneid, H., Edraki, A., Lawson, N. D., Rivera-Pérez, J. A., Sontheimer, E. J., Watts, J. K., & Mello, C. C. (2021). 5′-Modifications improve potency and efficacy of DNA donors for precision genome editing. *ELife*, *10*. https://doi.org/10.7554/eLife.72216

Ghanta, K. S., & Mello, C. C. (2020). Melting dsDNA Donor Molecules Greatly Improves Precision Genome Editing in *Caenorhabditis elegans*. *Genetics*, *216*(3), 643–650. https://doi.org/10.1534/genetics.120.303564

Gho, M., & Schweisguth, F. (1998). Frizzled signalling controls orientation of asymmetric sense organ precursor cell divisions in Drosophila. *Nature*, *393*(6681), 178–181. https://doi.org/10.1038/30265

Gleason, J. E., Korswagen, H. C., & Eisenmann, D. M. (2002). Activation of Wnt signaling bypasses the requirement for RTK/Ras signaling during *C. elegans* vulval induction. *Genes & Development*, *16*(10), 1281–1290. https://doi.org/10.1101/gad.981602

Gleason, J. E., Szyleyko, E. A., & Eisenmann, D. M. (2006a). Multiple redundant Wnt signaling components function in two processes during C. elegans vulval development. *Developmental Biology*, *298*(2), 442–457. https://doi.org/10.1016/J.YDBIO.2006.06.050

Gleason, J. E., Szyleyko, E. A., & Eisenmann, D. M. (2006b). Multiple redundant Wnt signaling components function in two processes during C. elegans vulval development. *Developmental Biology*, *298*(2), 442–457. https://doi.org/10.1016/j.ydbio.2006.06.050

Glinka, A., Wu, W., Delius, H., Monaghan, A. P., Blumenstock, C., & Niehrs, C. (1998). Dickkopf-1 is a member of a new family of secreted proteins and functions in head induction. *Nature*, *391*(6665), 357–362. https://doi.org/10.1038/34848

Green, J. L., Kuntz, S. G., & Sternberg, P. W. (2008). Ror receptor tyrosine kinases: orphans no more. *Trends in Cell Biology*, *18*(11), 536–544. https://doi.org/10.1016/j.tcb.2008.08.006

Guenther, C., & Garriga, G. (1996). Asymmetric distribution of the C. elegans HAM-1 protein in neuroblasts enables daughter cells to adopt distinct fates. *Development*, *122*(11), 3509–3518. https://doi.org/10.1242/dev.122.11.3509

Guo, S., & Kemphues, K. J. (1996). Molecular genetics of asymmetric cleavage in the early Caenorhabditis elegans embryo. *Current Opinion in Genetics & Development*, *6*(4), 408–415. https://doi.org/10.1016/S0959-437X(96)80061-X

Hardin, J. (2011). Imaging Embryonic Morphogenesis in C. elegans. *Methods in Cell Biology*, *106*, 377–412. https://doi.org/10.1016/B978-0-12-544172-8.00014-1

Harris, J., Honigberg, L., Robinson, N., & Kenyon, C. (1996). Neuronal cell migration in C. elegans: regulation of Hox gene expression and cell position. *Development (Cambridge, England)*, *122*(10), 3117–3131. https://doi.org/10.1242/DEV.122.10.3117

Harterink, M., Kim, D. hyun, Middelkoop, T. C., Doan, T. D., van Oudenaarden, A., & Korswagen, H. C. (2011). Neuroblast migration along the anteroposterior axis of *C. elegans* is controlled by opposing gradients of Wnts and a secreted Frizzled-related protein. *Development*, *138*(14), 2915–2924. https://doi.org/10.1242/dev.064733

Hartmann, C., Landgraf, M., Bate, M., & Jäckle, H. (1997). Krüppel target gene knockout participates in the proper innervation of a specific set of Drosophila larval muscles. *The EMBO Journal*, *16*(17), 5299. https://doi.org/10.1093/EMBOJ/16.17.5299

Hawkins, N., & Garriga, G. (1996). Asymmetric cell division: from A to Z Asymmetric cell divisions in Drosophila neurogenesis. In *Kemphues and Strome*. www.genesdev.org

Herman, M. A., & Robert Horvitz, H. (1994). The Caenorhabditis elegans gene lin-44 controls the polarity of asymmetric cell divisions. *Development (Cambridge, England)*, *120*(5), 1035–1047. https://doi.org/10.1242/DEV.120.5.1035

Herman, M. A., Vassilieva, L. L., Horvitz, H. R., Shaw, J. E., & Herman, R. K. (1995). The C. elegans gene lin-44, which controls the polarity of certain asymmetric cell divisions, encodes a Wnt protein and acts cell nonautonomously. *Cell*, *83*(1), 101–110. https://doi.org/10.1016/0092-8674(95)90238-4

Hilliard, M. A., & Bargmann, C. I. (2006a). Wnt signals and frizzled activity orient anterior-posterior axon outgrowth in C. elegans. *Developmental Cell*, *10*(3), 379–390. https://doi.org/10.1016/J.DEVCEL.2006.01.013

Hilliard, M. A., & Bargmann, C. I. (2006b). Wnt Signals and Frizzled Activity Orient Anterior-Posterior Axon Outgrowth in C. elegans. *Developmental Cell*, *10*(3), 379–390. https://doi.org/10.1016/j.devcel.2006.01.013

Hirata, J., Nakagoshi, H., Nabeshima, Y., & Matsuzaki, F. (1995). Asymmetric segregation of the homeodomain protein Prospero duringDrosophila development. *Nature*, *377*(6550), 627–630. https://doi.org/10.1038/377627a0

Horvitz, H. R., & Herskowitz, I. (1992). Mechanisms of asymmetric cell division: Two Bs or not two Bs, that is the question. *Cell*, *68*(2), 237–255. https://doi.org/10.1016/0092-8674(92)90468-R

Hsieh, J.-C., Kodjabachian, L., Rebbert, M. L., Rattner, A., Smallwood, P. M., Samos, C. H., Nusse, R., Dawid, I. B., & Nathans, J. (1999). A new secreted protein that binds to Wnt proteins and inhibits their activites. *Nature*, *398*(6726), 431–436. https://doi.org/10.1038/18899

Inoue, T., Oz, H. S., Wiland, D., Gharib, S., Deshpande, R., Hill, R. J., Katz, W. S., & Sternberg, P. W. (2004). C. elegans LIN-18 is a Ryk ortholog and functions in parallel to LIN-17/Frizzled in Wnt signaling. *Cell*, *118*(6), 795–806. https://doi.org/10.1016/j.cell.2004.09.001

Jackson, B. M., & Eisenmann, D. M. (2012). -Catenin-Dependent Wnt Signaling in C. elegans: Teaching an Old Dog a New Trick. *Cold Spring Harbor Perspectives in Biology*, *4*(8), a007948–a007948. https://doi.org/10.1101/cshperspect.a007948

Jensen, M., Hoerndli, F. J., Brockie, P. J., Wang, R., Johnson, E., Maxfield, D., Francis, M. M., Madsen, D. M., & Maricq, A. V. (2012). Wnt Signaling Regulates Acetylcholine Receptor Translocation and Synaptic Plasticity in the Adult Nervous System. *Cell*, *149*(1), 173–187. https://doi.org/10.1016/j.cell.2011.12.038

Jin, F., Jin, L., & Wang, Y. (2021). Downregulation of *STOX1* is a novel prognostic biomarker for glioma patients. *Open Life Sciences*, *16*(1), 1164–1174. https://doi.org/10.1515/biol-2021-0119

Kamb, A., Weir, M., Rudy, B., Varmus, H., & Kenyon, C. (1989). Identification of genes from pattern formation, tyrosine kinase, and potassium channel families by DNA amplification. *Proceedings of the National Academy of Sciences*, *86*(12), 4372–4376. https://doi.org/10.1073/pnas.86.12.4372

Kaur, S., Mélénec, P., Murgan, S., Bordet, G., Recouvreux, P., Lenne, P.-F., & Bertrand, V. (2020). Wnt ligands regulate the asymmetric divisions of neuronal progenitors in *C. elegans* embryos. *Development*, *147*(7). https://doi.org/10.1242/dev.183186

Kennerdell, J. R., Fetter, R. D., & Bargmann, C. I. (2009). Wnt-Ror signaling to SIA and SIB neurons directs anterior axon guidance and nerve ring placement in *C. elegans*. *Development*, *136*(22), 3801–3810. https://doi.org/10.1242/dev.038109

Komiya, Y., & Habas, R. (2008). Wnt signal transduction pathways. *Organogenesis*, *4*(2), 68–75. https://doi.org/10.4161/org.4.2.5851

Korswagen, H. C., Herman, M. A., & Clevers, H. C. (2000). Distinct β-catenins mediate adhesion and signalling functions in C. elegans. *Nature*, *406*(6795), 527–532. https://doi.org/10.1038/35020099

Kühl, M., Sheldahl, L. C., Park, M., Miller, J. R., & Moon, R. T. (2000). The Wnt/Ca2+ pathway A new vertebrate Wnt signaling pathway takes shape. *Trends in Genetics*, *16*(7), 279–283. https://doi.org/10.1016/S0168-9525(00)02028-X

Leung, A., Hua, K., Ramachandran, P., Hingwing, K., Wu, M., Koh, P. L., & Hawkins, N. (2016). C. elegans HAM-1 functions in the nucleus to regulate asymmetric neuroblast division. *Developmental Biology*, *410*(1), 56–69. https://doi.org/10.1016/j.ydbio.2015.12.011

Li, Z., Zhou, G., Jiang, L., Xiang, H., & Cao, Y. (2019). Effect of STOX1 on recurrent spontaneous abortion by regulating trophoblast cell proliferation and migration via the PI3K/AKT signaling pathway. *Journal of Cellular Biochemistry*, *120*(5), 8291–8299. https://doi.org/10.1002/jcb.28112

Lin, R., Hill, R. J., & Priess, J. R. (1998). POP-1 and Anterior–Posterior Fate Decisions in C. elegans Embryos. *Cell*, *92*(2), 229–239. https://doi.org/10.1016/S0092-8674(00)80917-4

Lin, R., Thompson, S., & Priess, J. R. (1995). pop-1 encodes an HMG box protein required for the specification of a mesoderm precursor in early C. elegans embryos. *Cell*, *83*(4), 599–609. https://doi.org/10.1016/0092-8674(95)90100-0

Loyer, N., & Januschke, J. (2020). Where does asymmetry come from? Illustrating principles of polarity and asymmetry establishment in Drosophila neuroblasts. *Current Opinion in Cell Biology*, *62*, 70–77. https://doi.org/10.1016/j.ceb.2019.07.018

Maduro, M. F. (2015). 20 Years of *unc-119* as a transgene marker. *Worm*, *4*(3), e1046031. https://doi.org/10.1080/21624054.2015.1046031

Maloof, J. N., Whangbo, J., Harris, J. M., Jongeward, G. D., & Kenyon, C. (1999). A Wnt signaling pathway controls Hox gene expression and neuroblast migration in *C. elegans*. *Development*, *126*(1), 37–49. https://doi.org/10.1242/dev.126.1.37

Maung, S. M. T. W., & Jenny, A. (2011). Planar cell polarity in Drosophila. *Organogenesis*, *7*(3), 165–179. https://doi.org/10.4161/org.7.3.18143

Menck, K., Heinrichs, S., Baden, C., & Bleckmann, A. (2021). The WNT/ROR Pathway in Cancer: From Signaling to Therapeutic Intervention. *Cells*, *10*(1), 142. https://doi.org/10.3390/cells10010142

Mizumoto, K., & Sawa, H. (2007). Cortical β-Catenin and APC Regulate Asymmetric Nuclear β-Catenin Localization during Asymmetric Cell Division in C. elegans. *Developmental Cell*, *12*(2), 287–299. https://doi.org/10.1016/j.devcel.2007.01.004

Neumüller, R. A., & Knoblich, J. A. (2009). Dividing cellular asymmetry: asymmetric cell division and its implications for stem cells and cancer. *Genes & Development*, *23*(23), 2675–2699. https://doi.org/10.1101/gad.1850809

Offenburger, S. L., Bensaddek, D., Murillo, A. B., Lamond, A. I., & Gartner, A. (2017). Comparative genetic, proteomic and phosphoproteomic analysis of C. elegans embryos with a focus on ham-1/STOX and pig-1/MELK in dopaminergic neuron development. *Scientific Reports 2017 7:1*, *7*(1), 1–17. https://doi.org/10.1038/s41598-017-04375-4

Ohno, S., Goulas, S., & Hirose, T. (2015). The PAR3-aPKC-PAR6 Complex. In *Cell Polarity 1* (pp. 3–23). Springer International Publishing. https://doi.org/10.1007/978-3-319-14463-4_1

Ou, G., Stuurman, N., D'Ambrosio, M., & Vale, R. D. (2010). Polarized myosin produces unequal-size daughters during asymmetric cell division. *Science*, *330*(6004), 677–680. https://doi.org/10.1126/science.1196112

Pacquelet, A. (2017). *Asymmetric Cell Division in the One-Cell C. elegans Embryo: Multiple Steps to Generate Cell Size Asymmetry* (pp. 115–140). https://doi.org/10.1007/978-3-319-53150-2_5

Pan, C. L., Howell, J. E., Clark, S. G., Hilliard, M., Cordes, S., Bargmann, C. I., & Garriga, G. (2006). Multiple Wnts and Frizzled receptors regulate anteriorly directed cell and growth cone migrations in Caenorhabditis elegans. *Developmental Cell*, *10*(3), 367–377. https://doi.org/10.1016/j.devcel.2006.02.010

Park, F. D., & Priess, J. R. (2003). Establishment of POP-1 asymmetry in early *C. elegans* embryos. *Development*, *130*(15), 3547–3556. https://doi.org/10.1242/dev.00563

Polakis, P. (2000). Wnt signaling and cancer. *Genes & Development*, *14*(15), 1837–1851. https://doi.org/10.1101/gad.14.15.1837

Prasad, B. C., & Clark, S. G. (2006). Wnt signaling establishes anteroposterior neuronal polarity and requires retromer in *C. elegans*. *Development*, *133*(9), 1757–1766. https://doi.org/10.1242/dev.02357

Puri, D., Ponniah, K., Biswas, K., Basu, A., Dey, S., Lundquist, E. A., & Ghosh-Roy, A. (2021). Wnt signaling establishes the microtubule polarity in neurons through regulation of Kinesin-13. *The Journal of Cell Biology*, *220*(9). https://doi.org/10.1083/JCB.202005080

Reich, J. D., Hubatsch, L., Illukkumbura, R., Peglion, F., Bland, T., Hirani, N., & Goehring, N. W. (2019). Regulated Activation of the PAR Polarity Network Ensures a Timely and Specific Response to Spatial Cues. *Current Biology*, *29*(12), 1911-1923.e5. https://doi.org/10.1016/j.cub.2019.04.058

Rhyu, M. S., Jan, L. Y., & Jan, Y. N. (1994). Asymmetric distribution of numb protein during division of the sensory organ precursor cell confers distinct fates to daughter cells. *Cell*, *76*(3), 477–491. https://doi.org/10.1016/0092-8674(94)90112-0

Rocheleau, C. E., Downs, W. D., Lin, R., Wittmann, C., Bei, Y., Cha, Y. H., Ali, M., Priess, J. R., & Mello, C. C. (1997). Wnt signaling and an APC-related gene specify endoderm in early C. elegans embryos. *Cell*, *90*(4), 707–716. https://doi.org/10.1016/S0092-8674(00)80531-0

Saneyoshi, T., Kume, S., Amasaki, Y., & Mikoshiba, K. (2002). The Wnt/calcium pathway activates NF-AT and promotes ventral cell fate in Xenopus embryos. *Nature*, *417*(6886), 295–299. https://doi.org/10.1038/417295a

Sasahira, T., Nishiguchi, Y., Fujiwara, R., Kurihara, M., Kirita, T., Bosserhoff, A. K., & Kuniyasu, H. (2016). Storkhead box 2 and melanoma inhibitory activity promote oral squamous cell carcinoma progression. *Oncotarget*, *7*(18), 26751–26764. https://doi.org/10.18632/oncotarget.8495

Schlesinger, A., Shelton, C. A., Maloof, J. N., Meneghini, M., & Bowerman, B. (1999). Wnt pathway components orient a mitotic spindle in the early Caenorhabditis elegans embryo without requiring gene transcription in the responding cell. *Genes & Development*, *13*(15), 2028–2038. https://doi.org/10.1101/gad.13.15.2028

Shackleford, G. M., Shivakumar, S., Shiue, L., Mason, J., Kenyon, C., & Varmus, H. E. (1993). Two wnt genes in Caenorhabditis elegans. *Oncogene*, *8*(7), 1857–1864. http://europepmc.org/abstract/MED/8510930

Sulston, J. E., & Horvitz, H. R. (1977). Post-embryonic cell lineages of the nematode, Caenorhabditis elegans. *Developmental Biology*, *56*(1), 110–156. https://doi.org/10.1016/0012-1606(77)90158-0

Sulston, J. E., Schierenberg, E., White, J. G., & Thomson, J. N. (1983). The embryonic cell lineage of the nematode Caenorhabditis elegans. *Developmental Biology*, *100*(1), 64–119. https://doi.org/10.1016/0012-1606(83)90201-4

Sunchu, B., & Cabernard, C. (2020). Principles and mechanisms of asymmetric cell division. *Development (Cambridge)*, *147*(13). https://doi.org/10.1242/DEV.167650/224234

Takada, R., Satomi, Y., Kurata, T., Ueno, N., Norioka, S., Kondoh, H., Takao, T., & Takada, S. (2006). Monounsaturated Fatty Acid Modification of Wnt Protein: Its Role in Wnt Secretion. *Developmental Cell*, *11*(6), 791–801. https://doi.org/10.1016/j.devcel.2006.10.003

Teuliere, J., Kovacevic, I., Bao, Z., & Garriga, G. (2018). The Caenorhabditis elegans gene ham-1 regulates daughter cell size asymmetry primarily in divisions that produce a small anterior daughter cell. *PLoS ONE*, *13*(4). https://doi.org/10.1371/journal.pone.0195855

Thorpe, C. J., Schlesinger, A., Clayton Carter, J., & Bowerman, B. (1997). Wnt signaling polarizes an early C. elegans blastomere to distinguish endoderm from mesoderm. *Cell*, *90*(4), 695–705. https://doi.org/10.1016/S0092-8674(00)80530-9

Tian, Y., Kang, Q., Shi, X., Wang, Y., Zhang, N., Ye, H., Xu, Q., Xu, T., & Zhang, R. (2021). SNX-3 mediates retromer-independent tubular endosomal recycling by opposing EEA-1-facilitated trafficking. *PLOS Genetics*, *17*(6), e1009607. https://doi.org/10.1371/journal.pgen.1009607

Trent, C., Tsuing, N., & Horvitz, H. R. (1983). Egg-laying defective mutants of the nematode Caenorhabditis elegans. *Genetics*, *104*(4), 619–647. https://doi.org/10.1093/GENETICS/104.4.619

van Abel, D., Hölzel, D. R., Jain, S., Lun, F. M. F., Zheng, Y. W. L., Chen, E. Z., Sun, H., Chiu, R. W. K., Lo, Y. M. D., van Dijk, M., & Oudejans, C. B. M. (2011). SFRS7-Mediated Splicing of Tau Exon 10 Is Directly Regulated by STOX1A in Glial Cells. *PLoS ONE*, *6*(7), e21994. https://doi.org/10.1371/journal.pone.0021994

van Dijk, M., Mulders, J., Poutsma, A., Könst, A. A. M., Lachmeijer, A. M. A., Dekker, G. A., Blankenstein, M. A., & Oudejans, C. B. M. (2005). Maternal segregation of the Dutch preeclampsia locus at 10q22 with a new member of the winged helix gene family. *Nature Genetics*, *37*(5), 514–519. https://doi.org/10.1038/ng1541

Van Dijk, M., Van Bezu, J., Poutsma, A., Veerhuis, R., Rozemuller, A. J., Scheper, W., Blankenstein, M. A., & Oudejans, C. B. (2010). The pre-eclampsia gene STOX1 controls a conserved pathway in placenta and brain upregulated in late-onset Alzheimer's disease. *Journal of Alzheimer's Disease*, *19*(2), 673–679. https://doi.org/10.3233/JAD-2010-1265

van Dijk, M., van Bezu, J., van Abel, D., Dunk, C., Blankenstein, M. A., Oudejans, C. B. M., & Lye, S. J. (2010). The STOX1 genotype associated with pre-eclampsia leads to a reduction of trophoblast invasion by α-T-catenin upregulation. *Human Molecular Genetics*, *19*(13), 2658–2667. https://doi.org/10.1093/hmg/ddq152

Vempati, U. D., Diaz, F., Barrientos, A., Narisawa, S., Mian, A. M., Millán, J. L., Boise, L. H., & Moraes, C. T. (2007). Role of Cytochrome *c* in Apoptosis: Increased Sensitivity to Tumor Necrosis Factor Alpha Is Associated with Respiratory Defects but Not with Lack of Cytochrome *c* Release. *Molecular and Cellular Biology*, *27*(5), 1771–1783. https://doi.org/10.1128/MCB.00287-06

Wallingford, J. B. (2012). Planar cell polarity and the developmental control of cell behavior in vertebrate embryos. *Annual Review of Cell and Developmental Biology*, *28*(Volume 28, 2012), 627–653. https://doi.org/10.1146/ANNUREV-CELLBIO-092910-154208/CITE/REFWORKS

Wallingford, J. B., Ewald, A. J., Harland, R. M., & Fraser, S. E. (2001). Calcium signaling during convergent extension in Xenopus. *Current Biology*, *11*(9), 652–661. https://doi.org/10.1016/S0960-9822(01)00201-9

Whangbo, J., Harris, J., & Kenyon, C. (2000). Multiple levels of regulation specify the polarity of an asymmetric cell division in C. elegans. *Development (Cambridge, England)*, *127*(21), 4587–4598. https://doi.org/10.1242/DEV.127.21.4587

Wodarz, A., & Nusse, R. (1998). Mechanisms of Wnt signaling in development. *Annual Review of Cell and Developmental Biology*, *14*, 59–88. https://doi.org/10.1146/ANNUREV.CELLBIO.14.1.59

Zacharias, A. L., Walton, T., Preston, E., & Murray, J. I. (2015). Quantitative Differences in Nuclear β-catenin and TCF Pattern Embryonic Cells in C. elegans. *PLOS Genetics*, *11*(10), e1005585. https://doi.org/10.1371/journal.pgen.1005585

Zhan, T., Rindtorff, N., & Boutros, M. (2017). Wnt signaling in cancer. *Oncogene*, *36*(11), 1461–1473. https://doi.org/10.1038/onc.2016.304

Zinovyeva, A. Y., & Forrester, W. C. (2005). The C. elegans Frizzled CFZ-2 is required for cell migration and interacts with multiple Wnt signaling pathways. *Developmental Biology*, *285*(2), 447–461. https://doi.org/10.1016/j.ydbio.2005.07.014

Appendix A. Supplementary Information

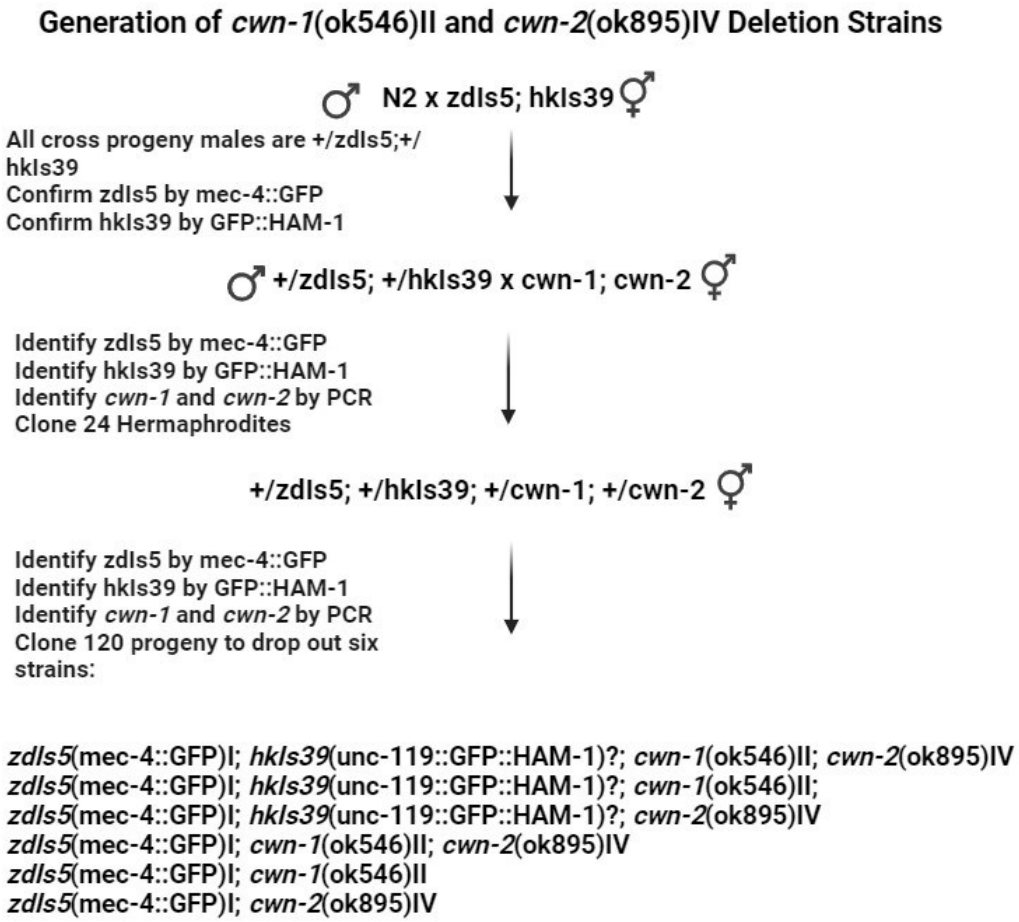

Figure A5-1. Genetic Cross for the Generation of Wnt Mutant strains in a GFP::HAM-1 overexpression and/or PLM reporter background.

Table A5-A. Primers for Detection of *cwn-1 (ok546)* and *cwn-2 (ok895)* deletion alleles

Wnt	Primers
cwn-1(ok546)	cwn-1 L: tgaaaatgacccaacagaccg cwn-1 R: TTAACATTGTCCGAGCAGCC cwn-1P2: AGTGTTCGTTCGGGATCTCT
cwn-2(ok895)	cwn-2IL: GATGCTTCTTGGTGGTTCGT cwn-2IR: TGAGCAAACGGGCTAAGATT cwn-2PL2: GGGTTTGCAAgtatgttgcc

Table A5-B. Sequencing Primers for Dendra-2::HAM-1 construct

Primer	Sequence
Dm8	TTCTACCTTTAAAGATGCCCACT
Dm9	ACATTTTGGAAGAAGCAATCACCT
Dm10	TGGCGAGACCCAAAAGCTAC
Dm11	TTTCCCCGAAAAGTGCCACC
Dm12	CCTGCAGGTCGACTCTAGAAA
Dm13	TCCTTCTGGAAACGATTGCTTG
Dm14	CTGACGATTGAGCTGTGCGA
Dm15	CTTCGTTCCGCTGGGAGATG

Dm16	ACTTCAGAGGAGCCCGAGAT
Dm17	ACGTCCAGCTGAGATCTTTCG
Dm18	TTCCAACTAAGGACCCCACA
Dm19	CCAATATGACTGAATGTCATTTTGG
hm115	GGTCTCTGGCATATCAACTG

Table A5-C. Primers for the generation of CRISPR/Cas9 Repair Templates

Primer	Sequence (5'-3')	Details
dm1 +5'TEG	TCTATTTGGGATTCTACAGA CAATAATACAACATGGAACA AAAACTTATTTCTGAAGAGG	Forward Primer for 3xMyc sequence: [35bp up to and including ham-1 start ATG] + [25bp 3xMyc homology from Hamida]
dm2 +5'TEG	GCTTTTGGTGCGTTGAGCA CAACGGCTAAGTAGGTCAA GTCTTCCTCGCTGATCAACT TC	Reverse Primer for 3xMyc sequence: [5' 35 bp homology to ham-1 - 3'] + [5' - 25bp 3xMyc homology from Hamida 3']
dm3	CCTGAATTTTCTTCCAGATT CC	Forward Primer For Het/homo detection. Made using Poison primer as "Right Primer" in Primer3: [5' - homology to upstream ham-1 sequence -3']
dm4	CGCCGAAGTGAGTTCTCTG	Reverse Primer For Het/homo detection (Made using "dm3" in Primer3): [5' - homology to downstream ham-1 sequence - 3']

dm5	AGAGTAATTGGACCTACAAG TCTTCCTCGCTGATCAACTT C	Reverse Primer for 3xMyc to *unc-54* Stitch:[5' - first 13bp of *unc-54*-3'UTR - 3']+[STOP] +[5'- 25bp end of 3xMyc homology from Hamida 3']
dm6	CGAGGAAGACTTGTAGGTC CAATTACTCTTCAACATCC	Forward Primer for 3xMyc to *unc-54* Stitch: [5'- 13bp end of 3xMyc homology from Hamida 3']+[STOP] +[5' - first 20bp of *unc-54*-3'UTR - 3'] 20bp *unc-54*-3'UTR TM=62
dm7 +5'TEG	GCTTTTGGTGCGTTGAGCA CAACGGCTAAGTAGGTTAT GATAAGGTATTTTGTGTGCG	Reverse Primer for *unc-54* 3'UTR to ham-1 Stitch: [5'-35bp ham-1 homology with mutated PAM - 3']+[5' - 23bp downstream of *unc-54* 3'UTR in pPD95_77 vector -3'] 23bp *unc-54*TM= 62
C-Myc-R	GAGGTCCTCCTCGGAGATG	Poison Primer Reverse "C-Myc-R" (From Hamida): [5' - mid 3xMyc sequence - 3']
dm20	GTAGAGGAGTCTCAGTCTAT TTGGGATTCTACAGA	Forward Extended Primer: to add 15bp to 35bp homology arms (has 15bp additional ham-1 upstream sequence, and 20bp of original homology arm)
dm21	TTCCGTCCATTCTTGGCTTT TGGTGCGTTGAGCAC	Reverse Extended Primer: to add 15bp to 35bp homology arms (has 15bp additional ham-1 downstream sequence, and 20bp of original homology arm)

Table A5-D. Wnt Primers for DNA amplification and generation of ssRNA

Primer Name	**PCR Role**	**Sequence (T7: GTCAGATCGTTAATACGACTCACTATAGGG)**

Dm22	cwn-1 F1	ATGCTGAAATCTACACAAGTGATC
Dm23	cwn-1 T7F1	GTCAGATCGTTAATACGACTCACTATAGGGATGCTGAAA TCTACACAAGTGATC
Dm24	cwn-1 R1	TGAGCGGAATCAACAAACTCT
Dm25	cwn-1 T7R1	GTCAGATCGTTAATACGACTCACTATAGGGTGAGCGGAA TCAACAAACTCT
Dm26	cwn-2 F1	ATGATTCCACGGAGAAGTTGT
Dm27	cwn-2 T7 F1	GTCAGATCGTTAATACGACTCACTATAGGGATGATTCCA CGGAGAAGTTGT
Dm28	cwn-2 R1	TGGATCGTGTTCTTTCTCTCG
Dm29	cwn-2 T7R1	GTCAGATCGTTAATACGACTCACTATAGGGTGGATCGTG TTCTTTCTCTCG
Dm30	egl-20 F1	ATGCAATTTTTCATTTGCCTGA
Dm31	egl-20 T7F1	GTCAGATCGTTAATACGACTCACTATAGGGATGCAATTTT TCATTTGCCTGA
Dm32	egl-20 R1	TCCTGGTTTACTGTCACATCCA
Dm33	egl-20T7R1	GTCAGATCGTTAATACGACTCACTATAGGGTCCTGGTTT ACTGTCACATCCA
Dm34	lin-44 F1	ATGCGAGCAGCTCCTTTTG
Dm35	lin-44 T7F1	GTCAGATCGTTAATACGACTCACTATAGGGATGCGAGCA GCTCCTTTTG
Dm36	lin-44 R1	CCCATCTGGTTGTTACACGC
Dm37	lin-44 T7R1	GTCAGATCGTTAATACGACTCACTATAGGGCCCATCTGG TTGTTACACGC